アルゼンティン共和国
ネウケン州北部地熱開発計画調査
(第1,2年次)
中間報告書 (付図集)

1983年11月

国際協力事業団

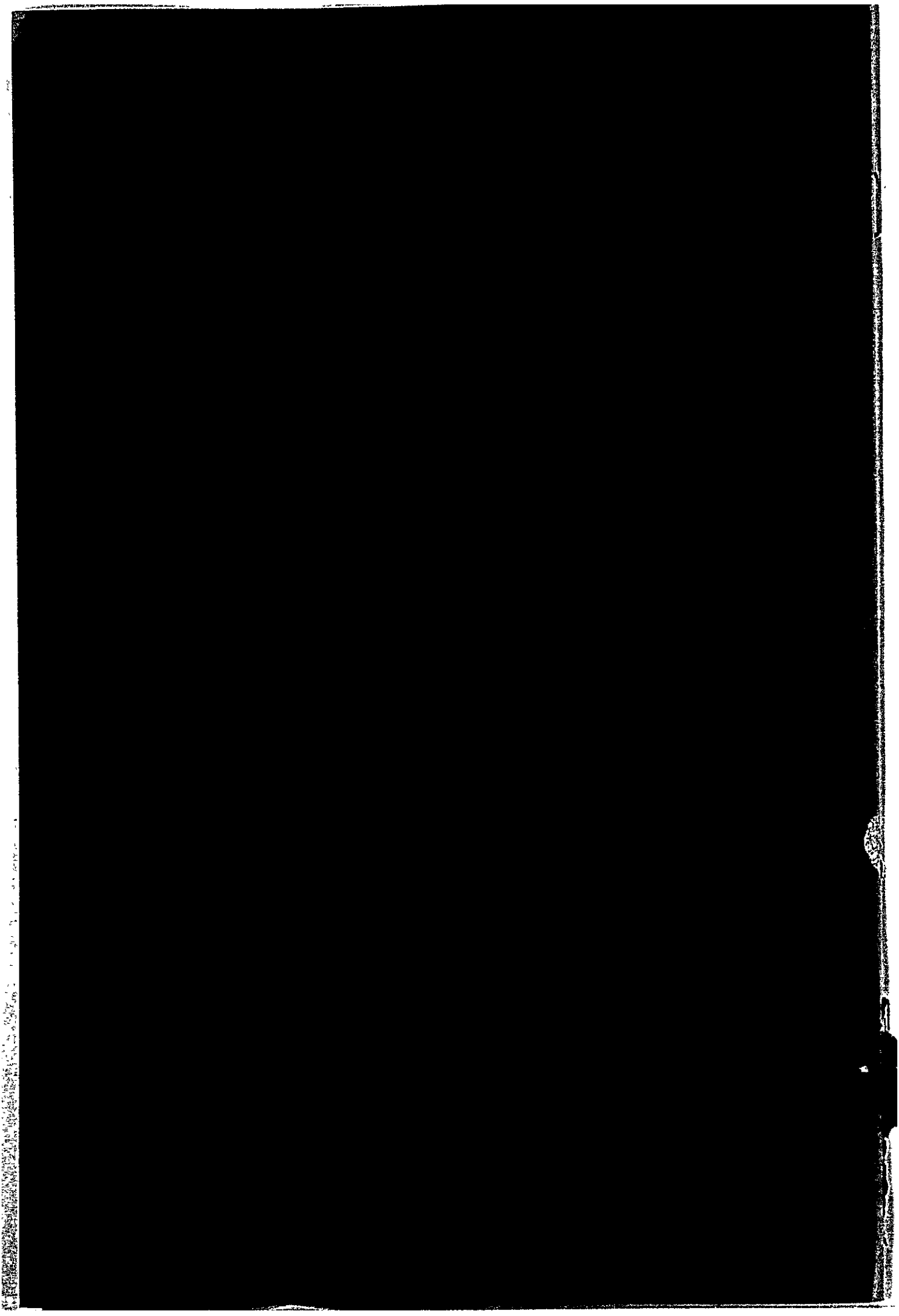

アルゼンティン共和国

ネウケン州北部地熱開発計画調査

（第１，２年次）

中 間 報 告 書 （付図集）

1983年11月

国 際 協 力 事 業 団

付 図 リ ス ト

1. 総　　説

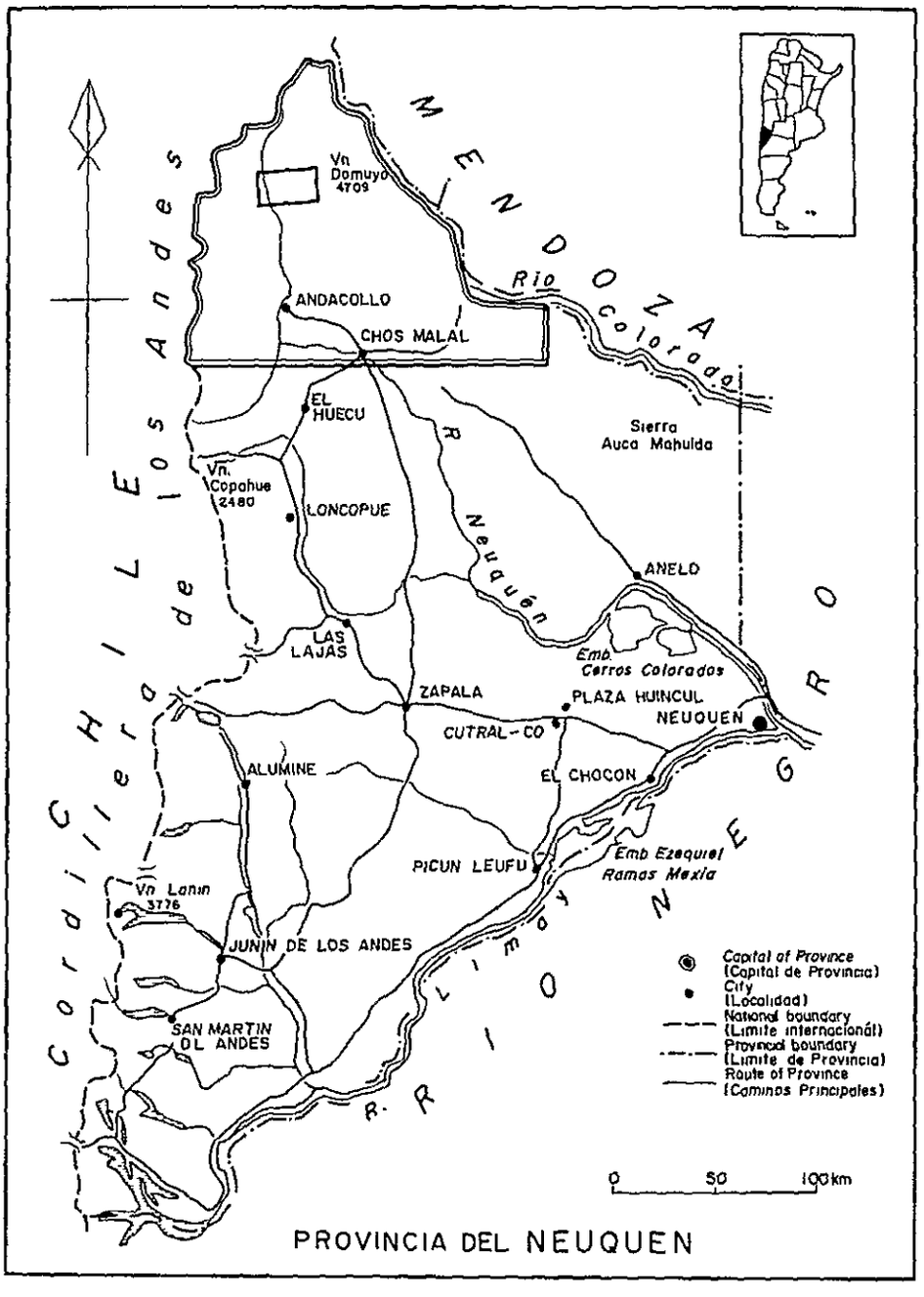

15,000 km^2 First phase survey area
(Area estudiada en la primera etapa)

200 km^2 Second phase survey area
(Area en estudio segunda etapa)

Fig.1-1 Location map of the survey areas

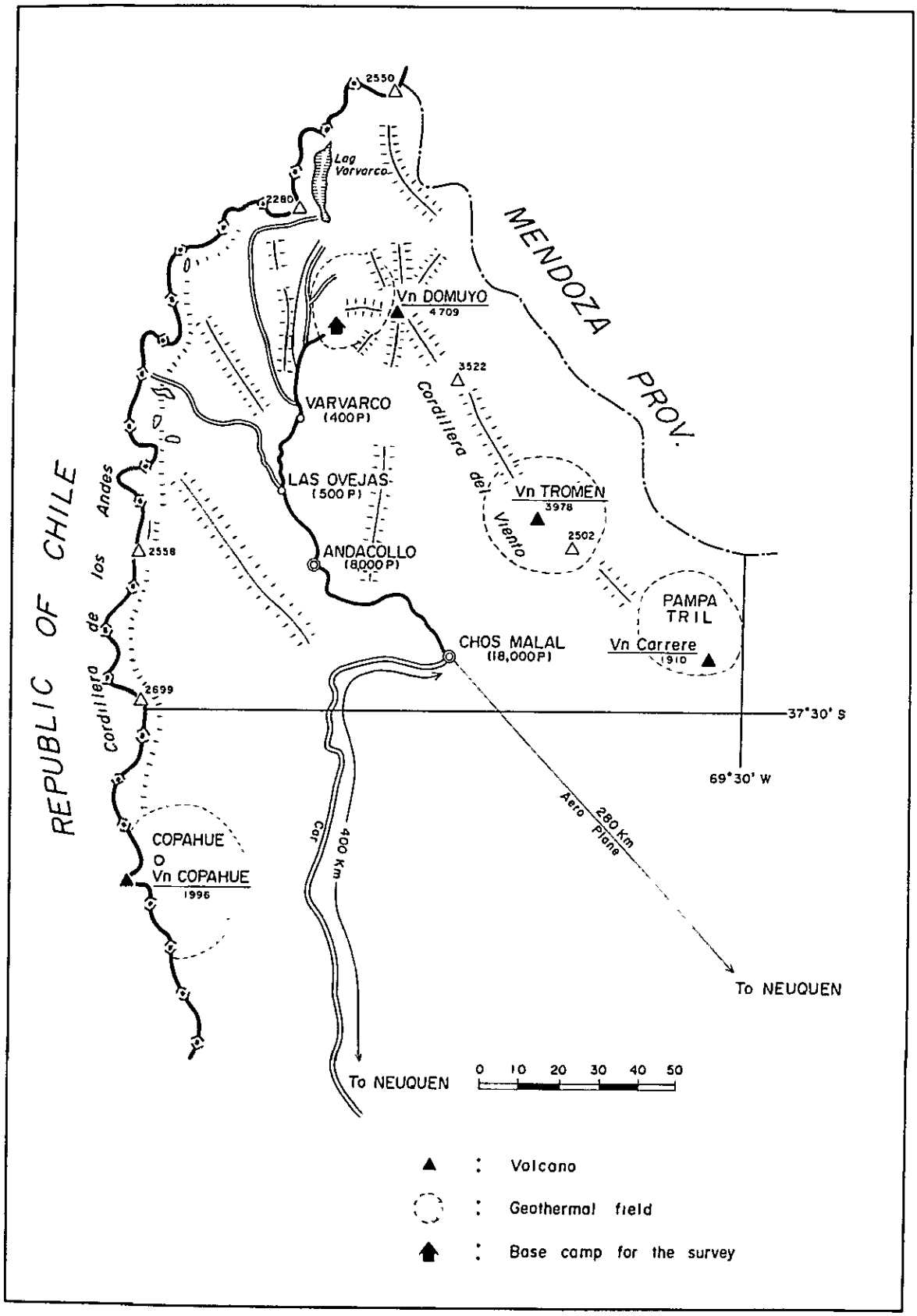

Fig.1-2 Explanatory map of northern parts of the Province of Neuquen

2.　第１次調査(広域調査)の概要

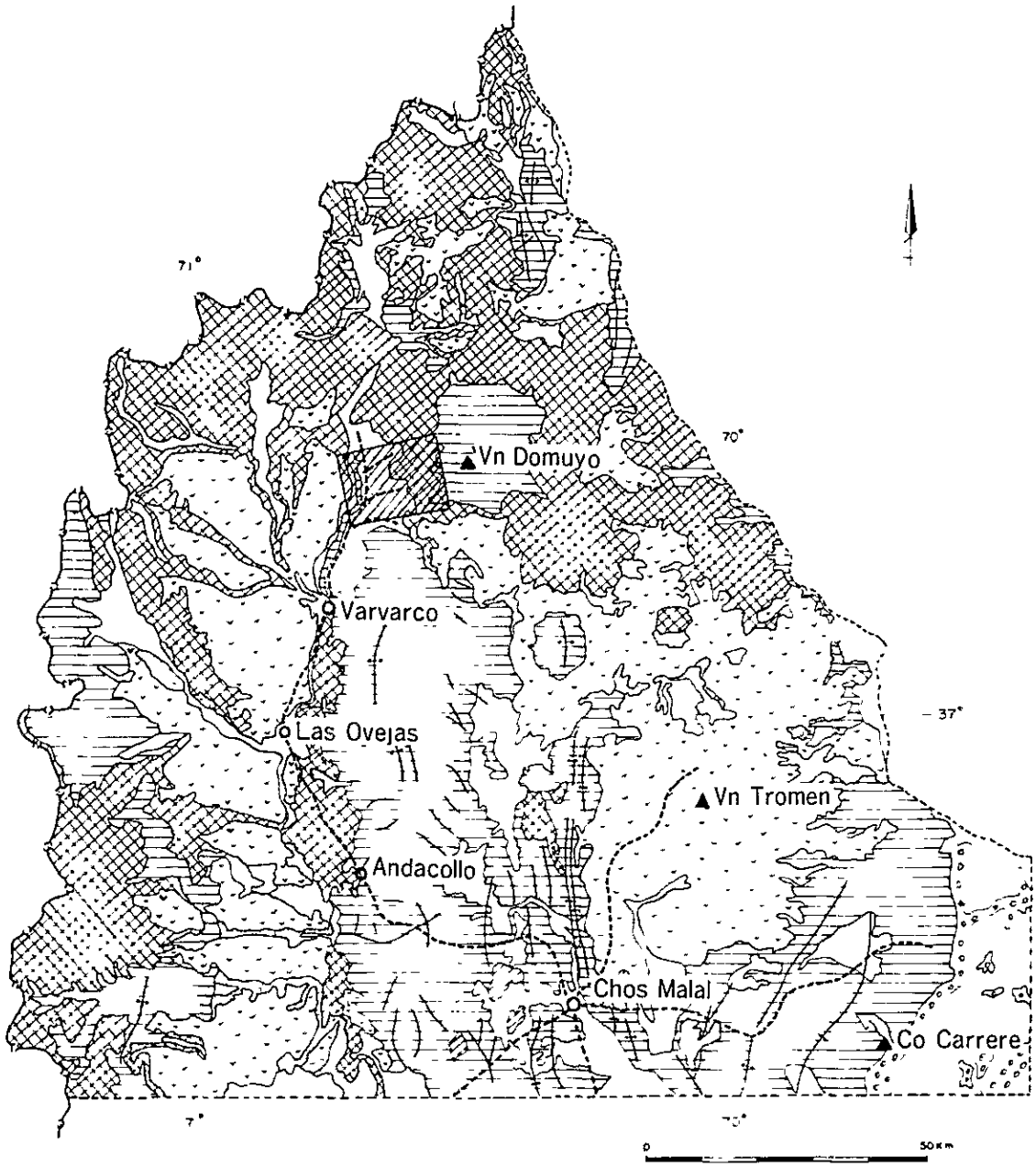

REGEND

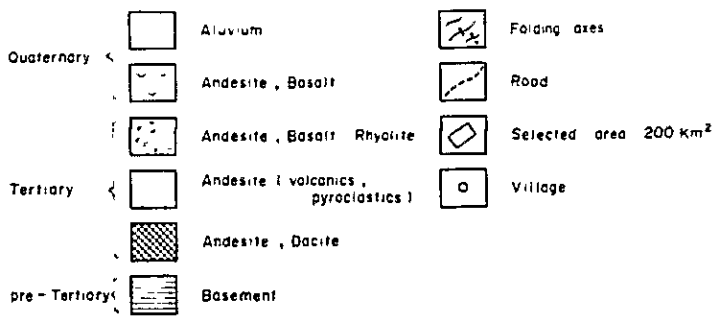

Fig.2-1 Geological interpretation map of Landsat image

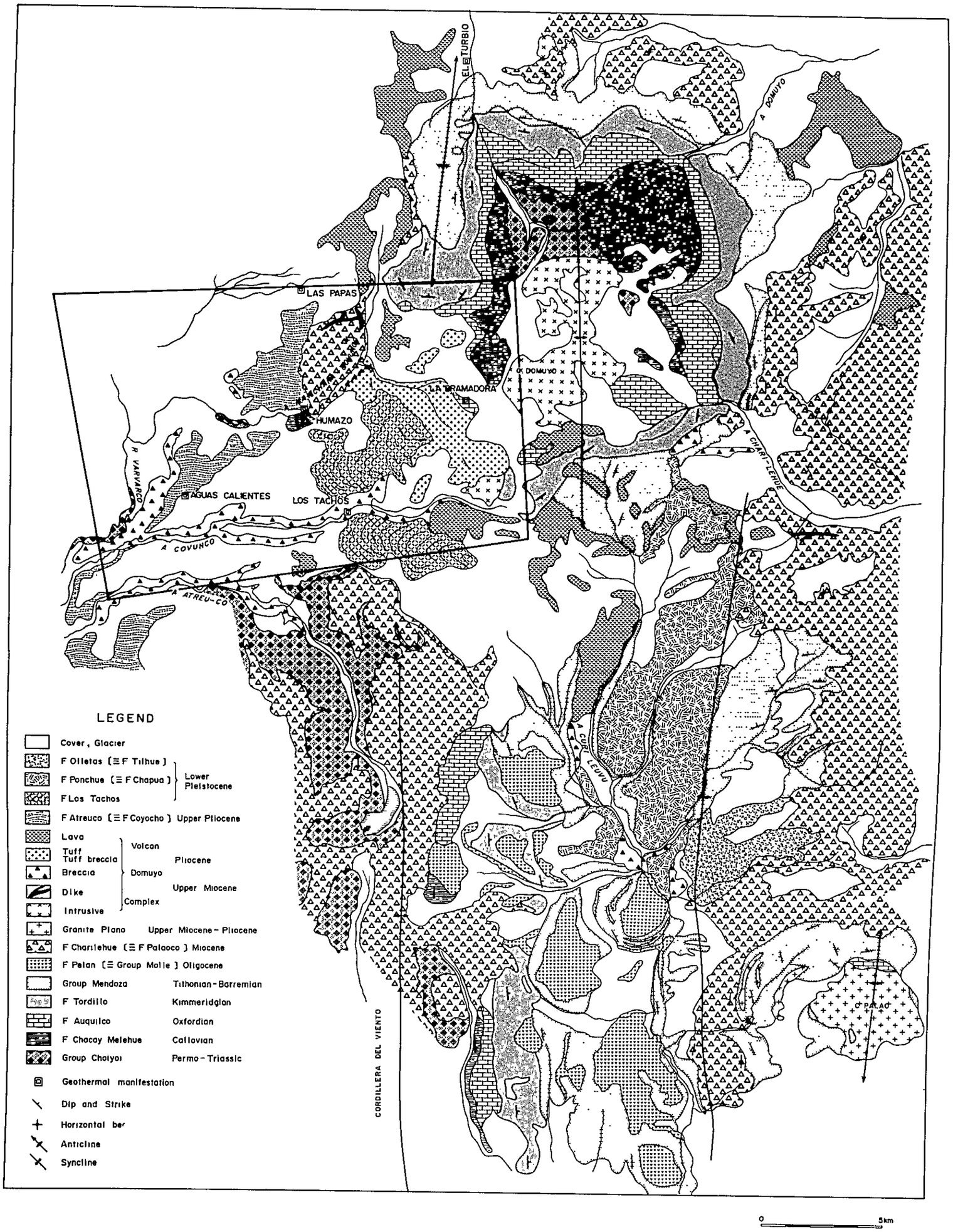

Fig.2-2 Regional geological map

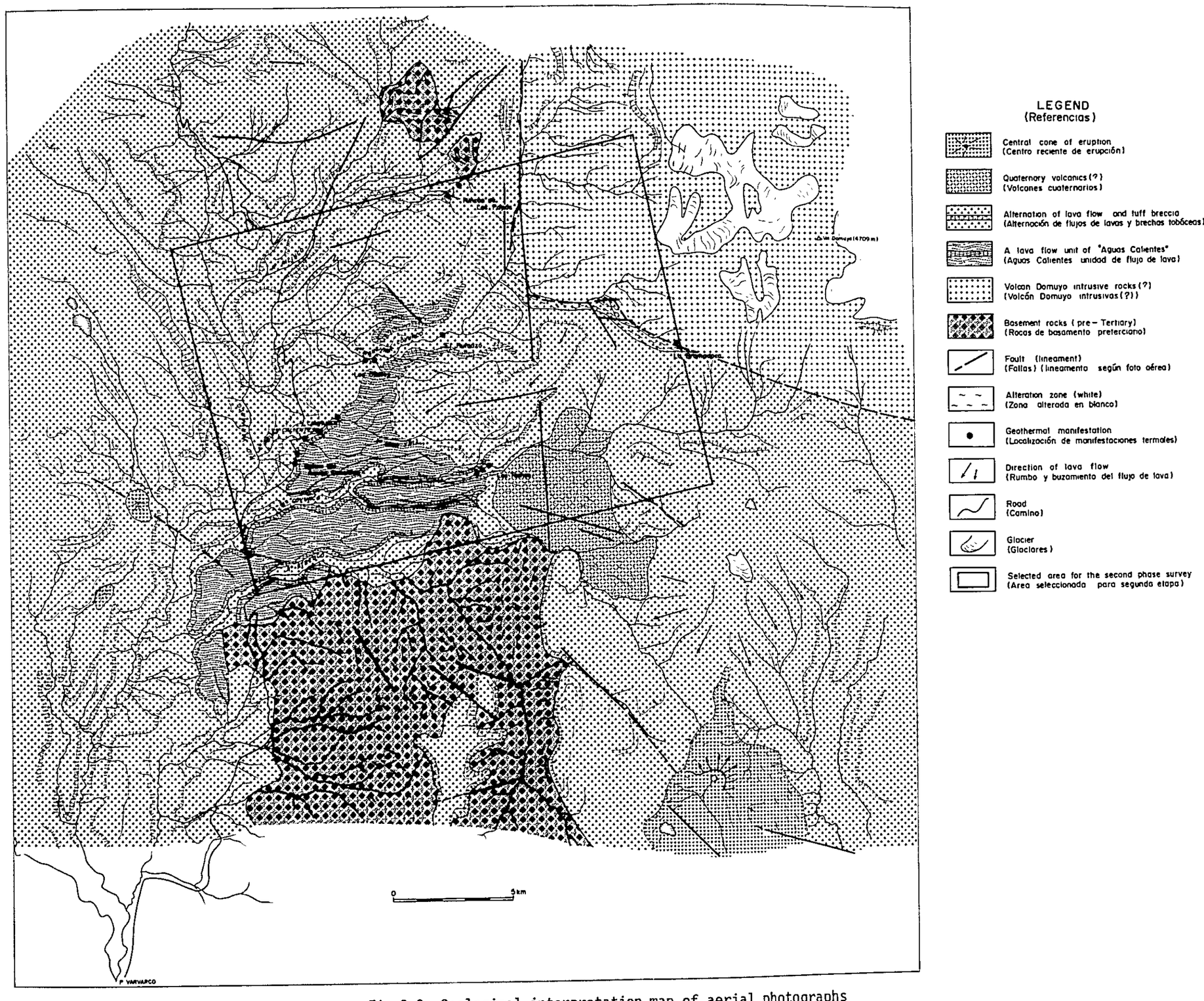

Fig.2-3 Geological interpretation map of aerial photographs

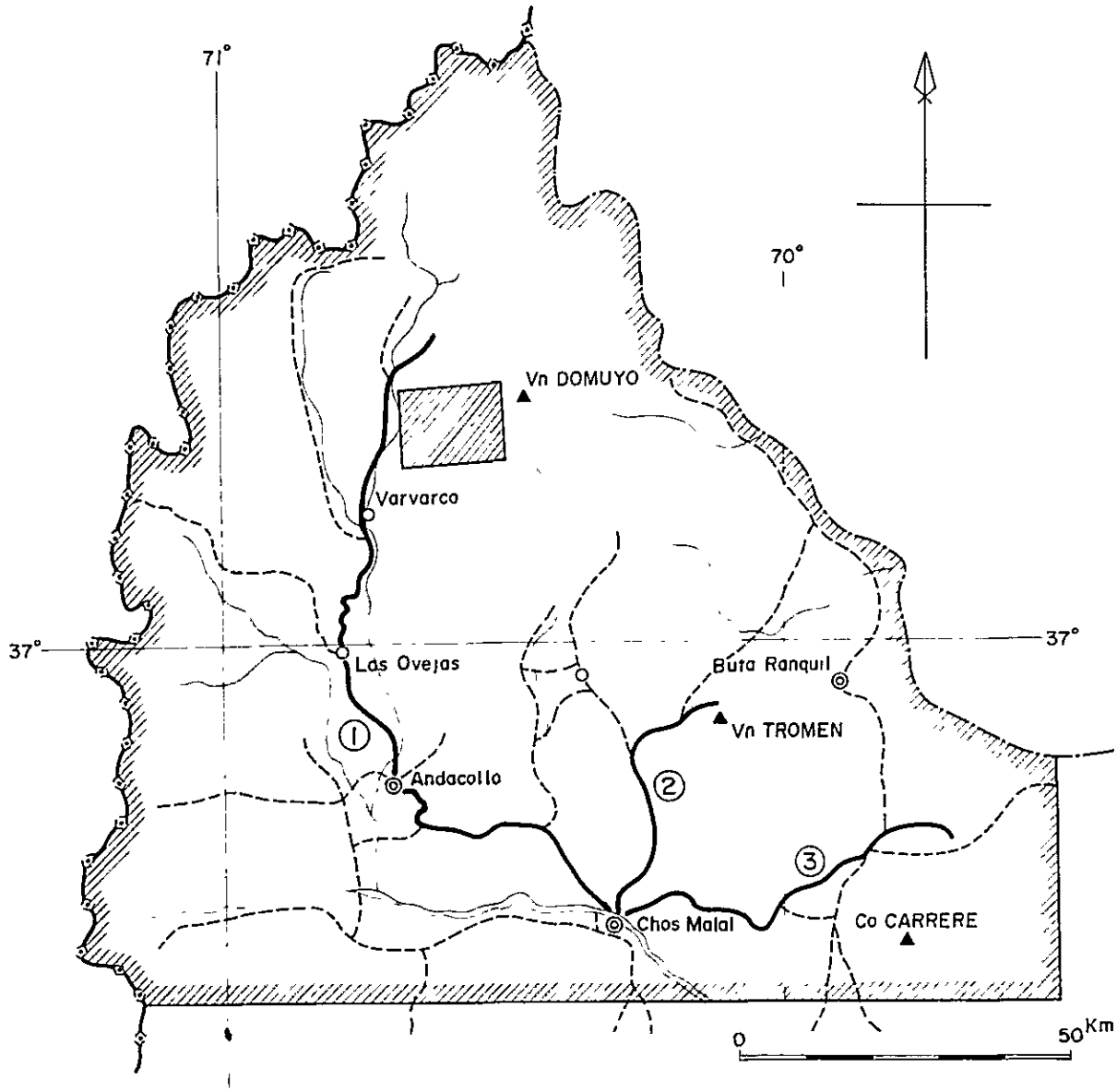

First phase survey area : 15,000Km²
(Limite del area de 15,000 Km²)

Second phase survey area : 200Km²
(Area seleccionada de 200Km²)

Routes of reconnaisance geological survey
(Rutas de reconocimiento efectuadas)

Roads
(Rutas y accesos a la zona)

Rivers
(Detalle de drenaje)

Fig.2-4 Map of the survey areas and routes of reconnaissance geological survey

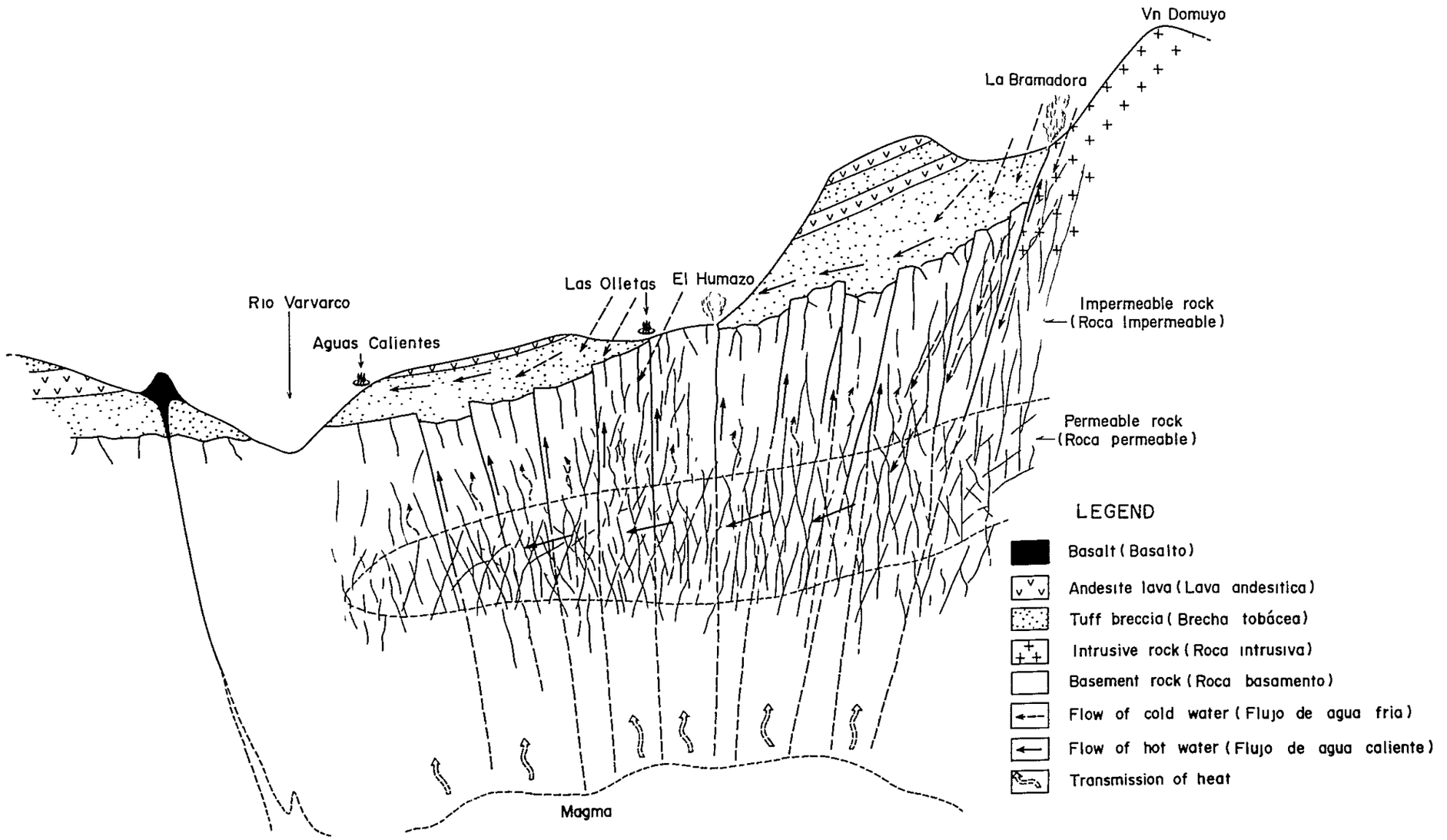

Fig.2-5 Schematic profile of geology and geothermal system

3. 調 査 地 域 の 地 質

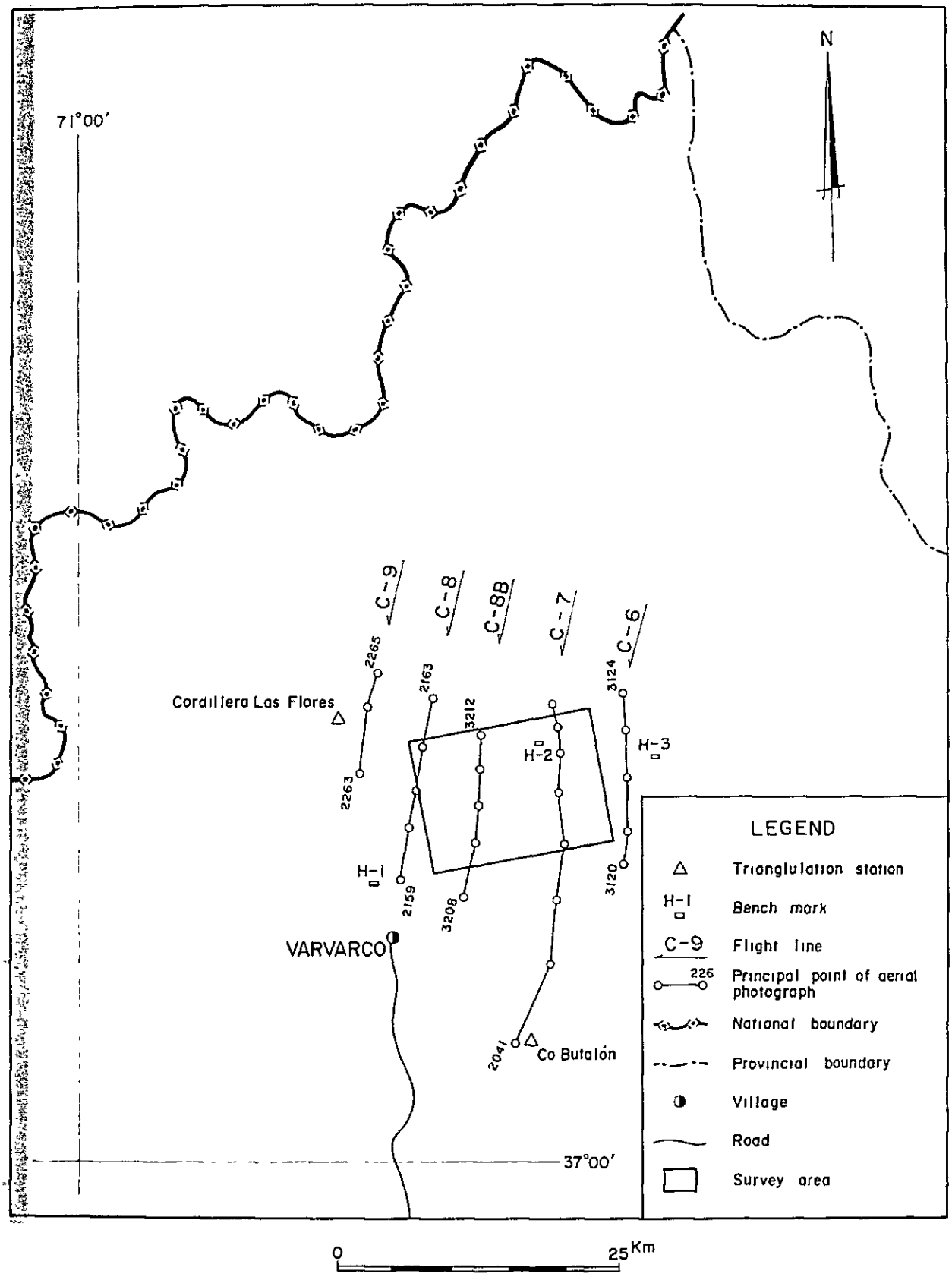

Fig.3-1 Principal points of aerial photographs and topographic standard points

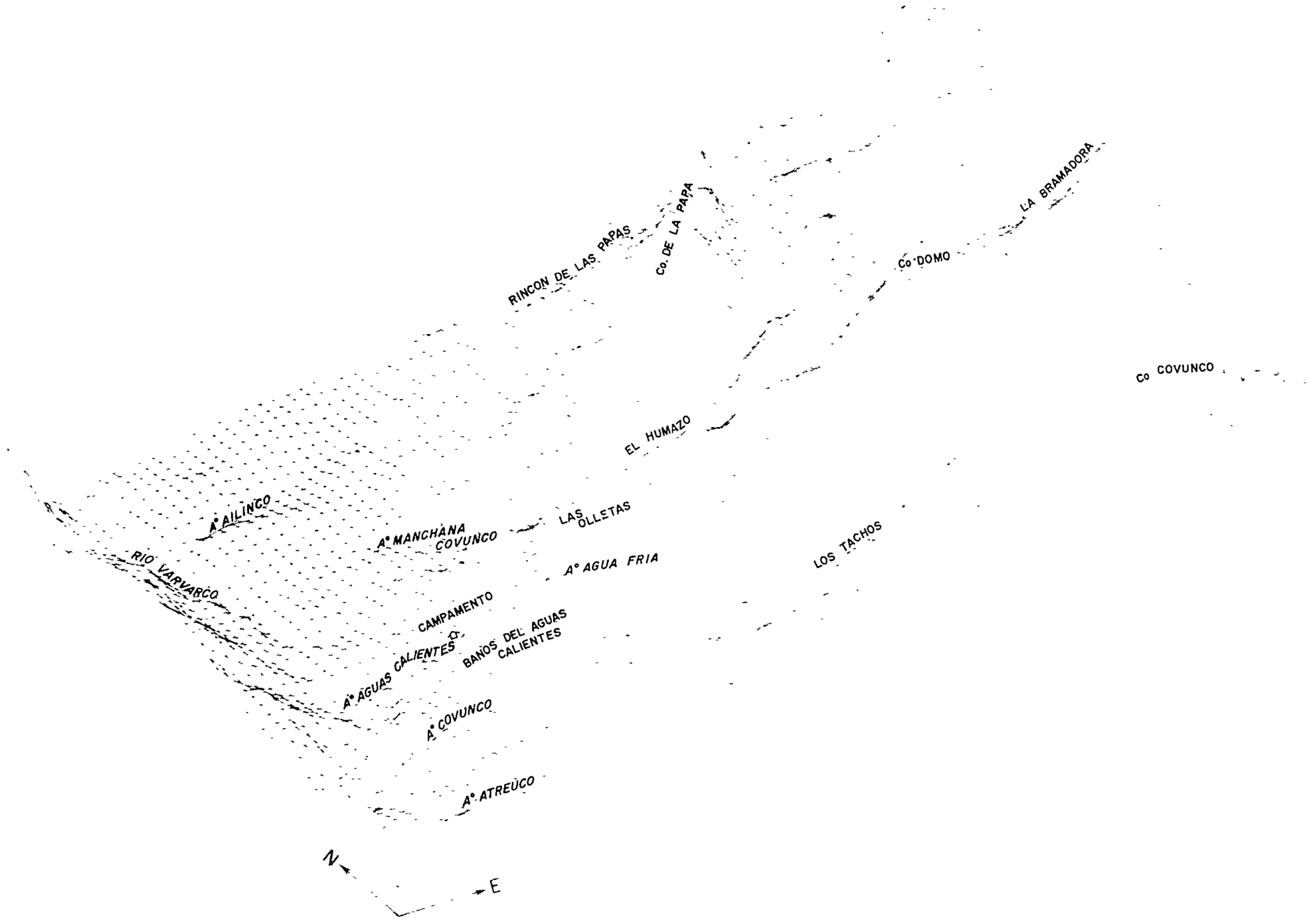

Fig.3-2 Bird's-eye view map of the survey area

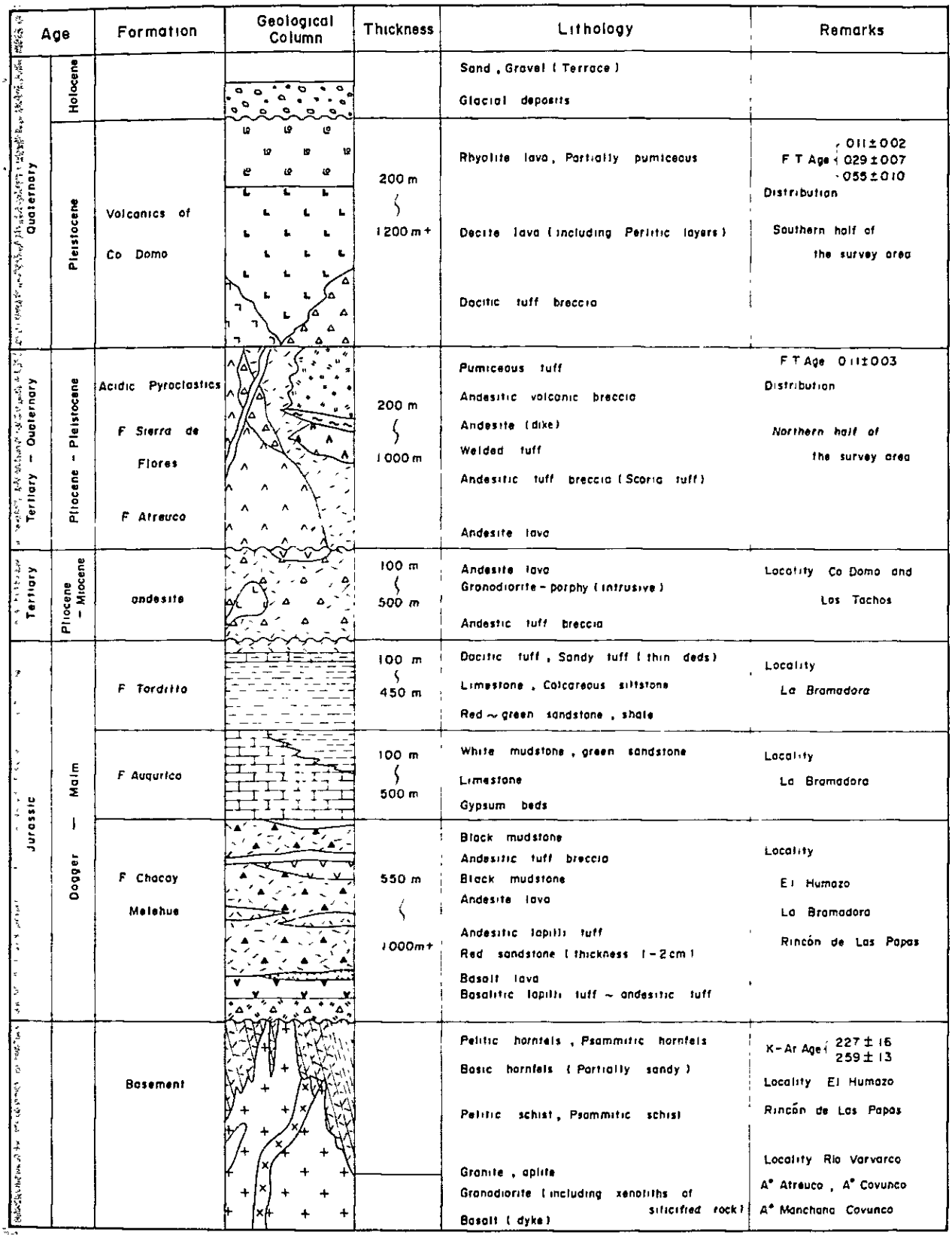

Fig.3-3 Geological columnar section of the survey area

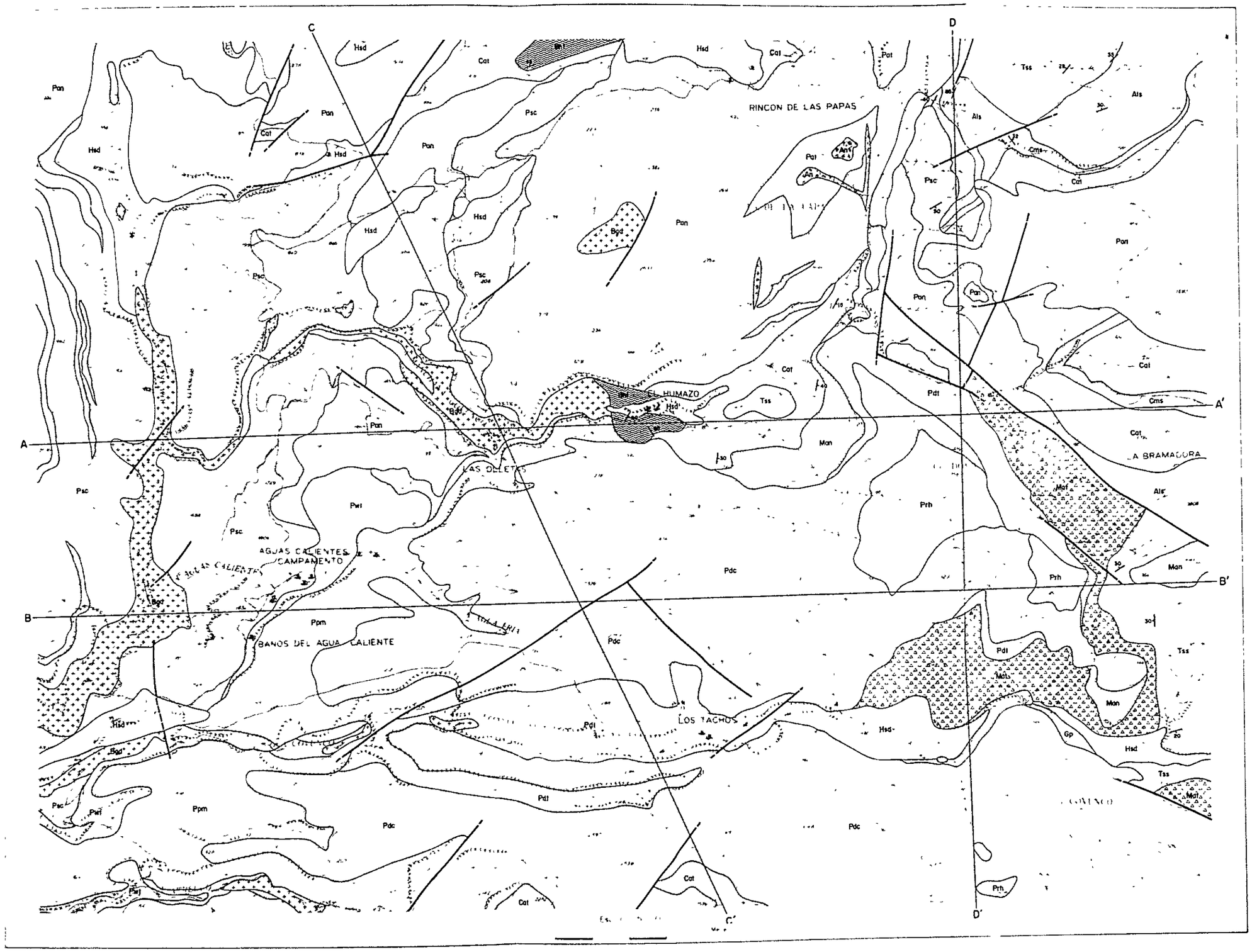

LEGEND

Quaternary	Holocene	Hsd	Sand, gravel
	Pleistocene	Prh	Rhyolite lava
		Pdc	Dacite lava
		Pdt	Dacitic tuff breccia
Quaternary–Tertiary	Pleistocene \ Pliocene	Pat	Andesitic volcanic breccia
		Pan	Andesite
		Ppm	Pumiceous tuff
		Pwl	Welded tuff
		Psc	Scoria tuff
Tertiary	Pliocene Miocene	Man	Andesite lava
		Mat	Andesitic tuff breccia
Jurassic	F Tordillo	Tss	Red sandstone, Dacitic tuff, Limestone
	F Auquilco	Als	Limestone, sandstone, mudstone, Gypsum
	F Chacay Melehue	Cms	Black mudstone
		Cat	Andesitic tuff breccia, Sandstone
Basement		Hnf	Hornfels schist
		Bgd	Granodiorite
Intrusive rocks		Andesite	
		Gp	Granodiorite porphyry

30 Bedding plane

Fault

A—A' Section line

Fig.3-4 Geological map of the survey area

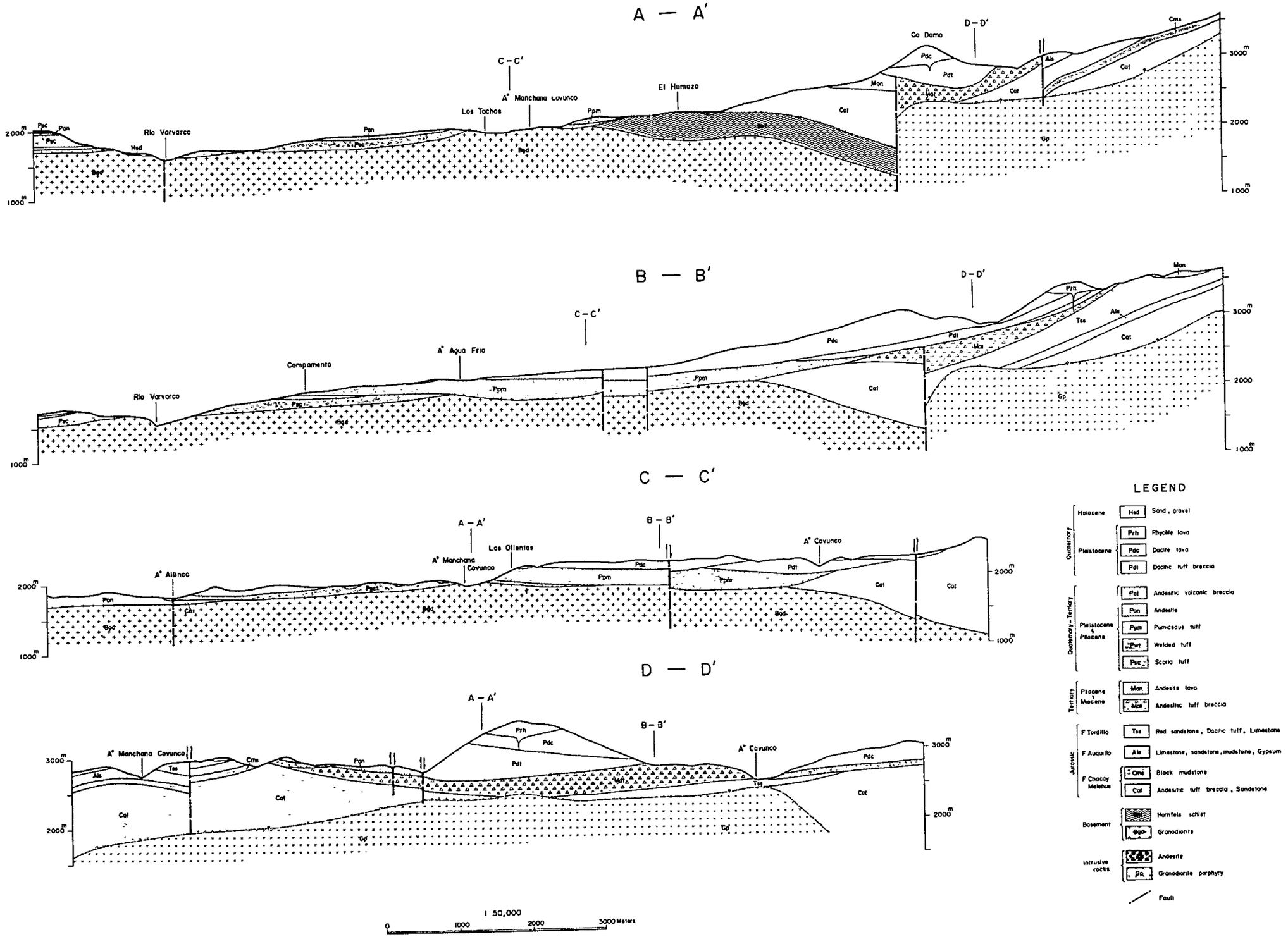

Fig.3-5 Geological cross-sections

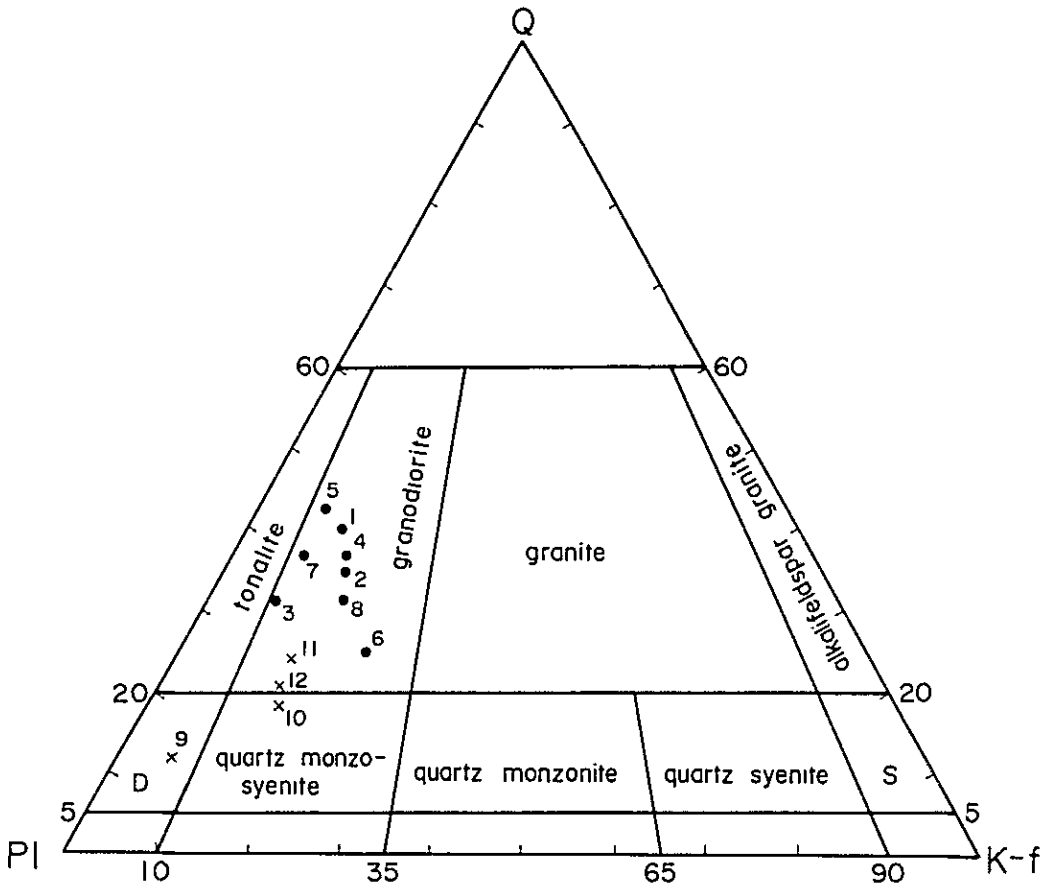

Varvarco intrusive
- 1 : F-1
- 2 : F-26
- 3 : F-42-2
- 4 : TM-8
- 5 : TM-11
- 6 : TM-16
- 7 : TM-27
- 8 : 83-2-12-5

Domuyo complex
- 9 : F-14
- 10 : TM-12
- 11 : TM-48
- 12 : TM-201

D : quartz diorite etc

S : alkalifeldspar-quartz syenite

Fig.3-6 Modal diagram of quartz - potash feldspar plagioclase

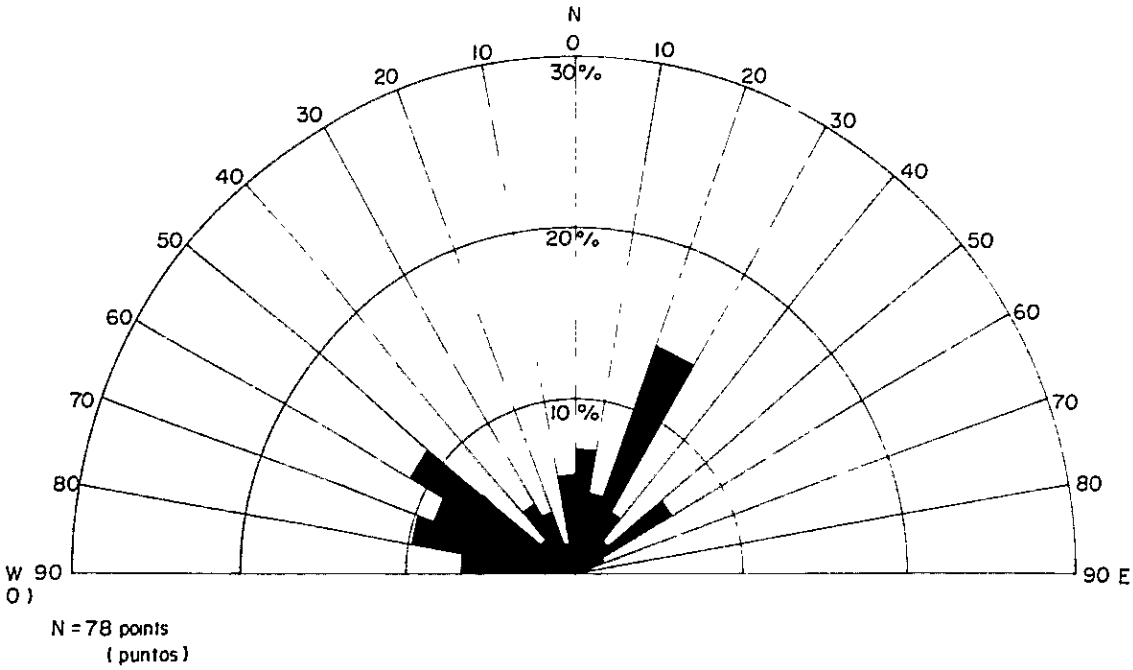

Fig.3-7 Rose diagram of joints in granodiorite

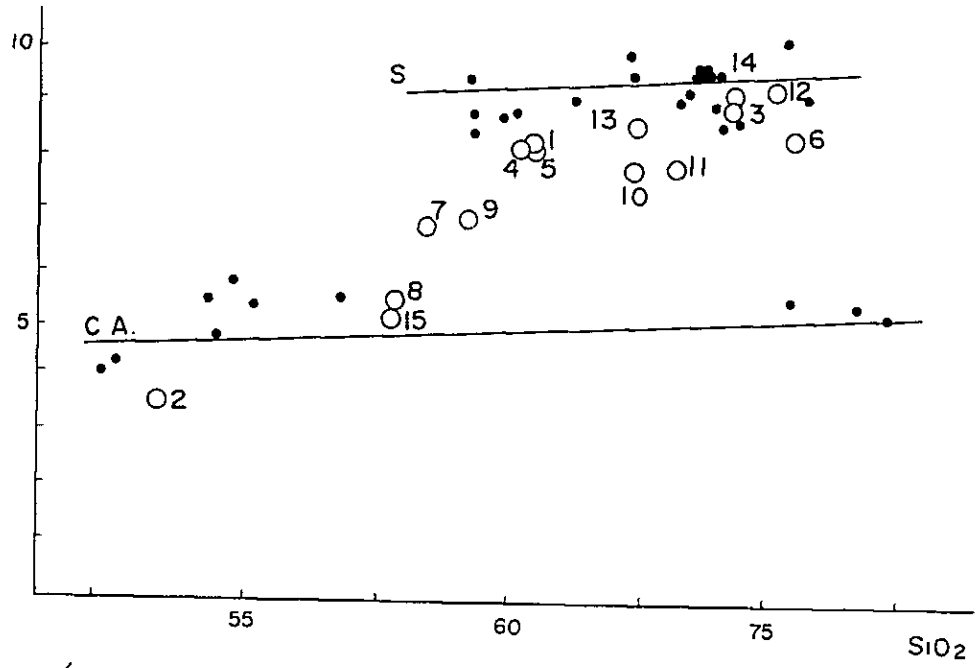

1	F-3	9	TM-44	S	Shoshonitic series (Serie shoshonitica)
2	F-8	10	TM-45	C A	Calc-alkaline series (Serie calco-alca lina)
3	F-23	11	TM-48		
4	F-46	12	TM-50		
5	TM-6	13	TM-52		
6	TM-13	14	TM-53		
7	TM-20	15	TM-69		
8	TM-31				

○

• Brousse, Pesco (1982)

Fig.3-8 Alkali - silica diagram of younger volcanic rocks

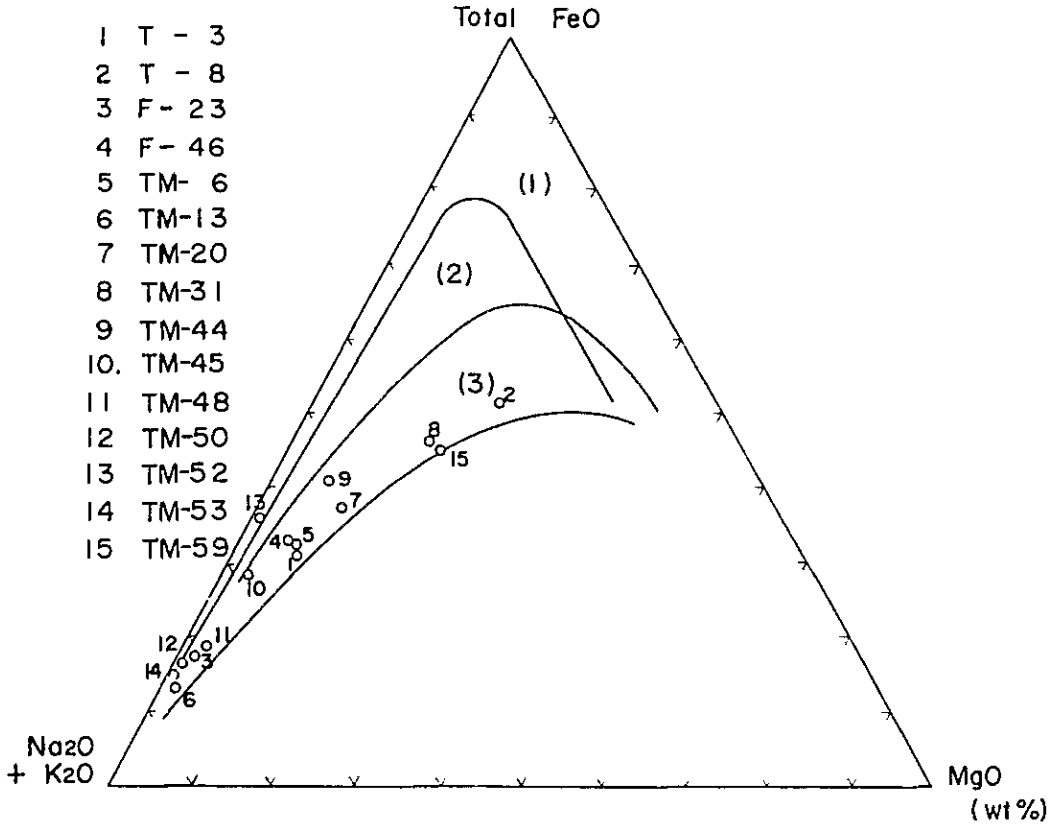

(1) Chemical variation in rocks of Skaergaard intrusion

(2) Chemical variation in tholeiitic volcanics of Izu-Hakone area, Japan

(3) Chemical variation in calc-alkaline volcanics of Izu-Hakone area, Japan

Fig.3-9 MgO - total FeO - (Na_2O + K_2O) diagram of younger volcanic rocks

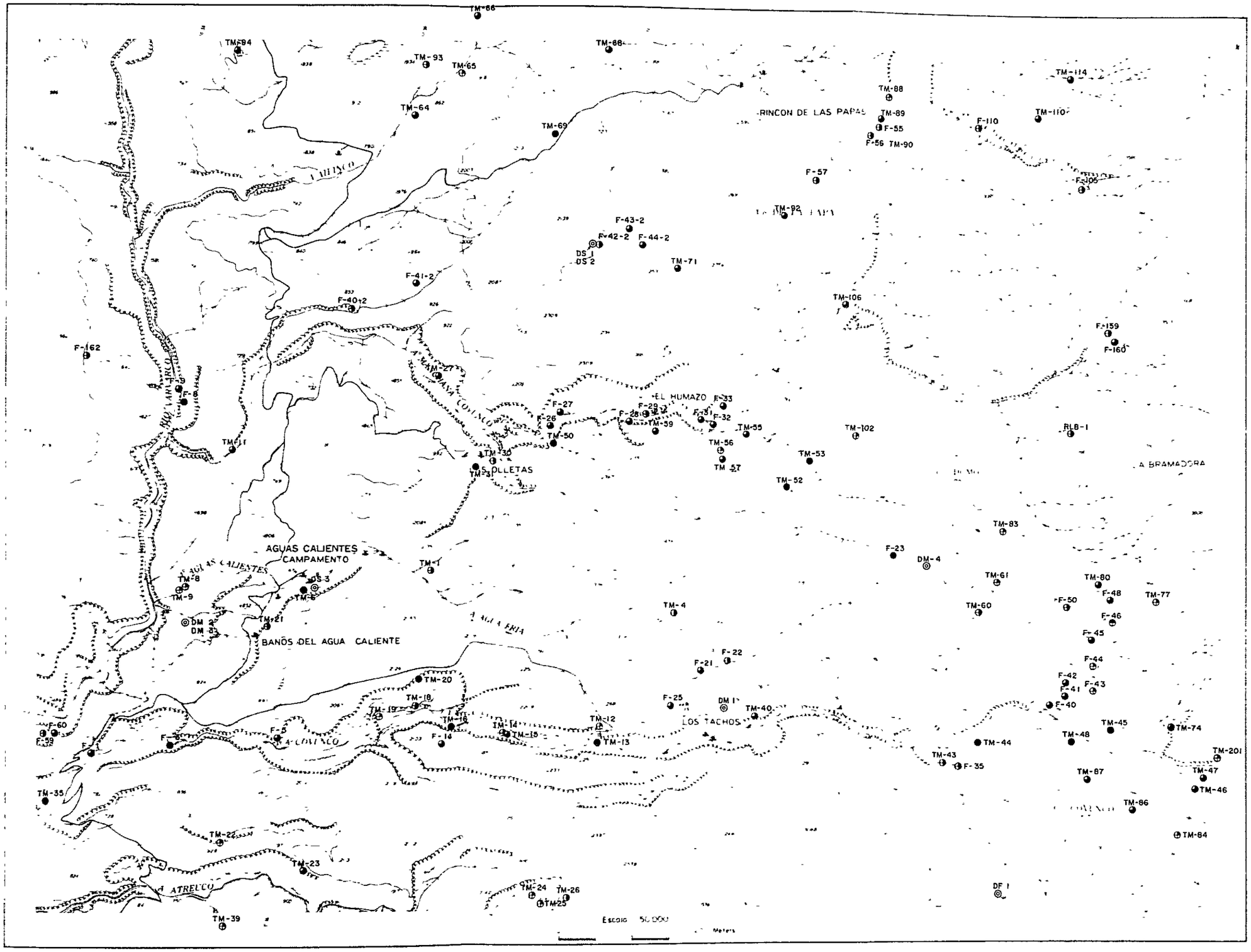

Fig.3-10 Location map of rock sampling

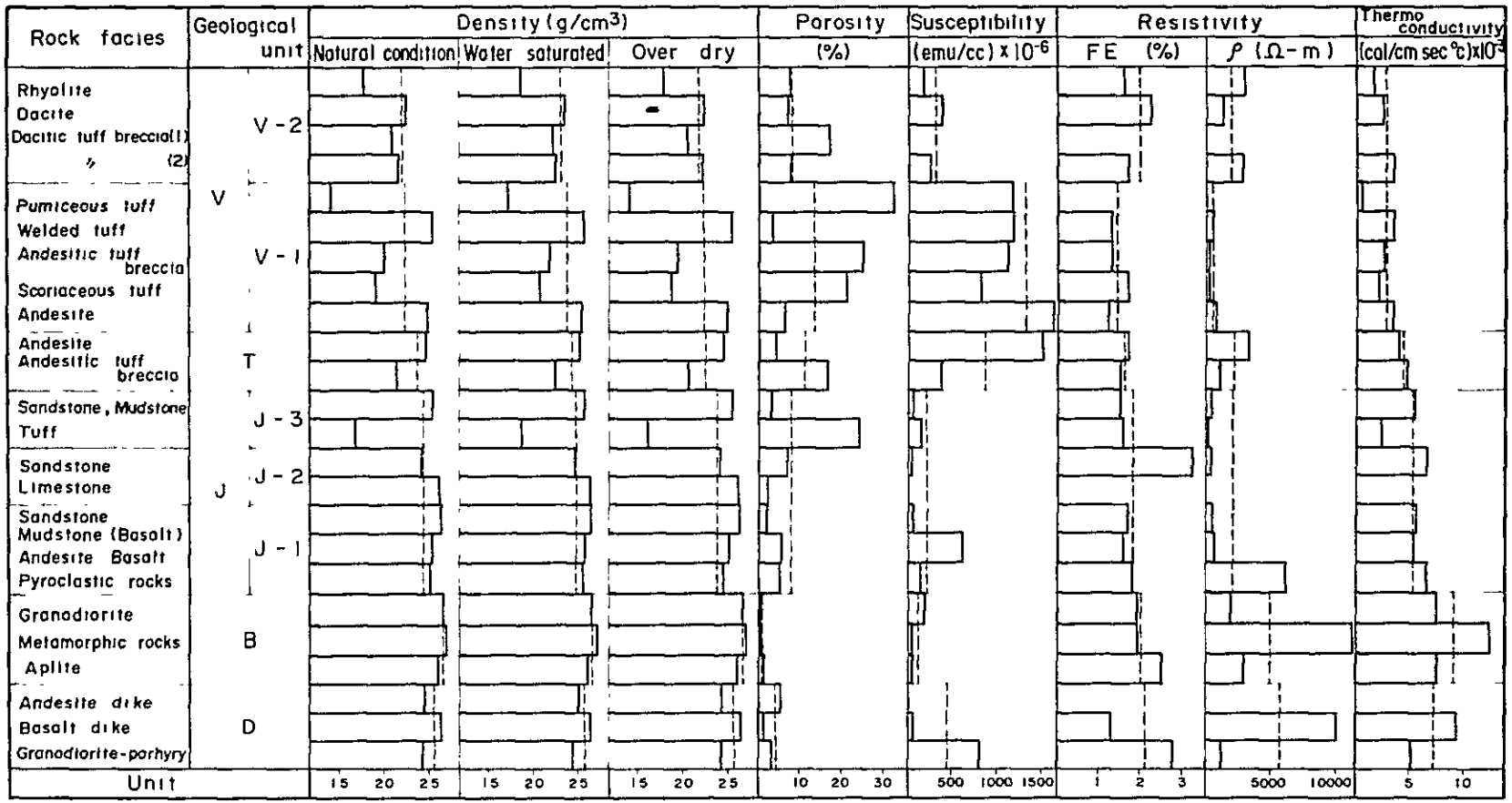

Mean value of rock facies, - - - - Mean value of geological unit

V Quaternary – Tertiary
- V-2 Pleistocene, Volcanics of Co Domo
- V-1 Pleistocene – Pliocene, Acidic Pyroclastics, Sierra de Flores Formation, Atreuco Formation

T Tertiary, Pliocene – Miocene, Andesite

J Jurassic, Dogger – Malm,
- J-3 Tordillo Formation
- J-2 Auquilco Formation
- J-1 Chacay Melehue Formation

B Basement

D Dike rock etc

Fig.3-11 Physical properties of rocks

4. 調 査 地 域 の 地 質 構 造

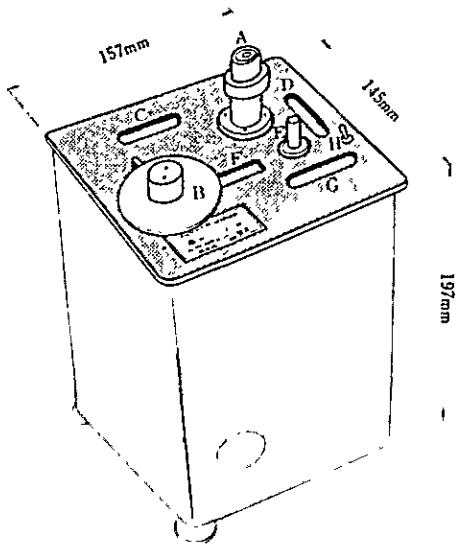

A : Eyepiece
B : Dial
C : Long Level
D : Cross Level
E : Arrestment Knob
F : Counter
G : Thermometer
H : Light Switch

Fig.4-1 LaCoste & Romberg gravity meter Model - G

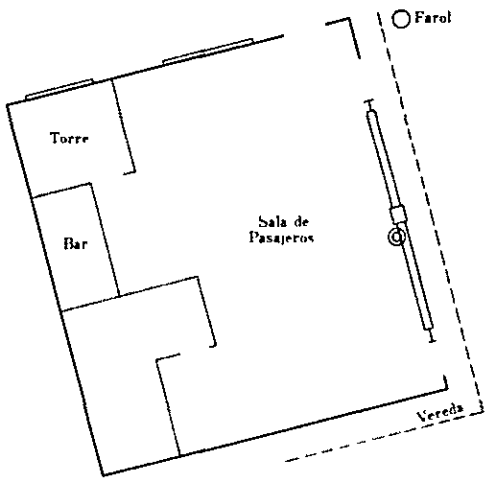

NEUQUEN AEROPUERTO

a Reference station
No.9310 68'

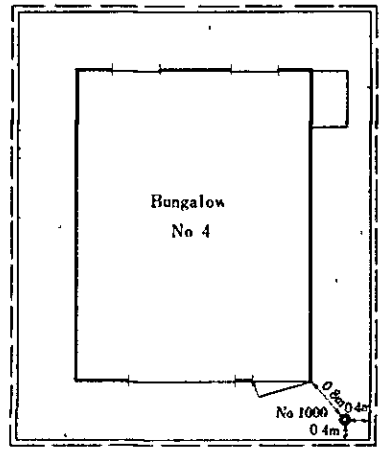

CAMPAMENTO

(b) Base station
(No.1000)

Fig.4-2 Sketches of reference station(a) and base station(b)

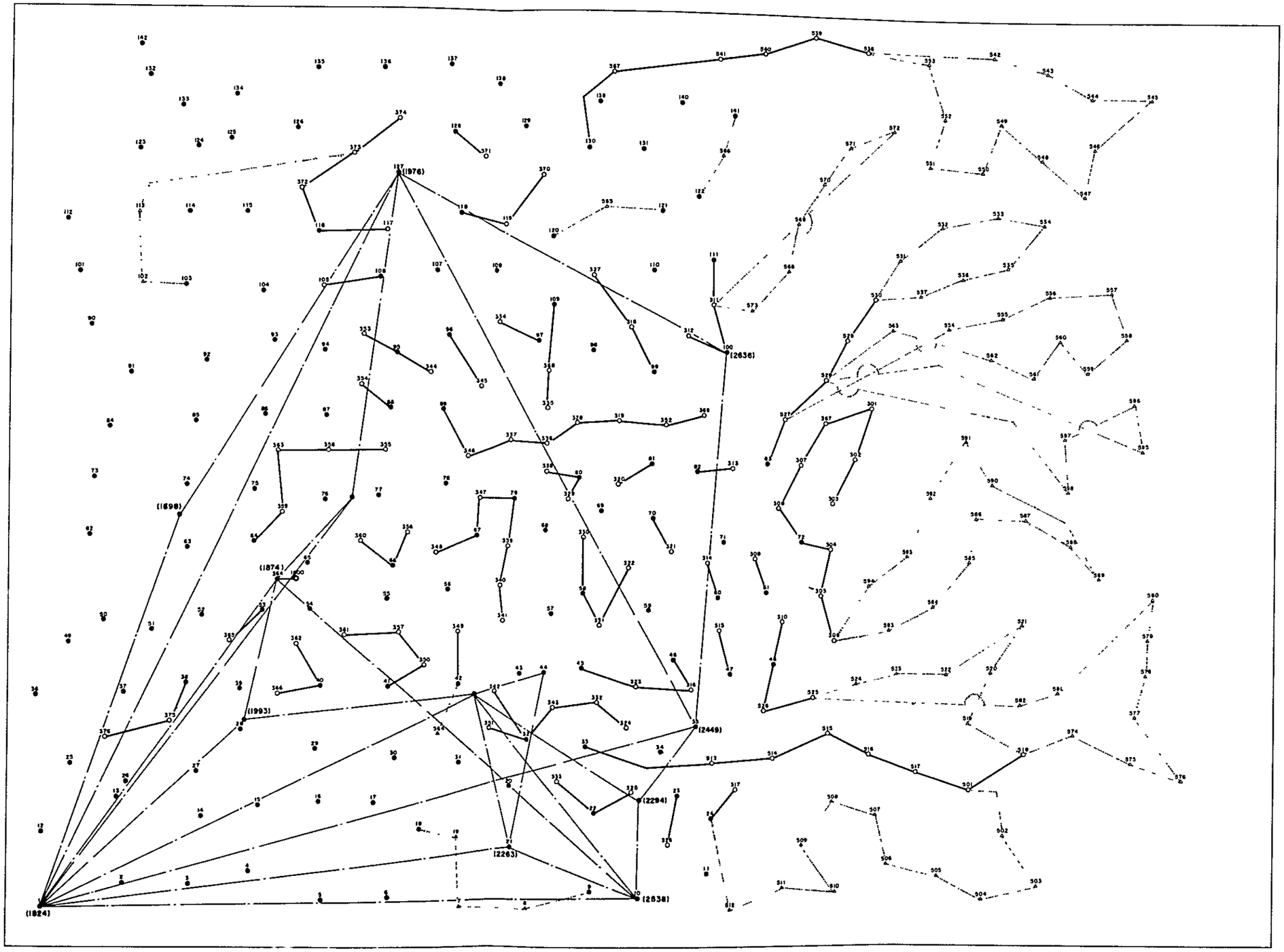

Fig.4-3 Network of leveling

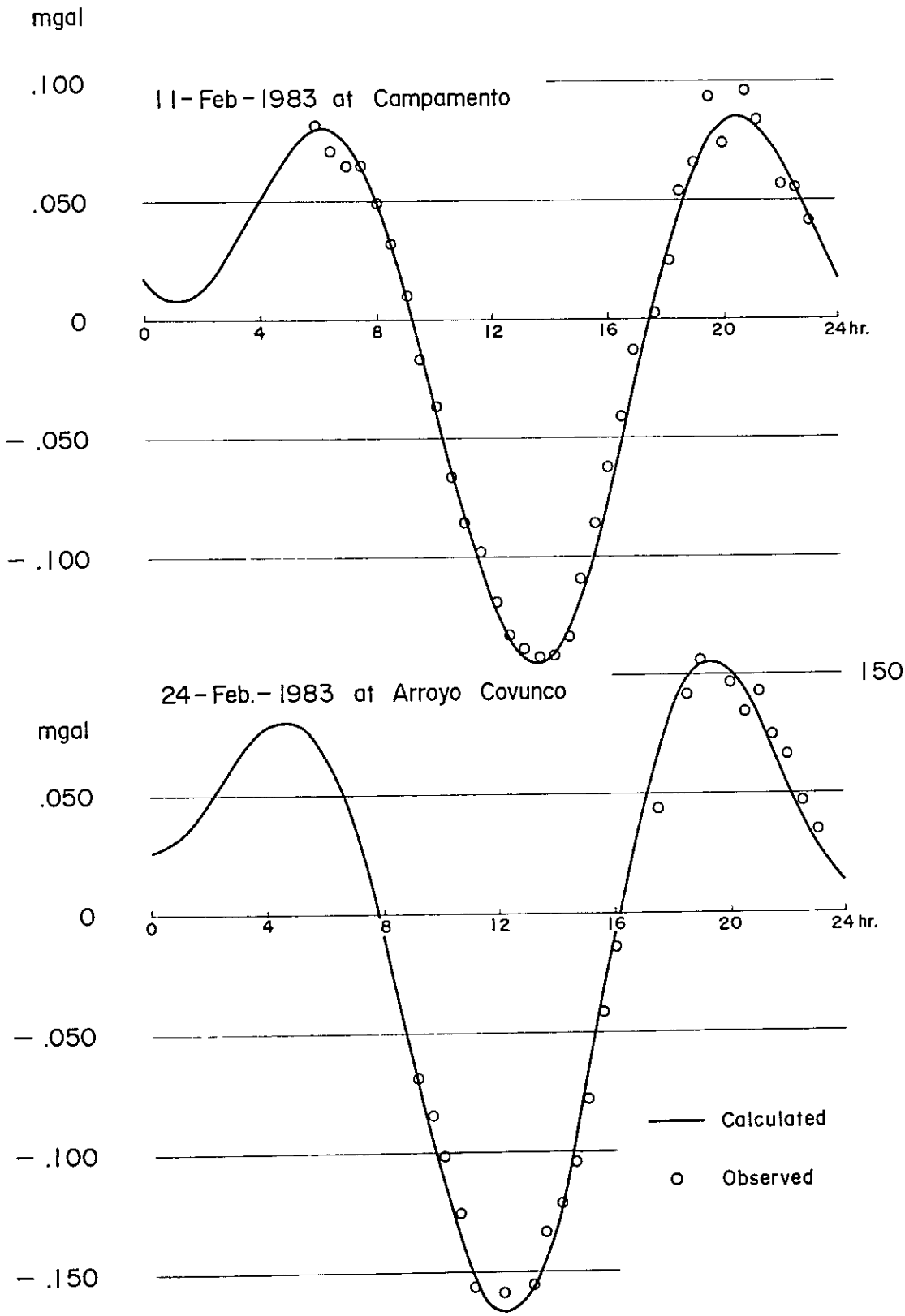

Fig.4-4 Observations of diurnal gravity variation

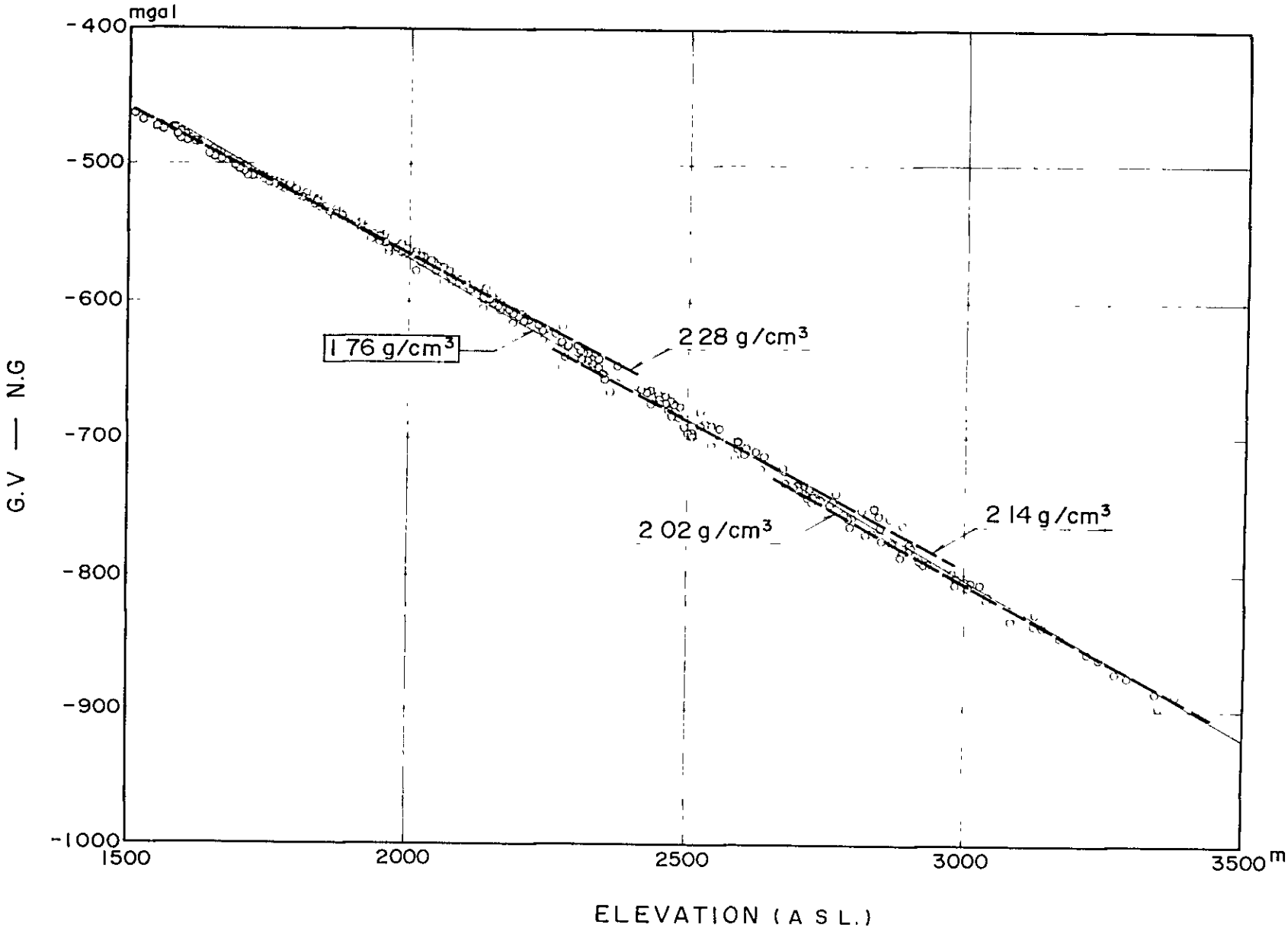

Fig.4-5 Relation between gravity and altitude

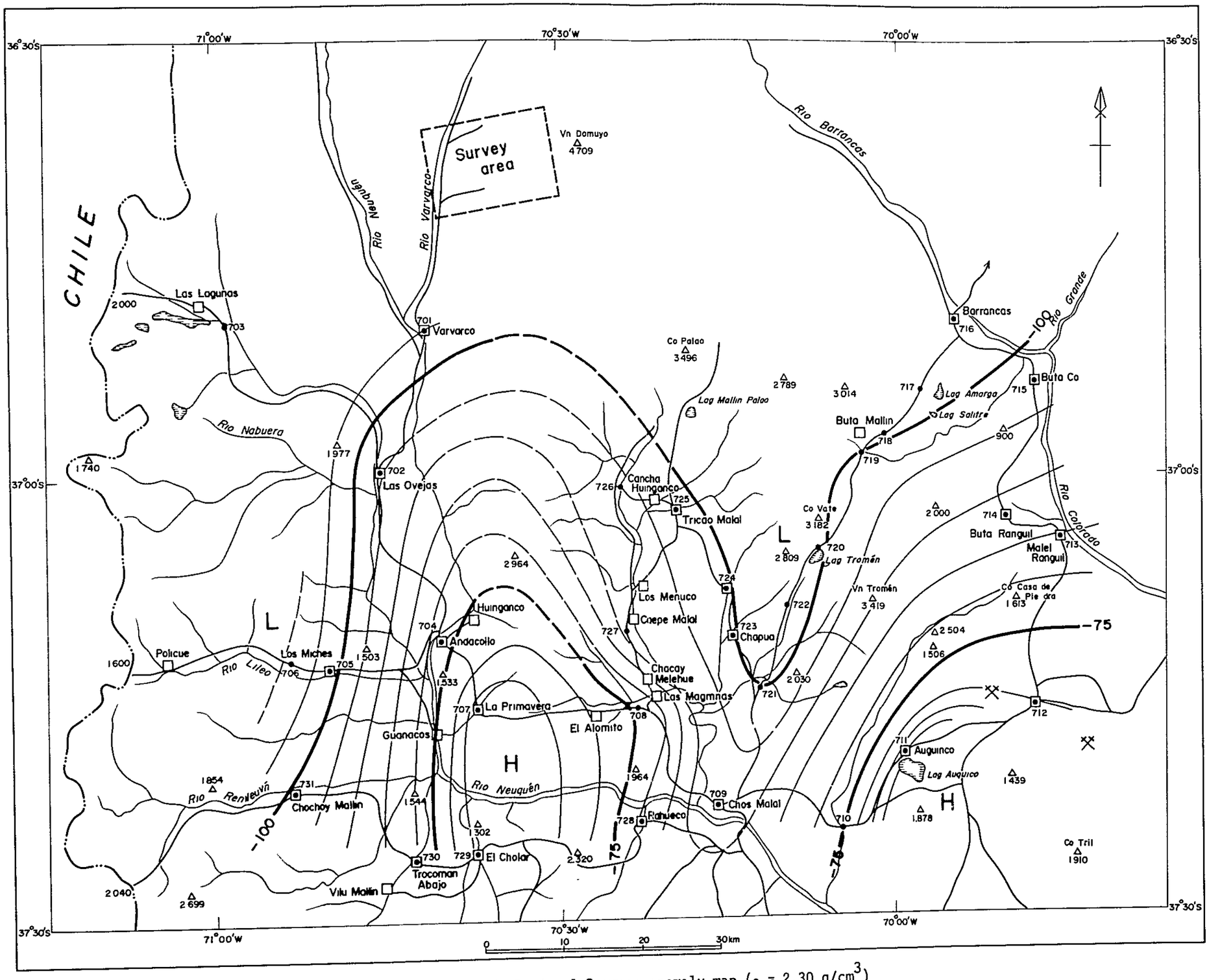

Fig.4-6 Regional Bouguer anomaly map (ρ = 2.30 g/cm^3)

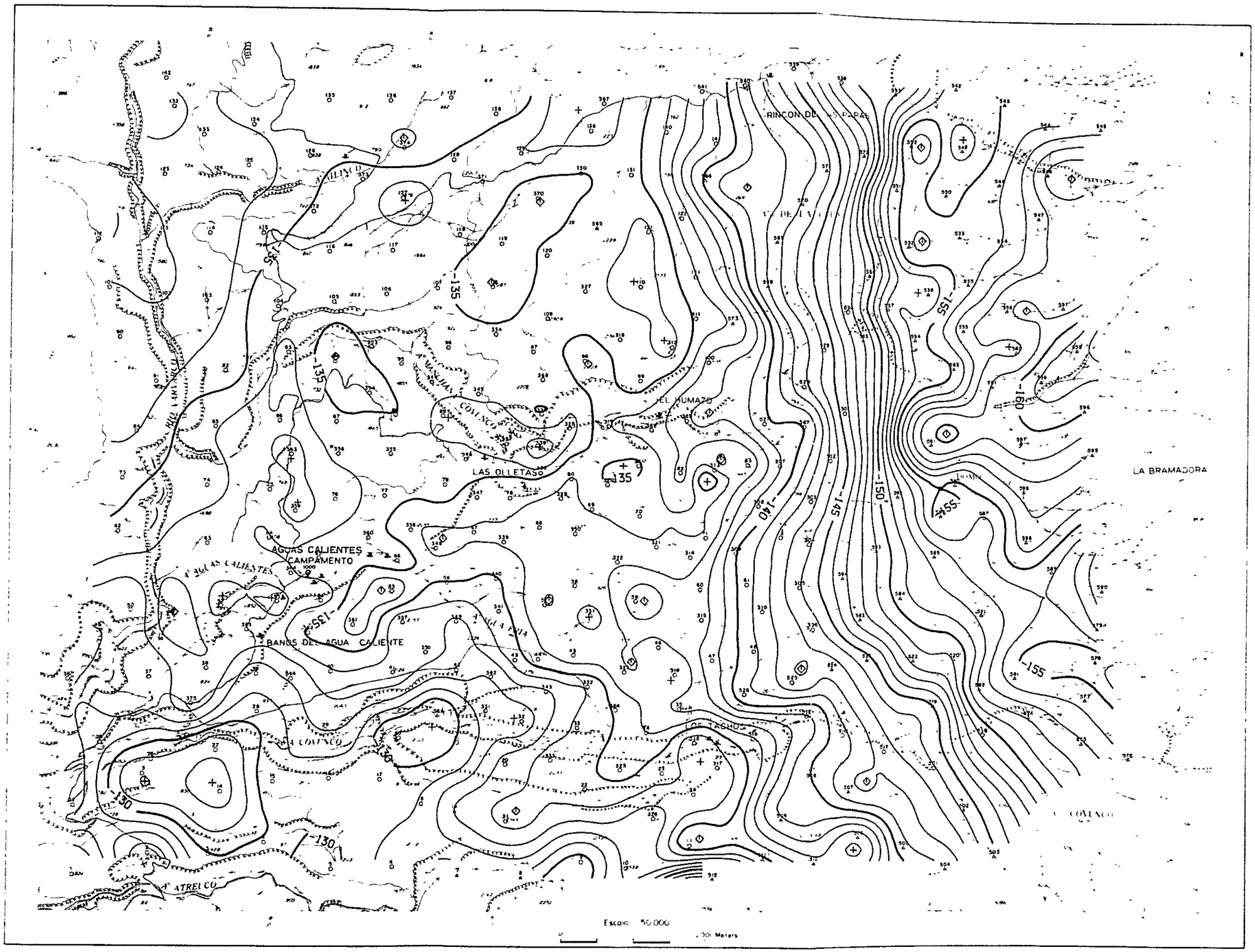

Fig.4-7 Bouguer anomaly map (ρ = 2.30 g/cm^3)

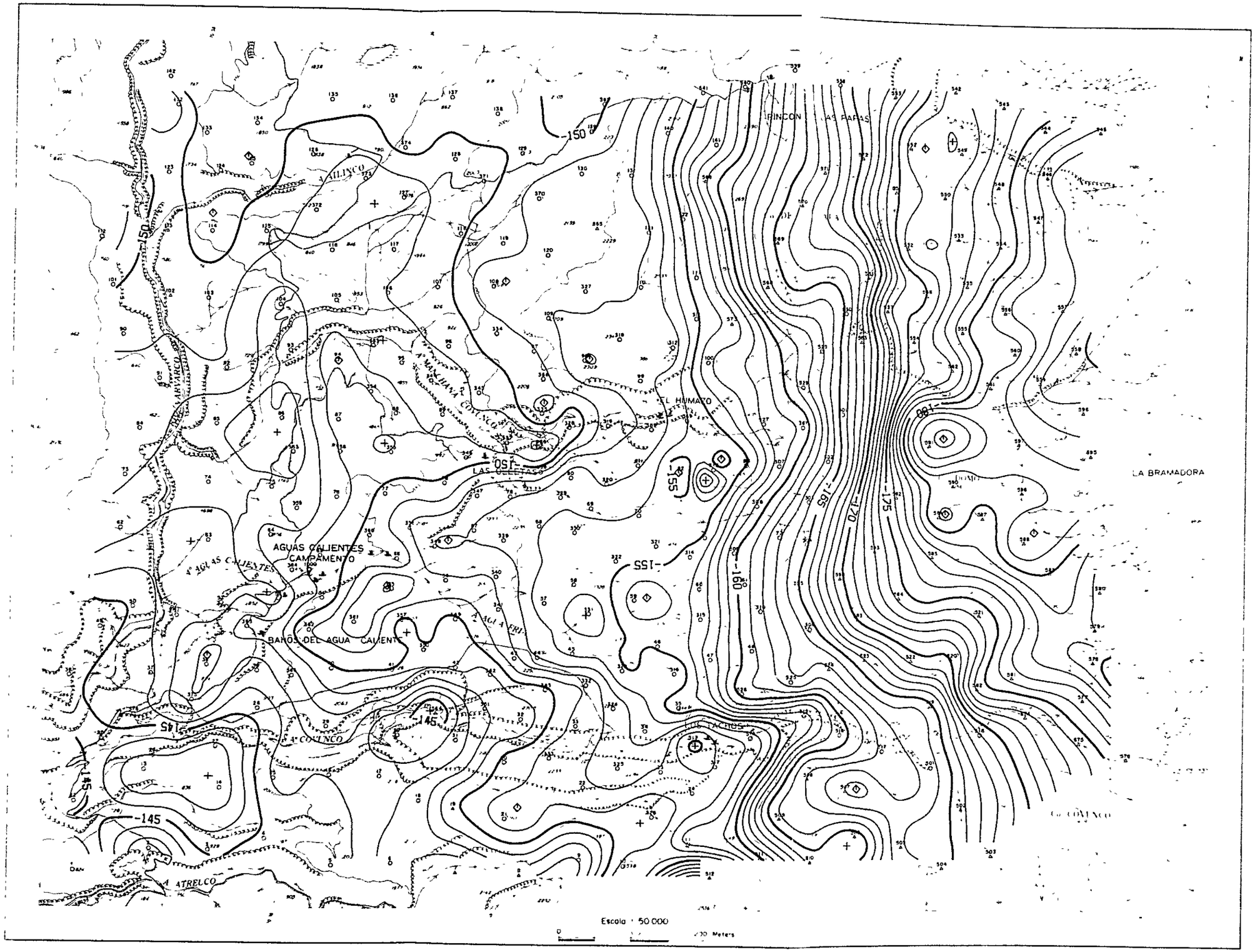

Fig.4-8 Bouguer anomaly map (ρ = 2.00 g/cm^3)

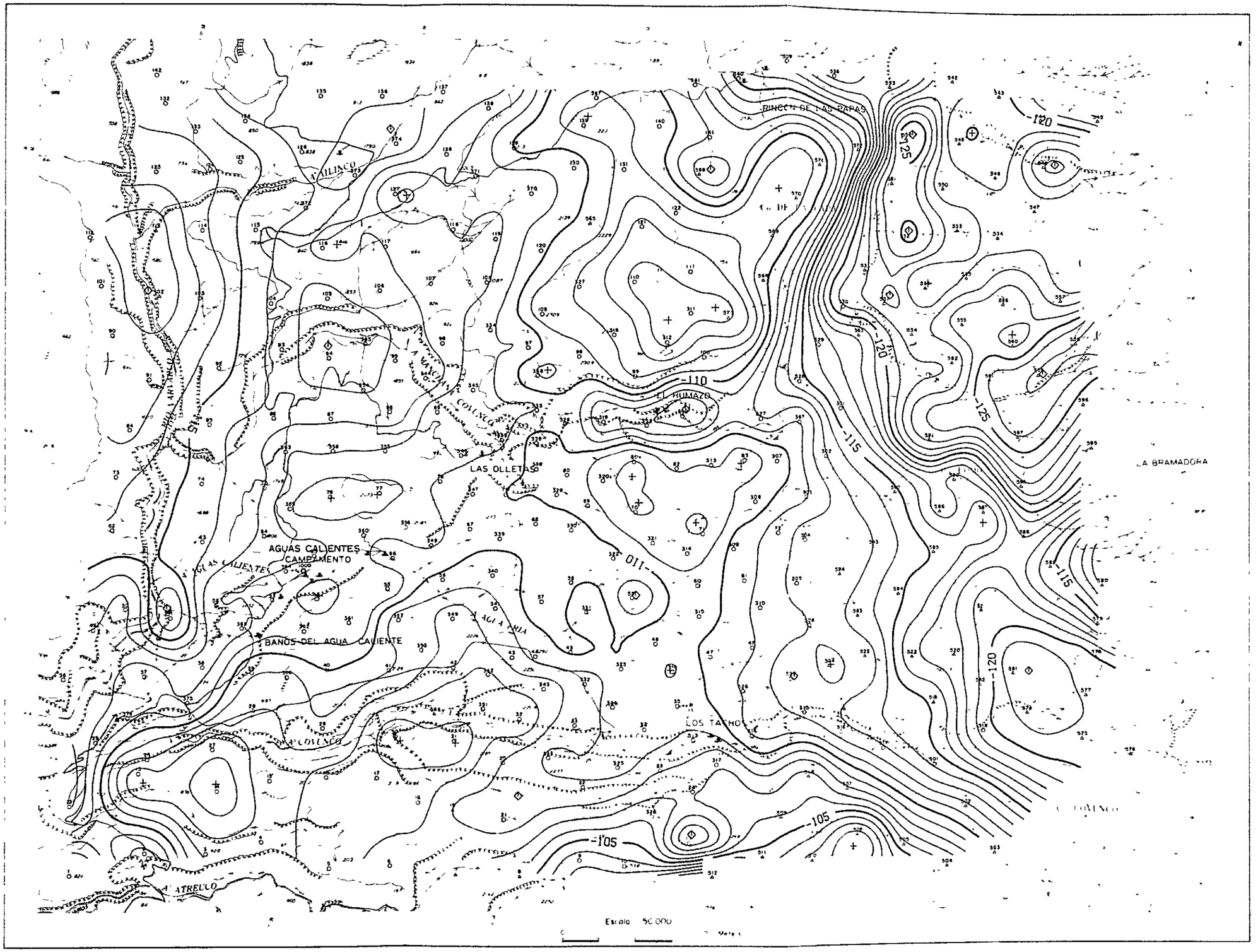

Fig.4-9 Bouguer anomaly map (ρ = 2.50 g/cm^3)

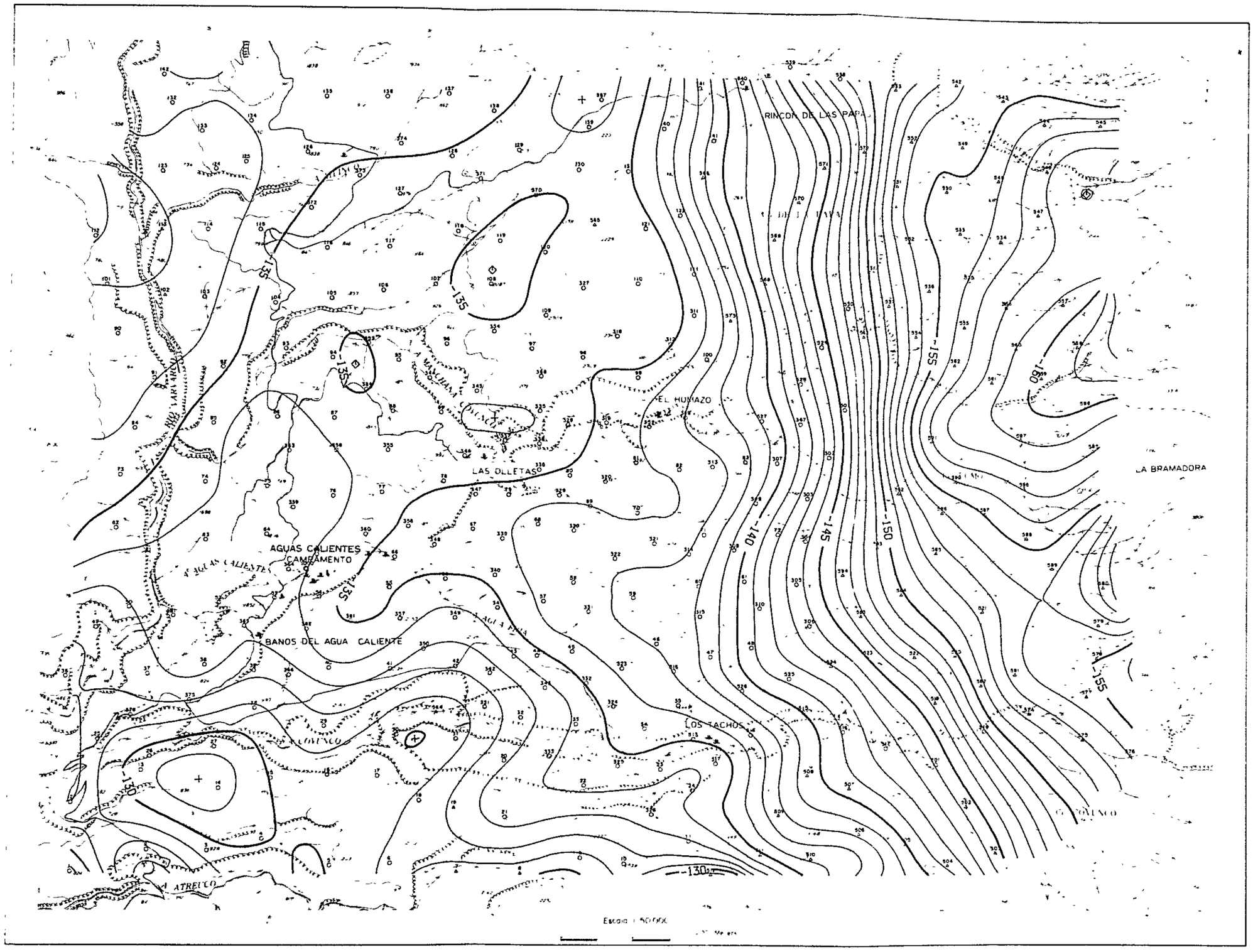

Fig.4-10 Long-wave Bouguer anomaly map (ρ = 2.30 g/cm^3)

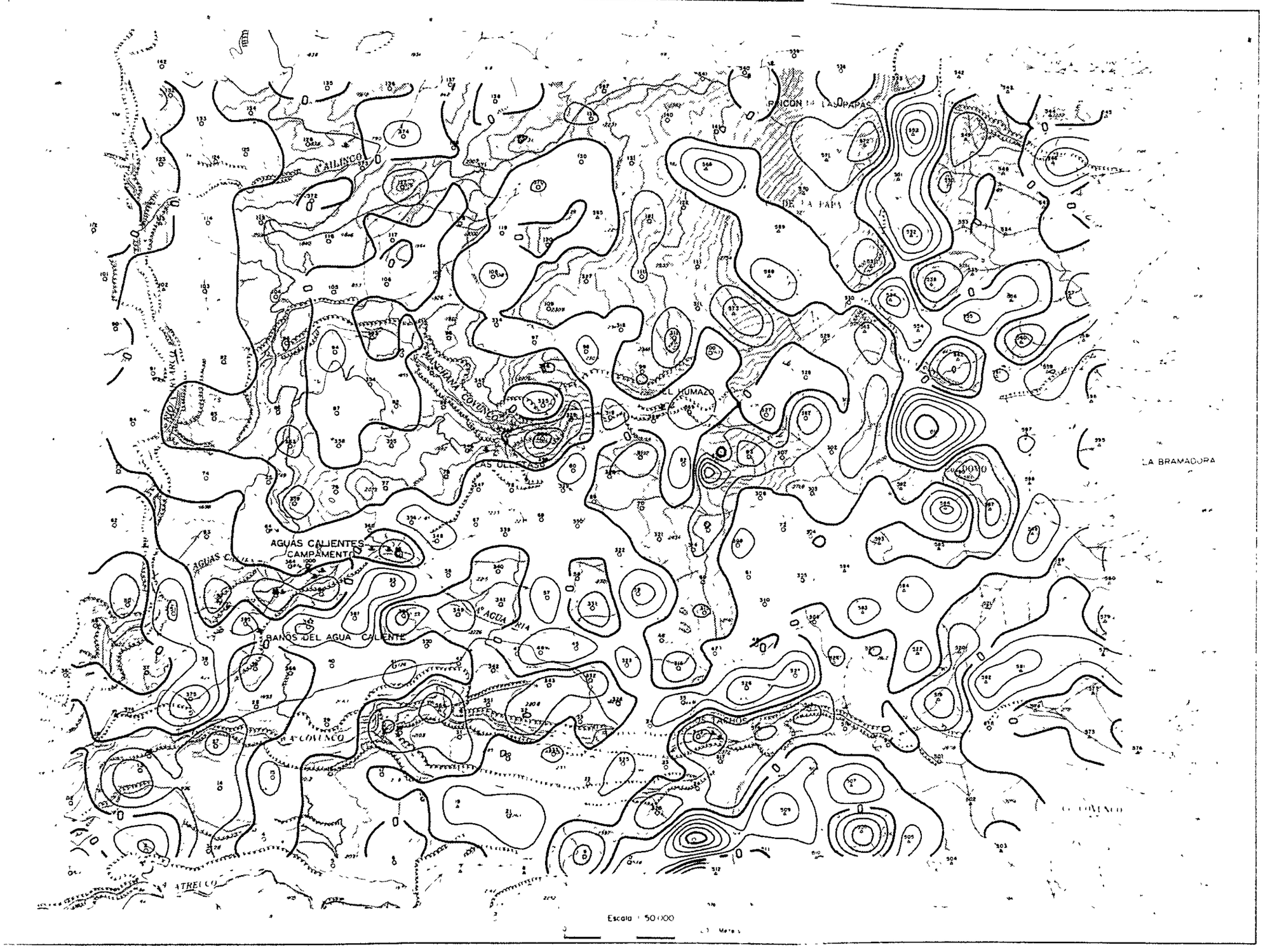

Fig.4-11 Short-wave Bouguer anomaly map (ρ = 2.30 g/cm^3)

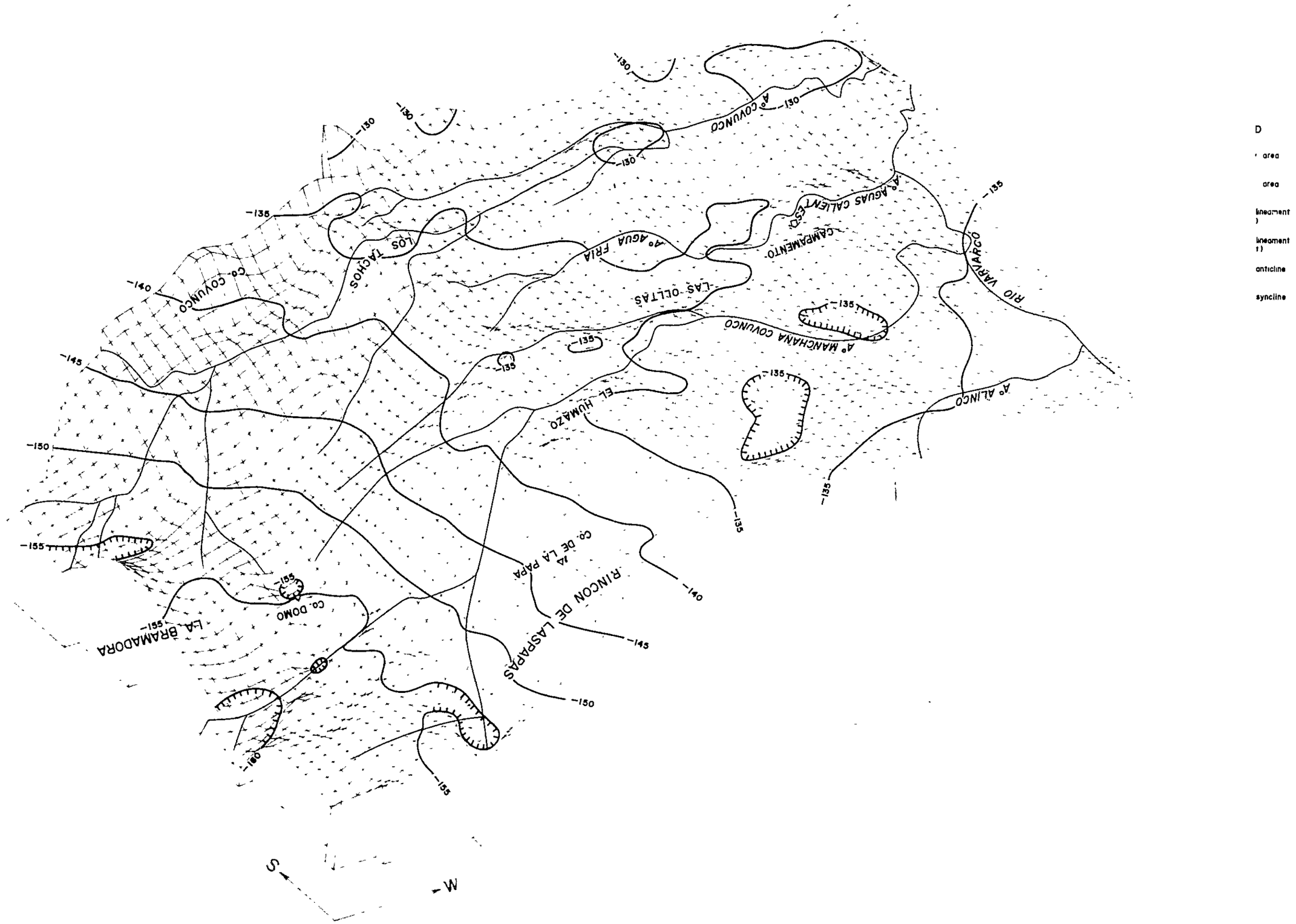

Fig.4-12 Three-dimensional image of Bouguer anomaly map (ρ = 2.30 g/cm^3)

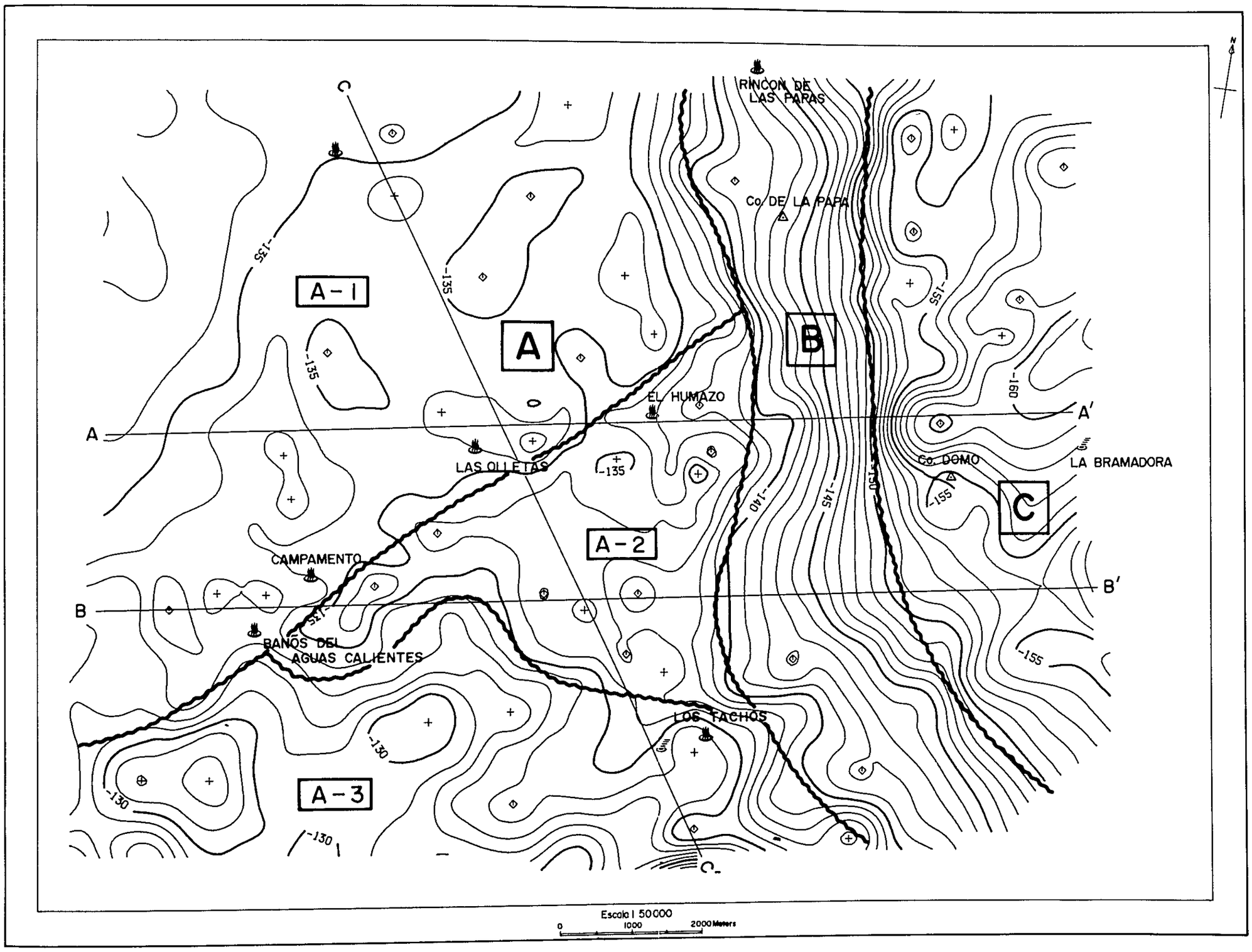

Fig.4-13 Zoning of Bouguer anomaly map

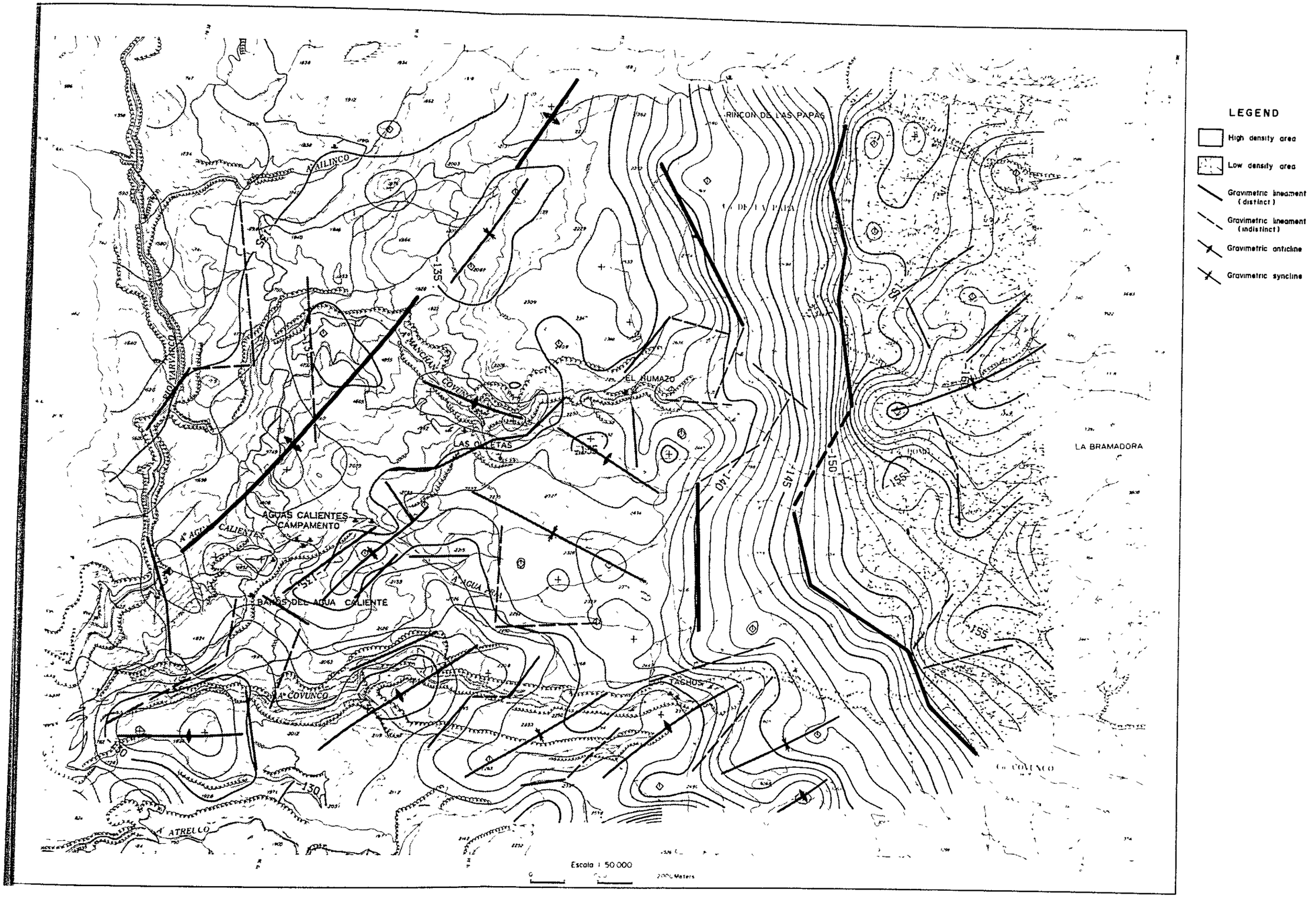

Fig.4-14 Gravimetric interpretation map

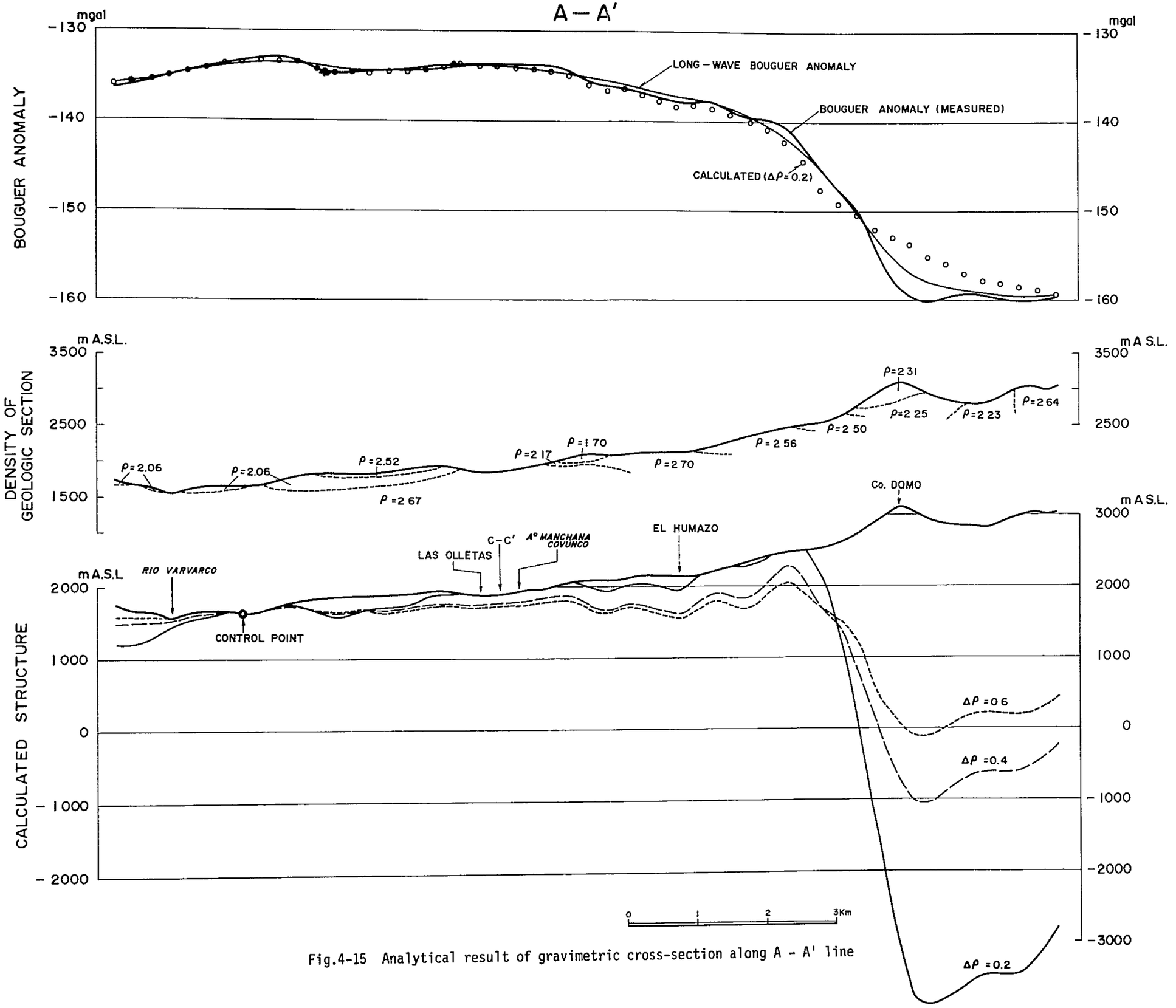

Fig.4-15 Analytical result of gravimetric cross-section along A - A' line

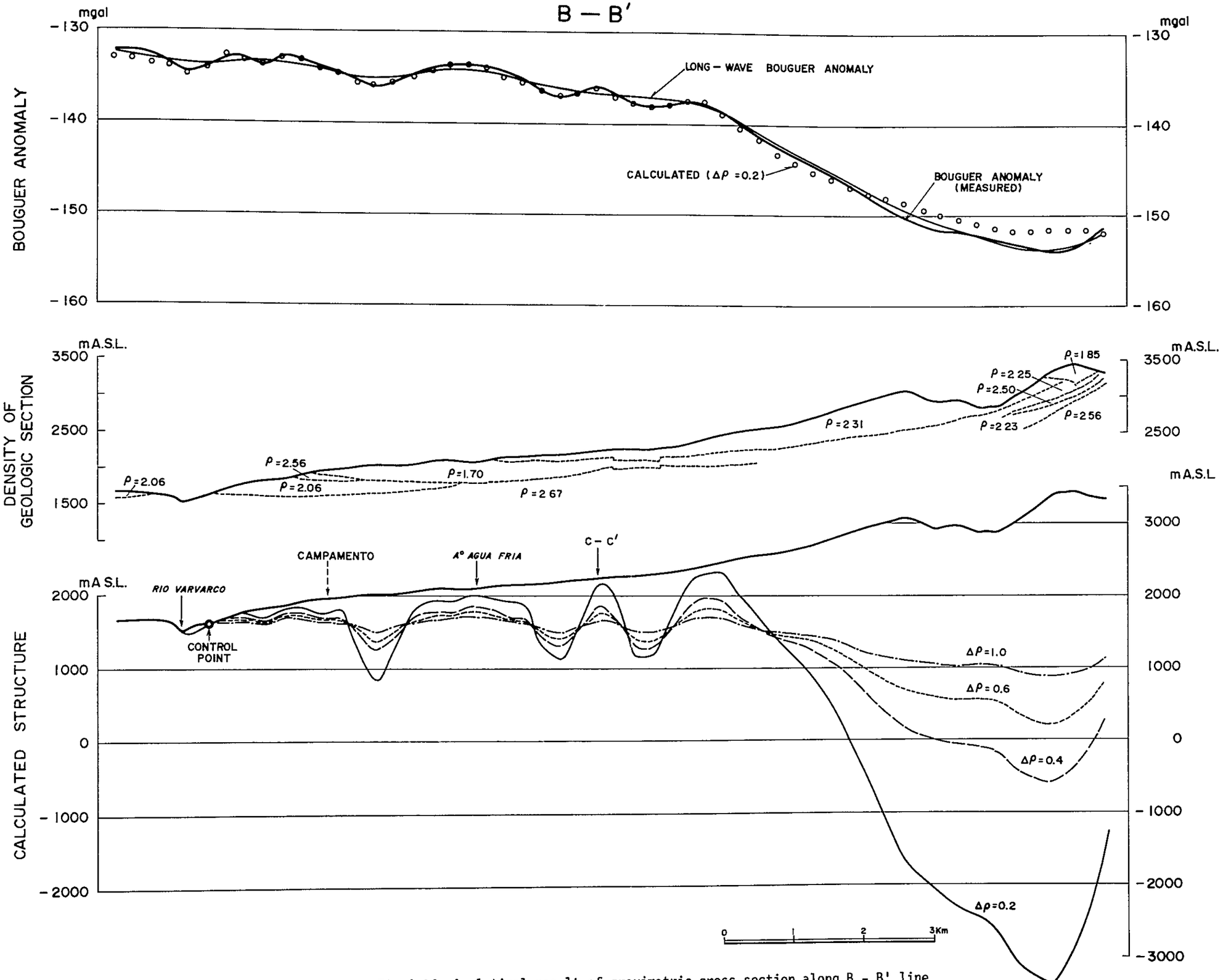

Fig.4-16 Analytical result of gravimetric cross-section along B - B' line

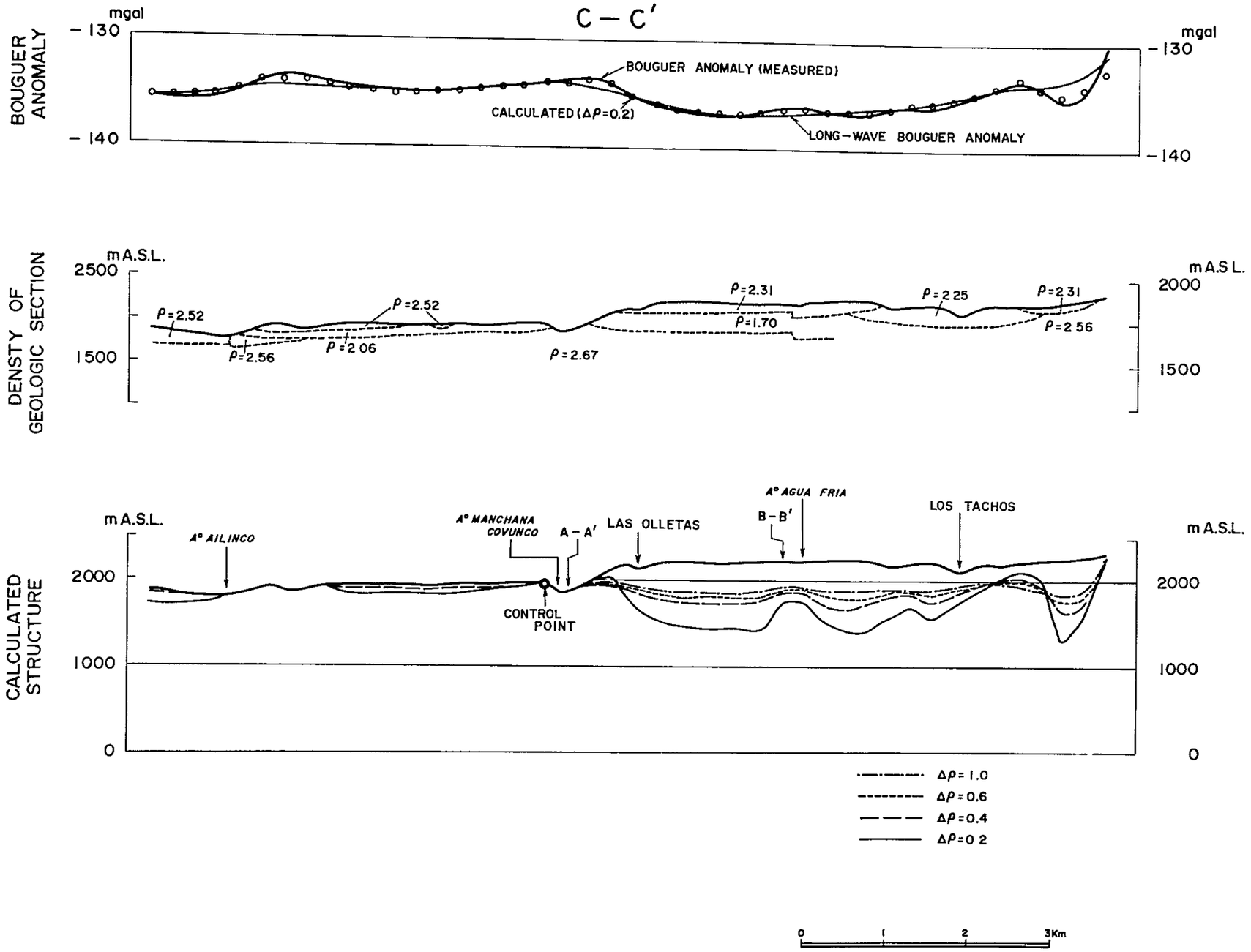

Fig.4-17 Analytical result of gravimetric cross-section along C - C' line

5. 調 査 地 域 の 熱 構 造

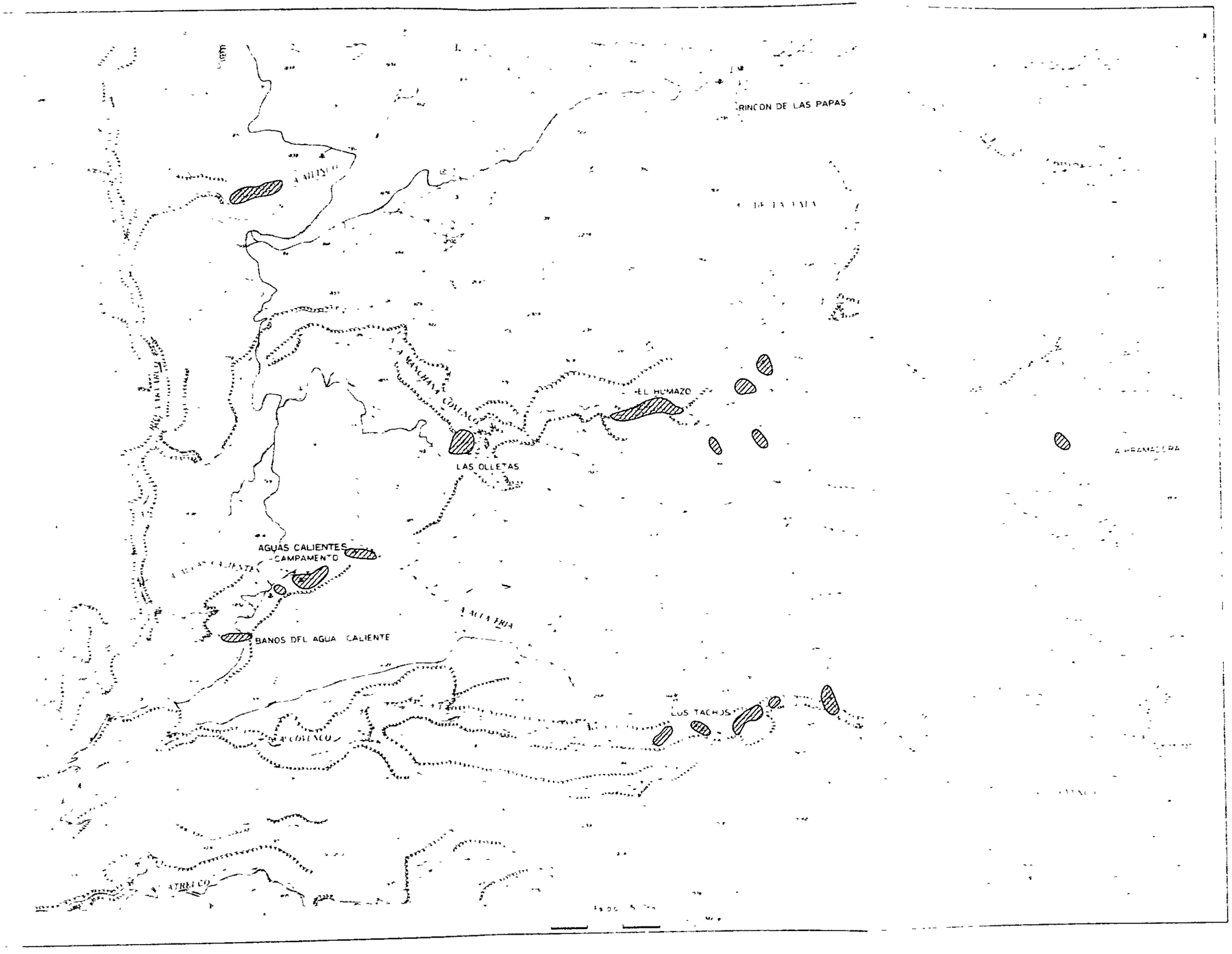

Fig.5-1 Location map of alteration zones

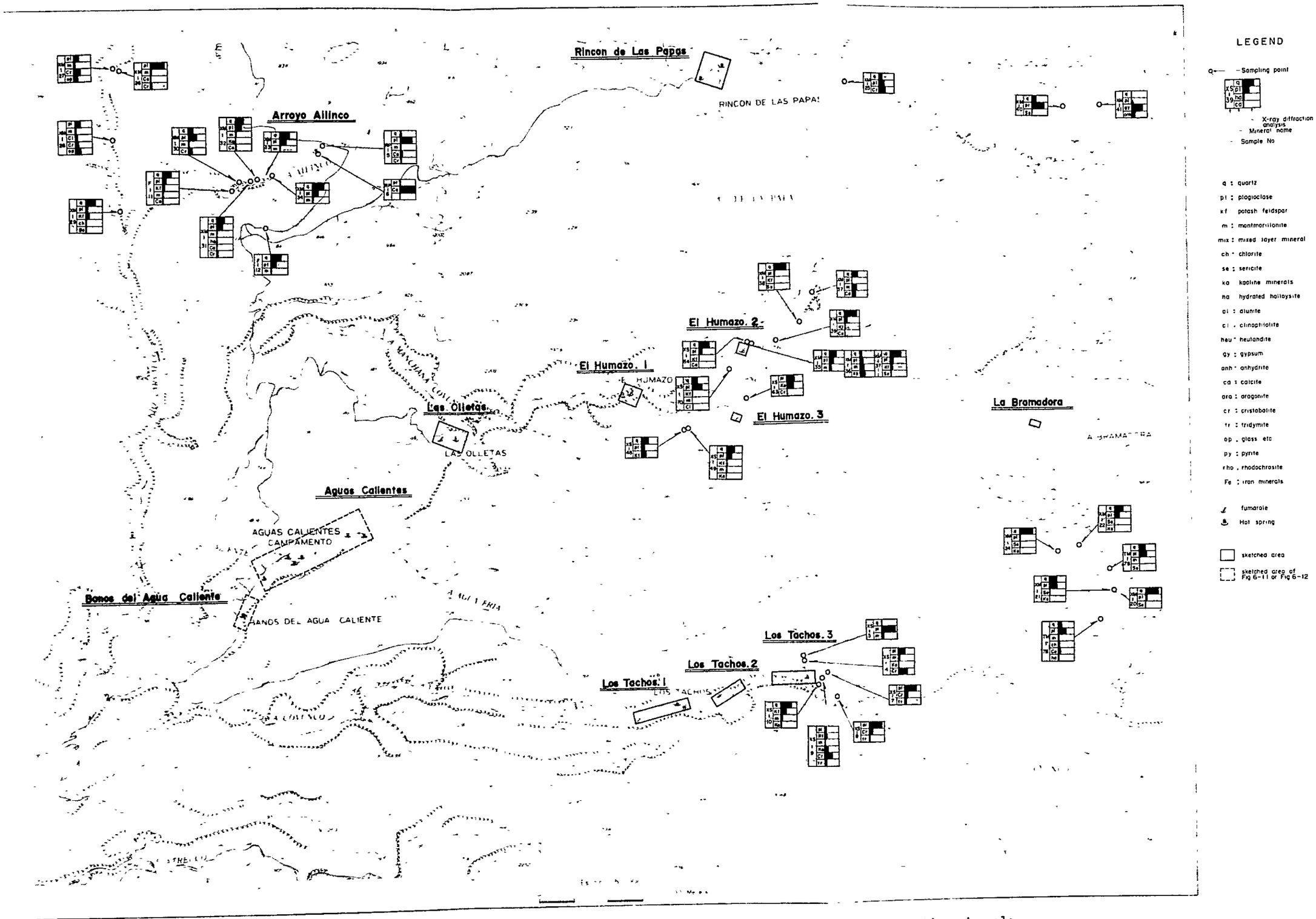

Fig.5-2 Sketched areas of alteration zone and regional distributions of alteration minerals

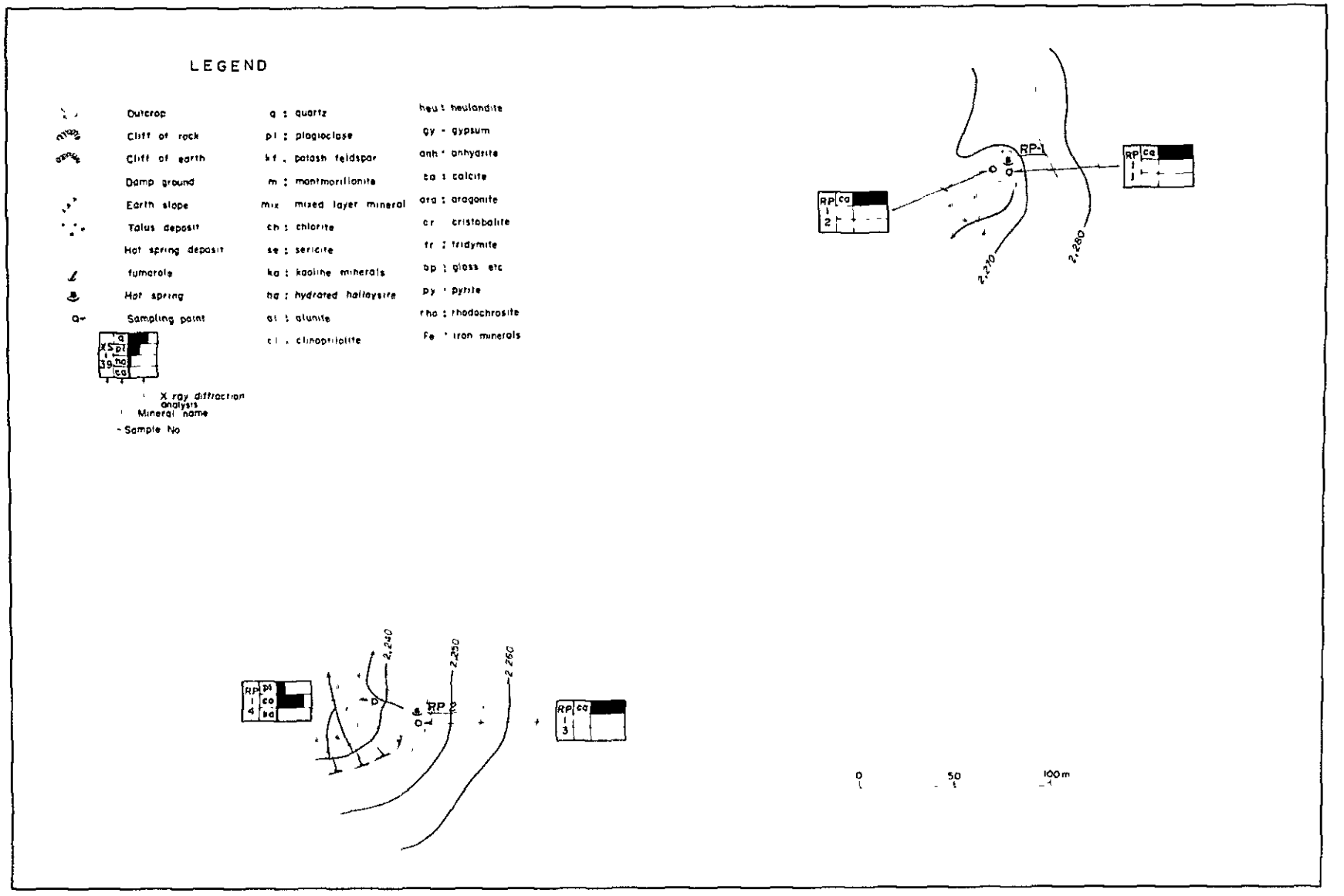

Fig.5-3 Sketch of alteration zone and diagrams of alteration minerals
(1) Rincon de Las Papas

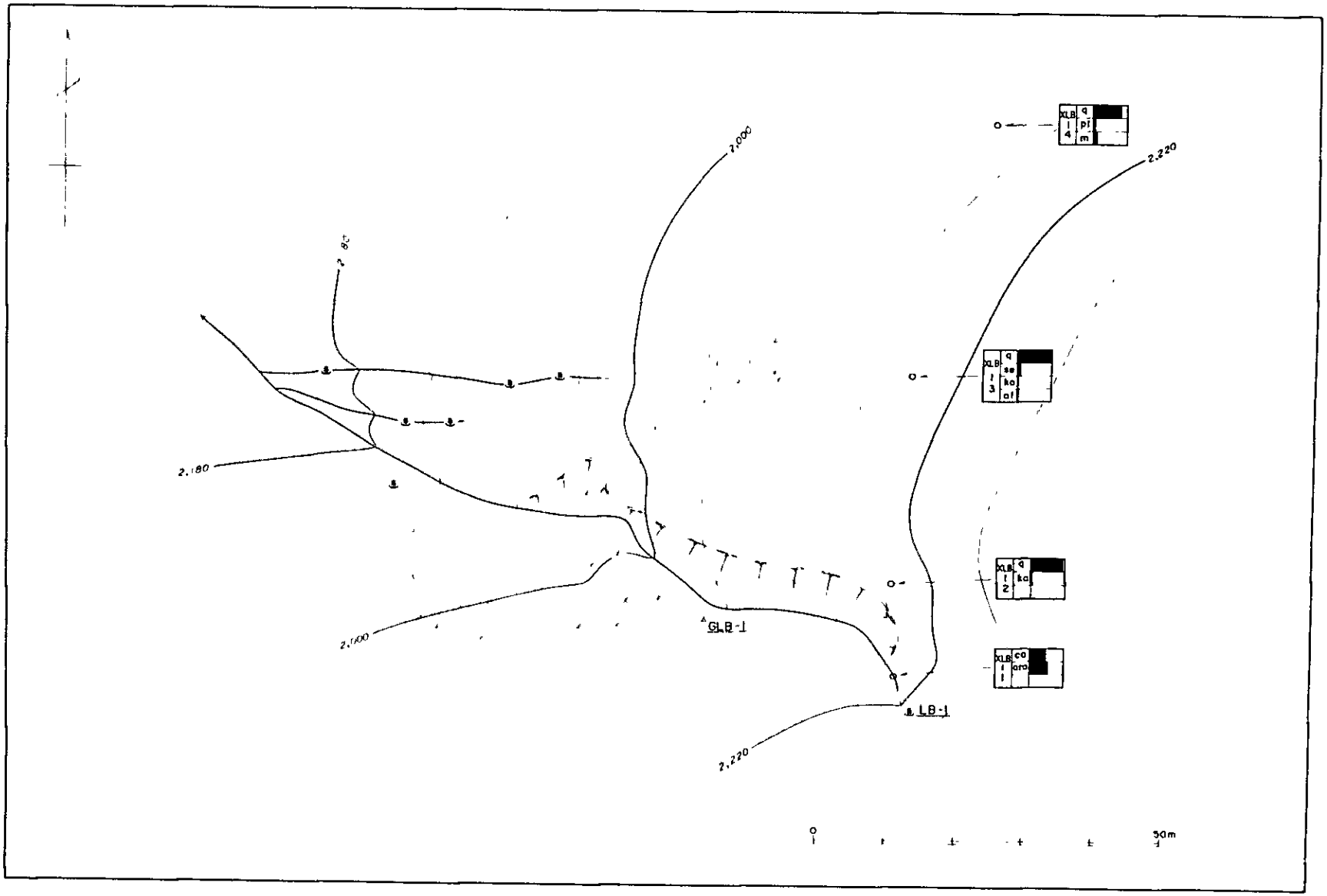

Fig.5-4 Sketch of alteration zone and diagrams of alteration minerals
(2) La Bramadora

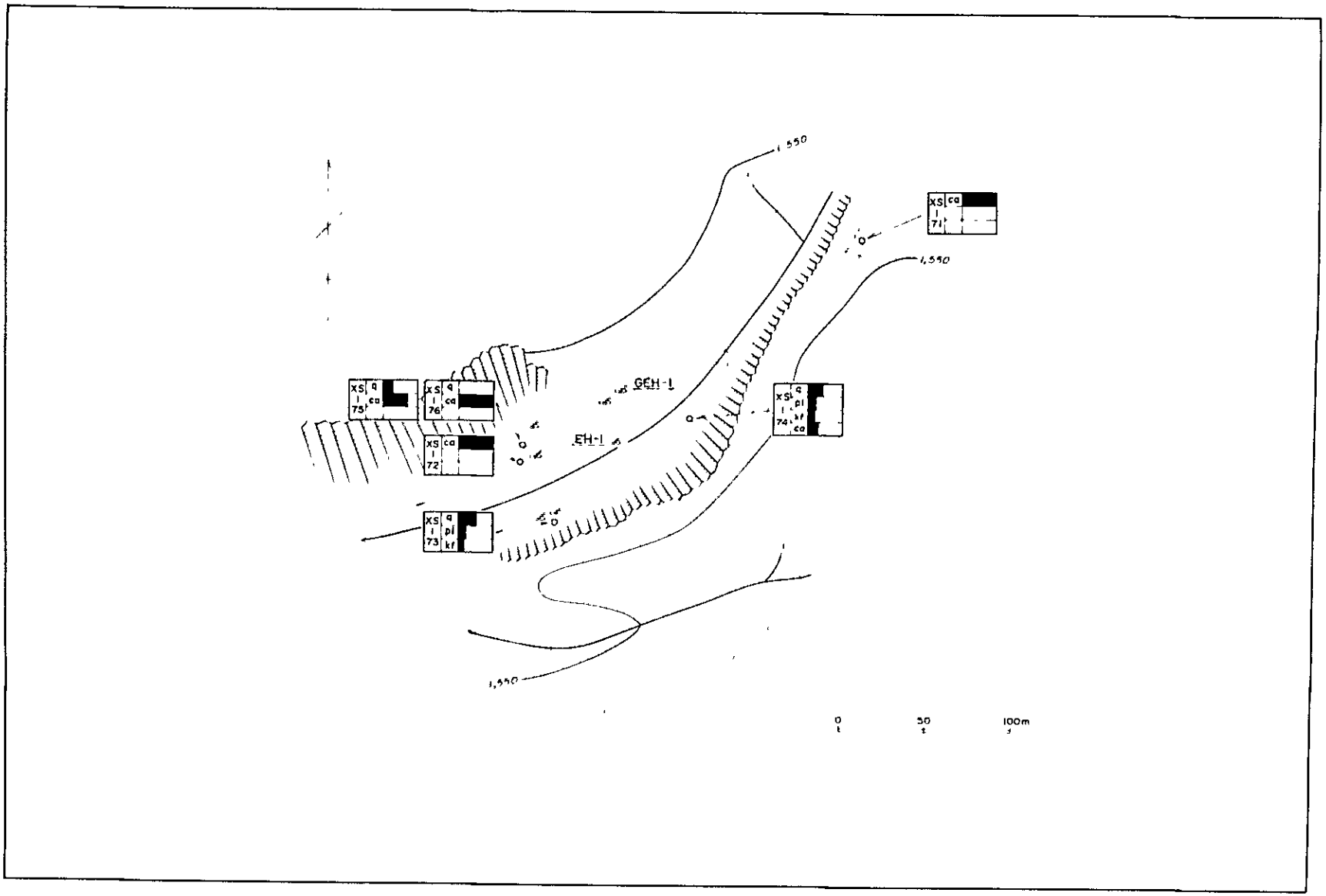

Fig.5-5 Sketch of alteration zone and diagrams of alteration minerals
(3) El Humazo - 1

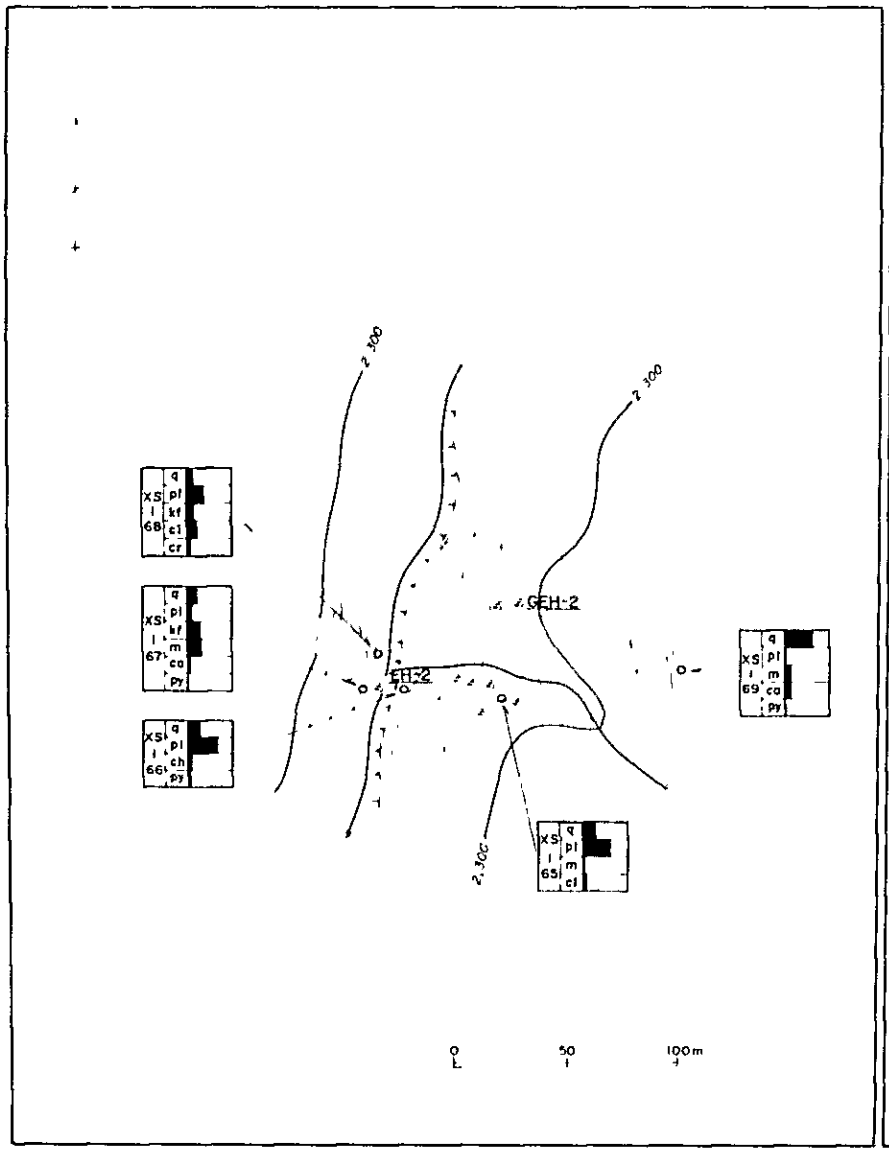

Fig.5-6 Sketch of alteration zone and diagrams of alteration minerals (4) El Humazo - 2

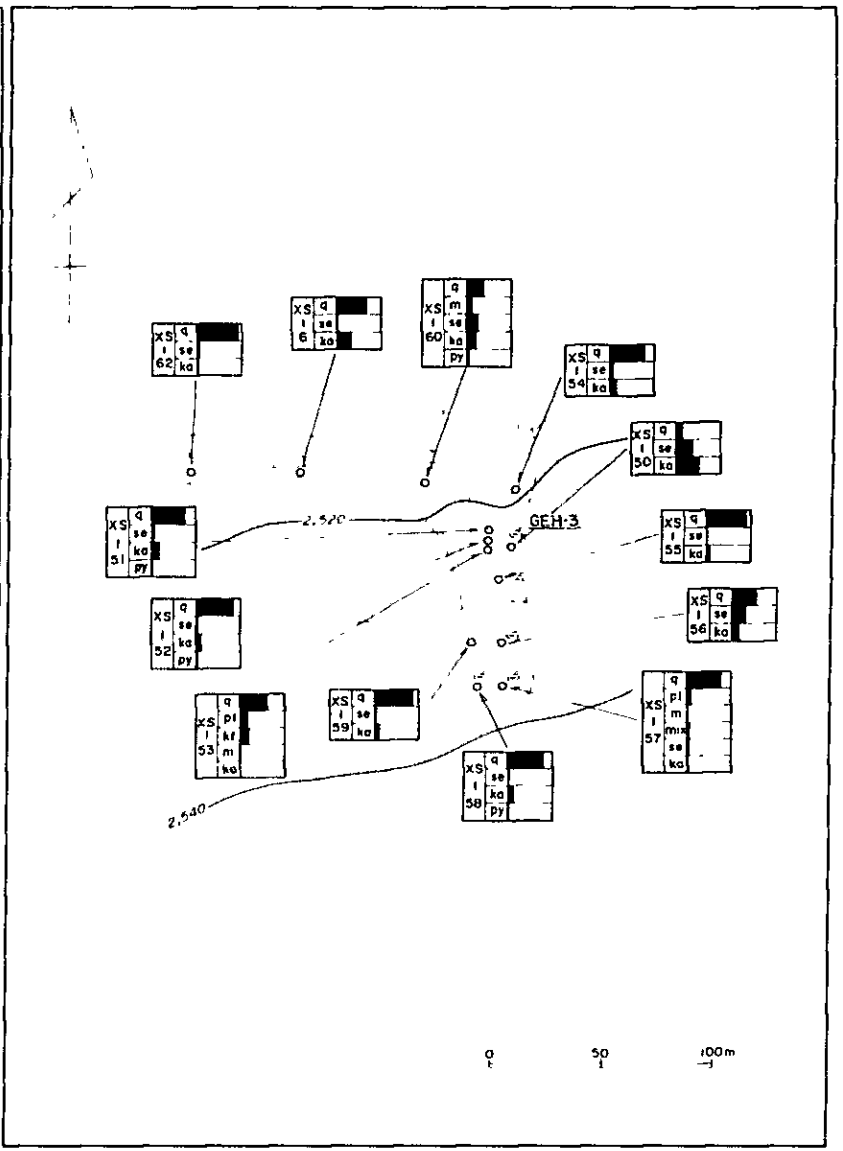

Fig.5-7 Sketch of alteration zone and diagrams of alteration minerals (5) El Humazo - 3

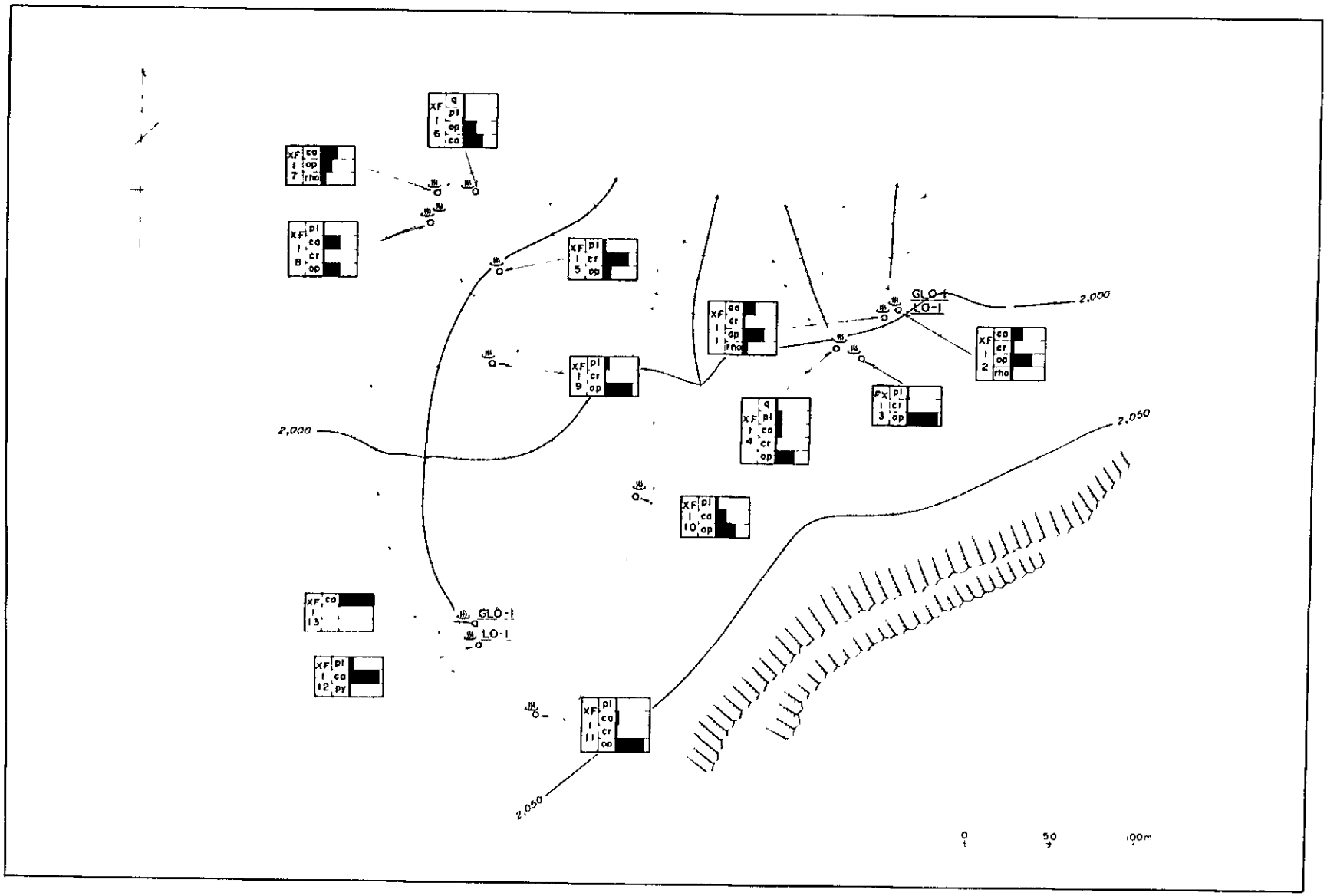

Fig.5-8 Sketch of alteration zone and diagrams of alteration minerals
(6) Las Olletas

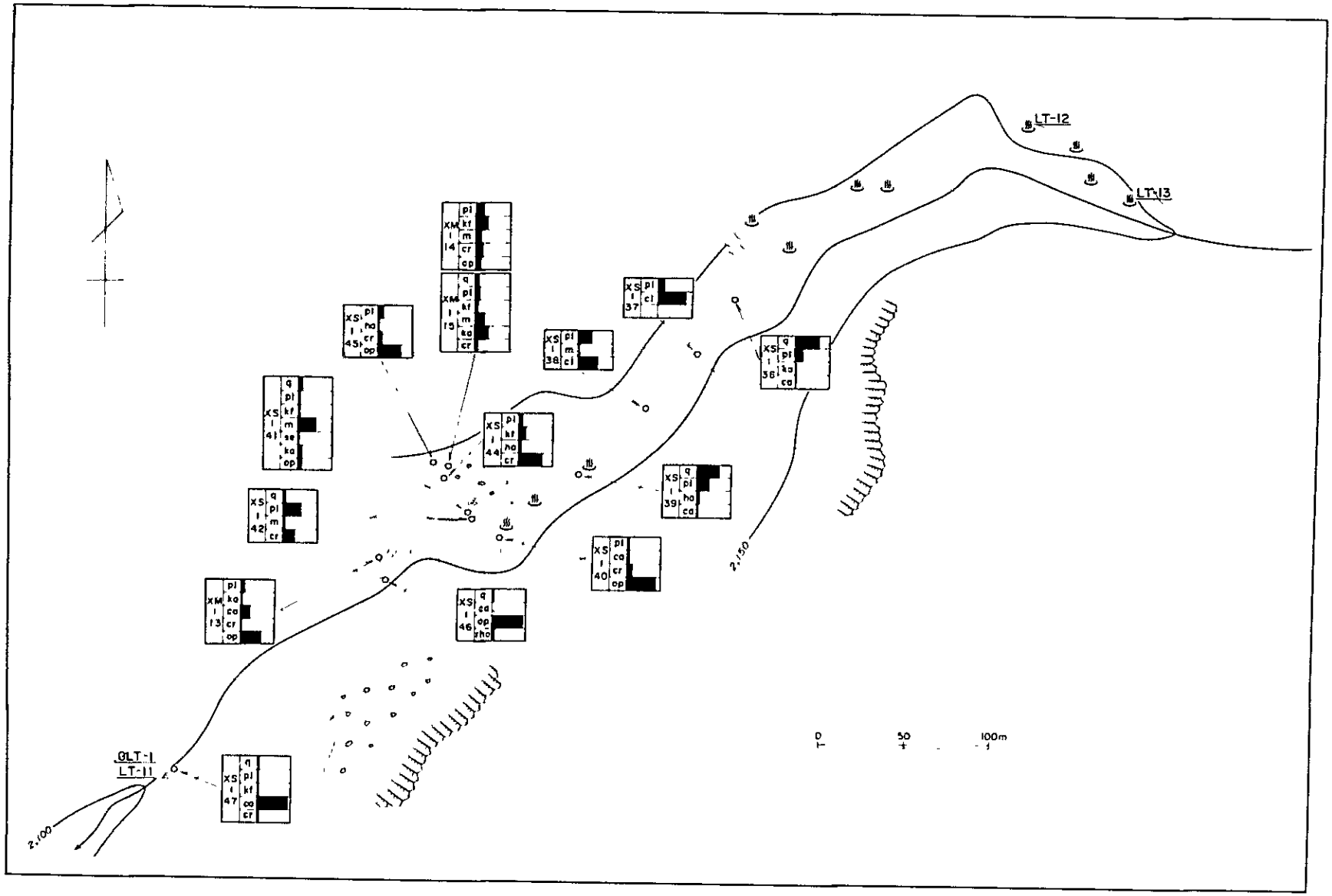

Fig.5-9 Sketch of alteration zone and diagrams of alteration minerals
(7) Los Tachos - 1

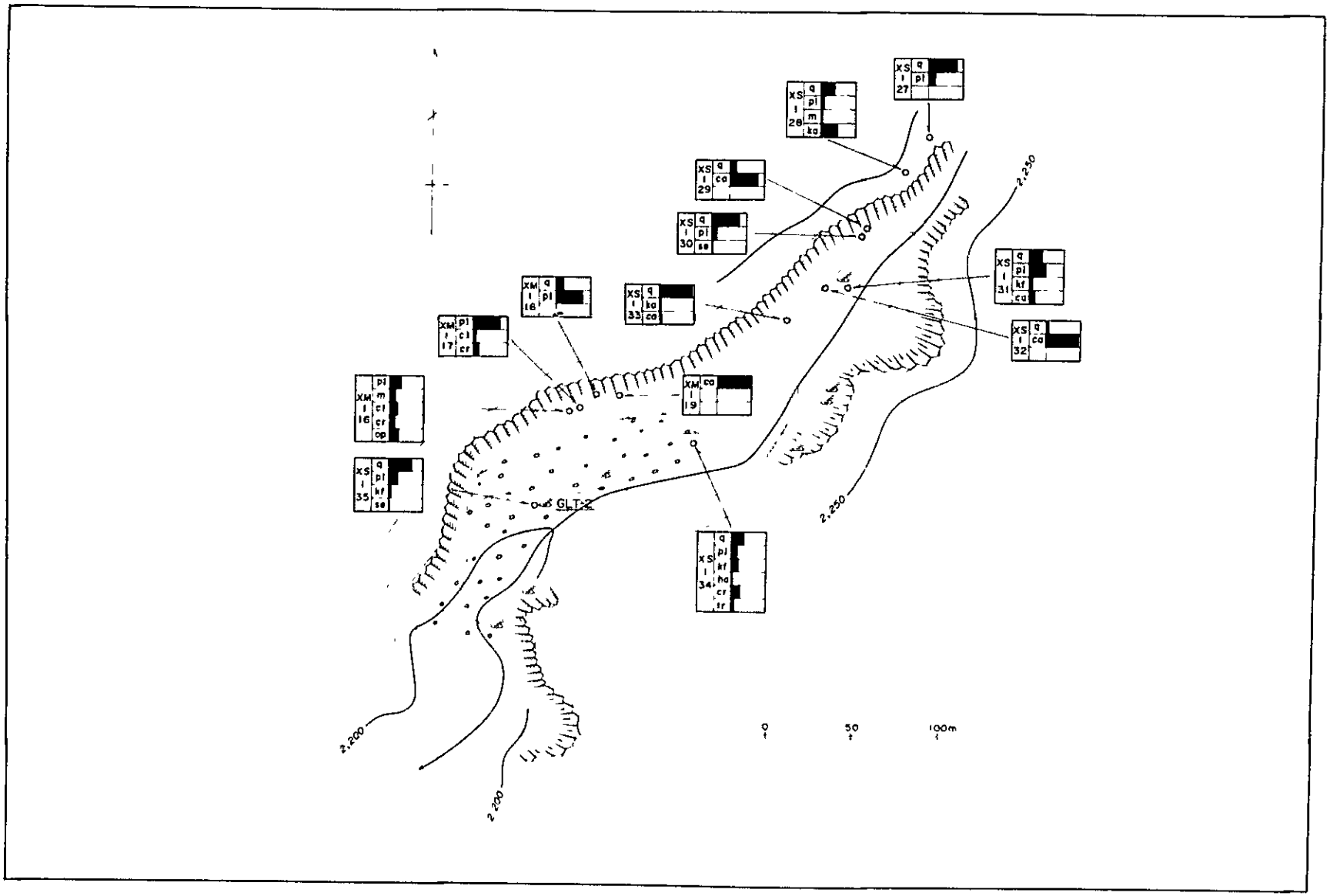

Fig.5-10 Sketch of alteration zone and diagrams of alteration minerals
(8) Los Tachos - 2

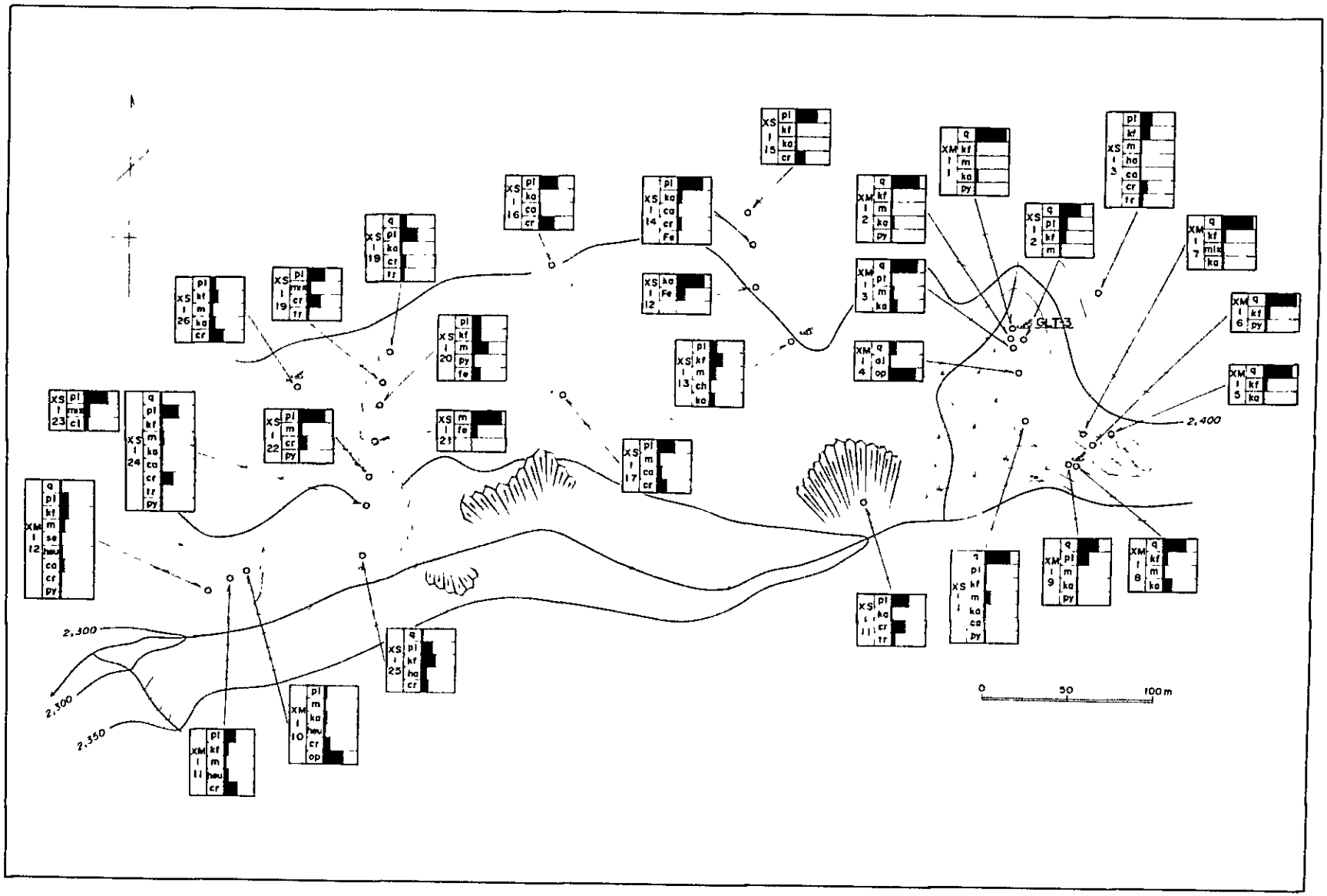

Fig.5-11 Sketch of alteration zone and diagrams of alteration minerals
(9) Los Tachos - 3

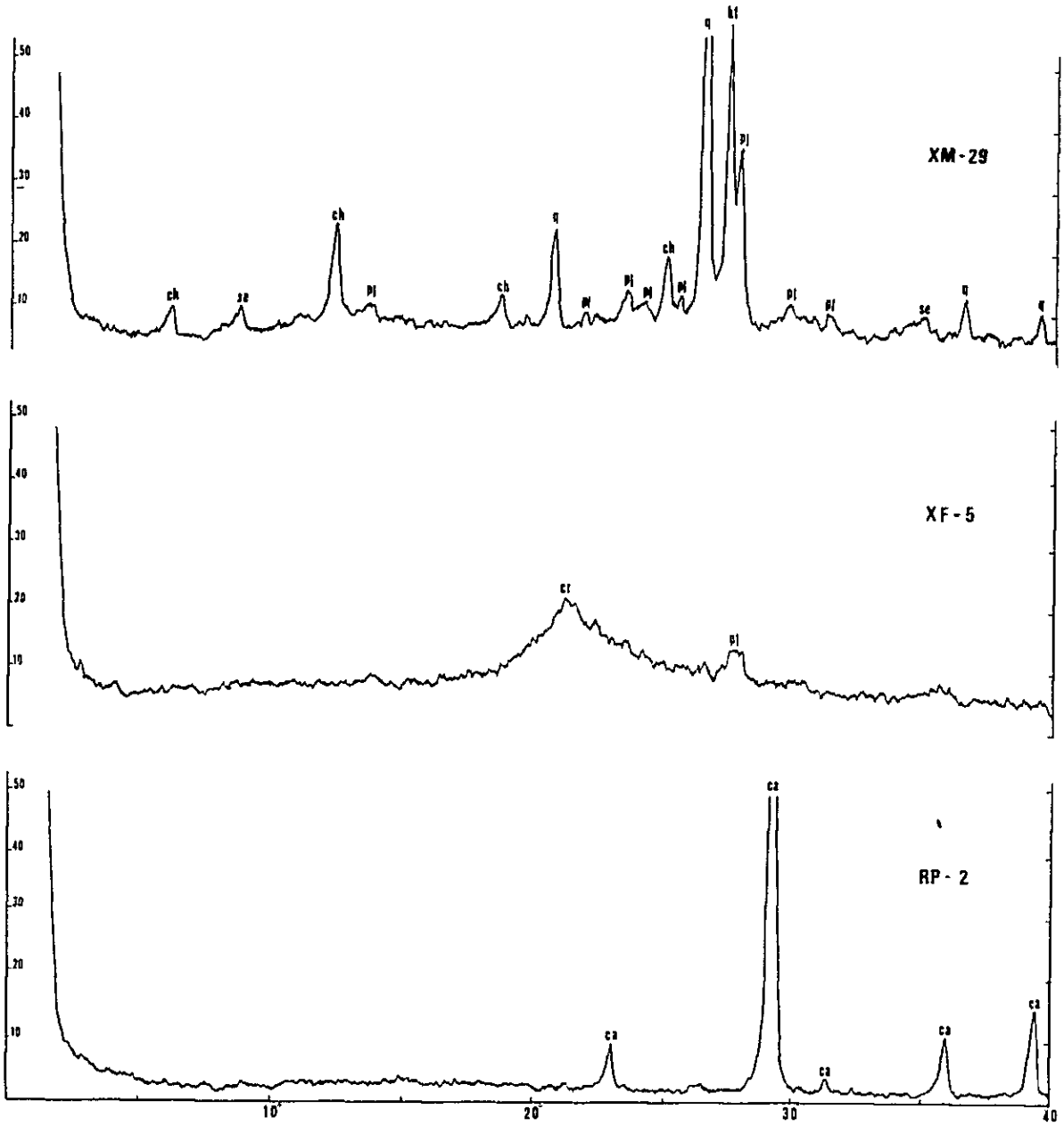

LEGEND

m:	montmorillonite	q:	quartz
ch:	chlorite	kf:	potash feldspar
se:	sericite	pl:	plagioclase
k:	kaolinite	ca:	calcite
ka:	hydrated halloysite	cr:	cristobalite

Fig. 5-12 (1) Typical charts of X-ray diffraction analysis

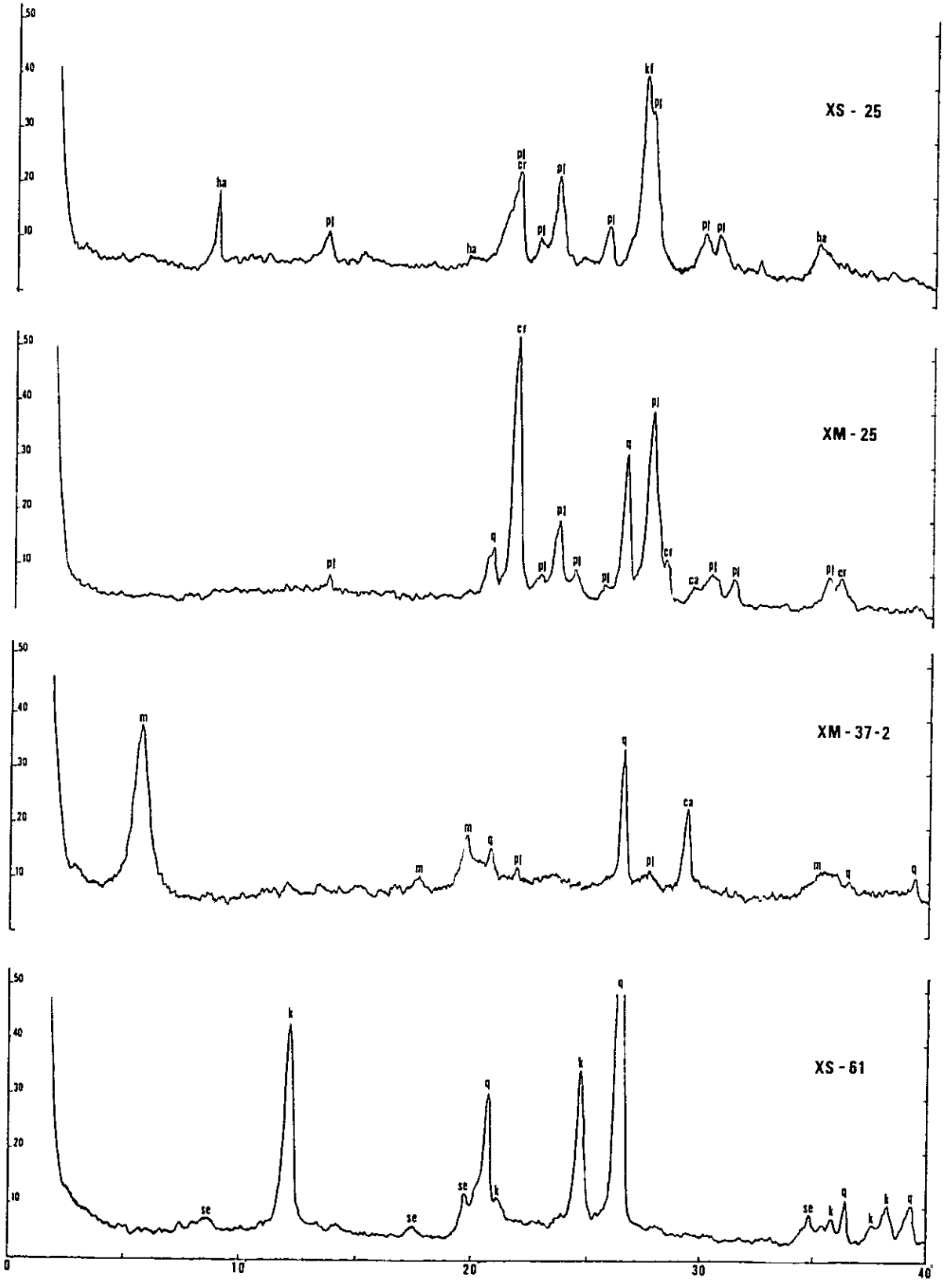

LEGEND

m:	montmorillonite	q:	quartz
ch:	chlorite	kf:	potash feldspar
se:	sericite	pl:	plagioclase
k:	kaolinite	ca:	calcite
ha:	hydrated halloysite	cr:	cristobalite

Fig. 5-12 (2) Typical charts of X-ray diffraction analysis

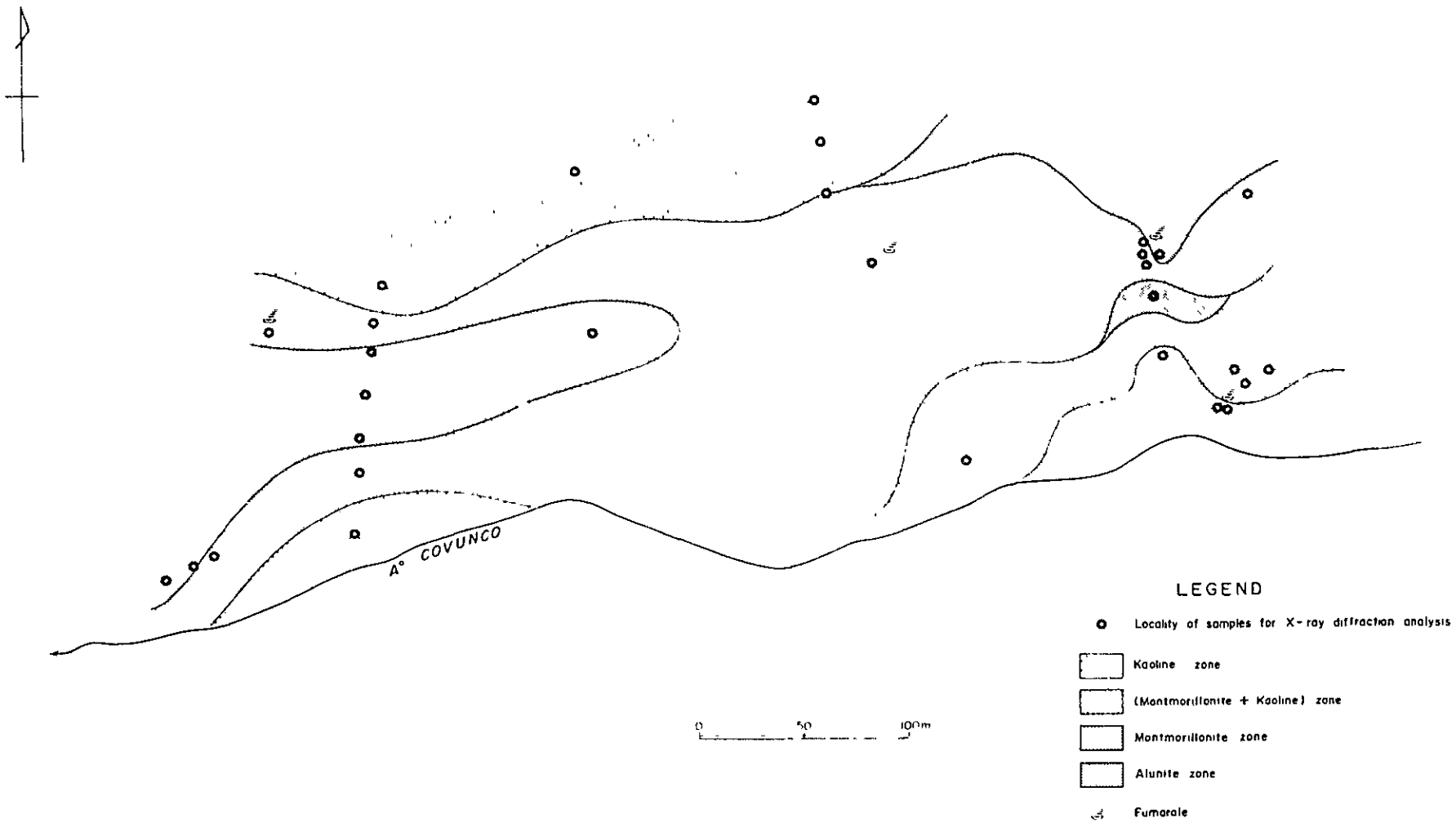

Fig.5-13 Alteration zoning map of Los Tachos - 3

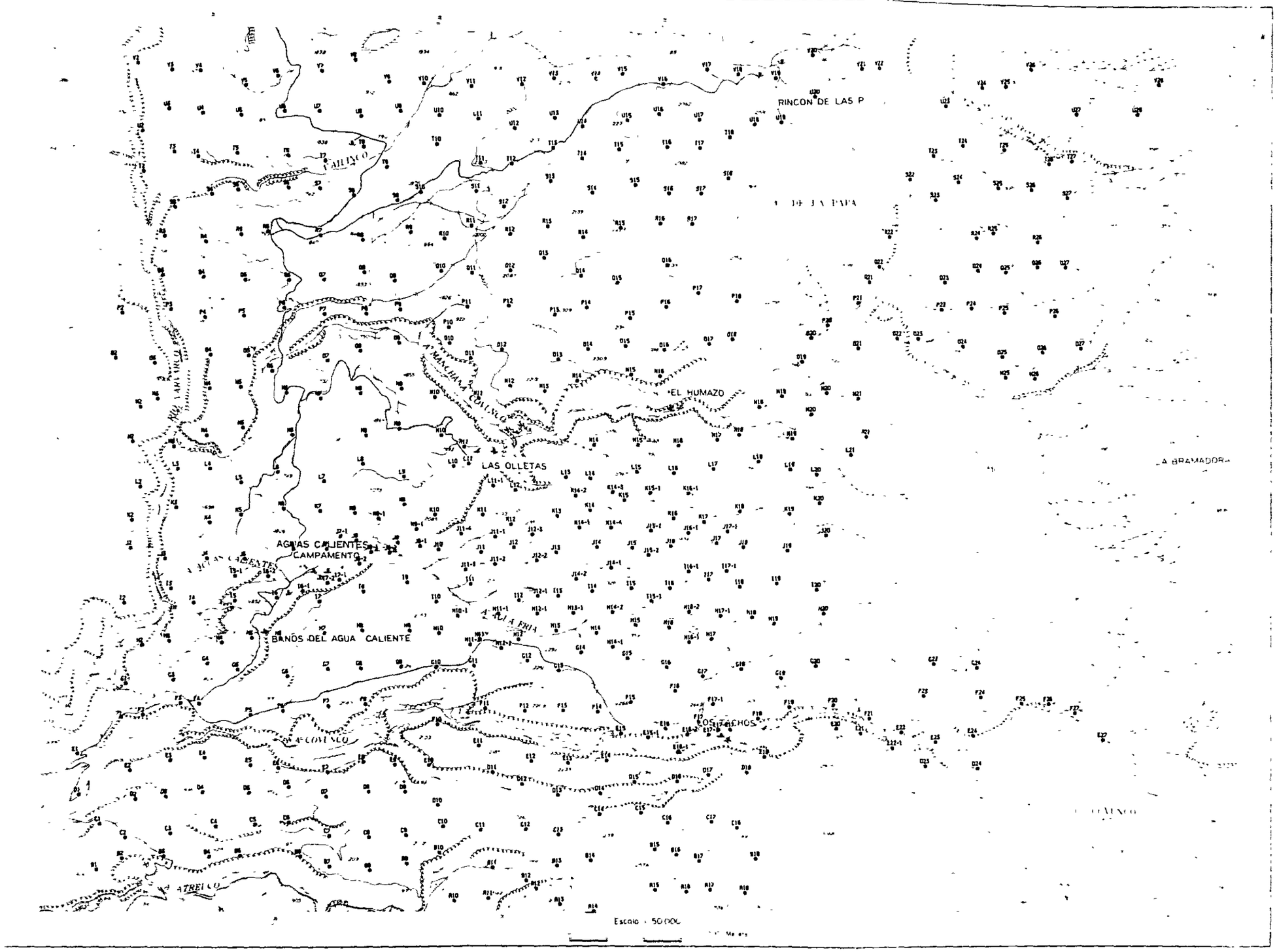

Fig.5-14 Location map of test holes at 1 meter depth

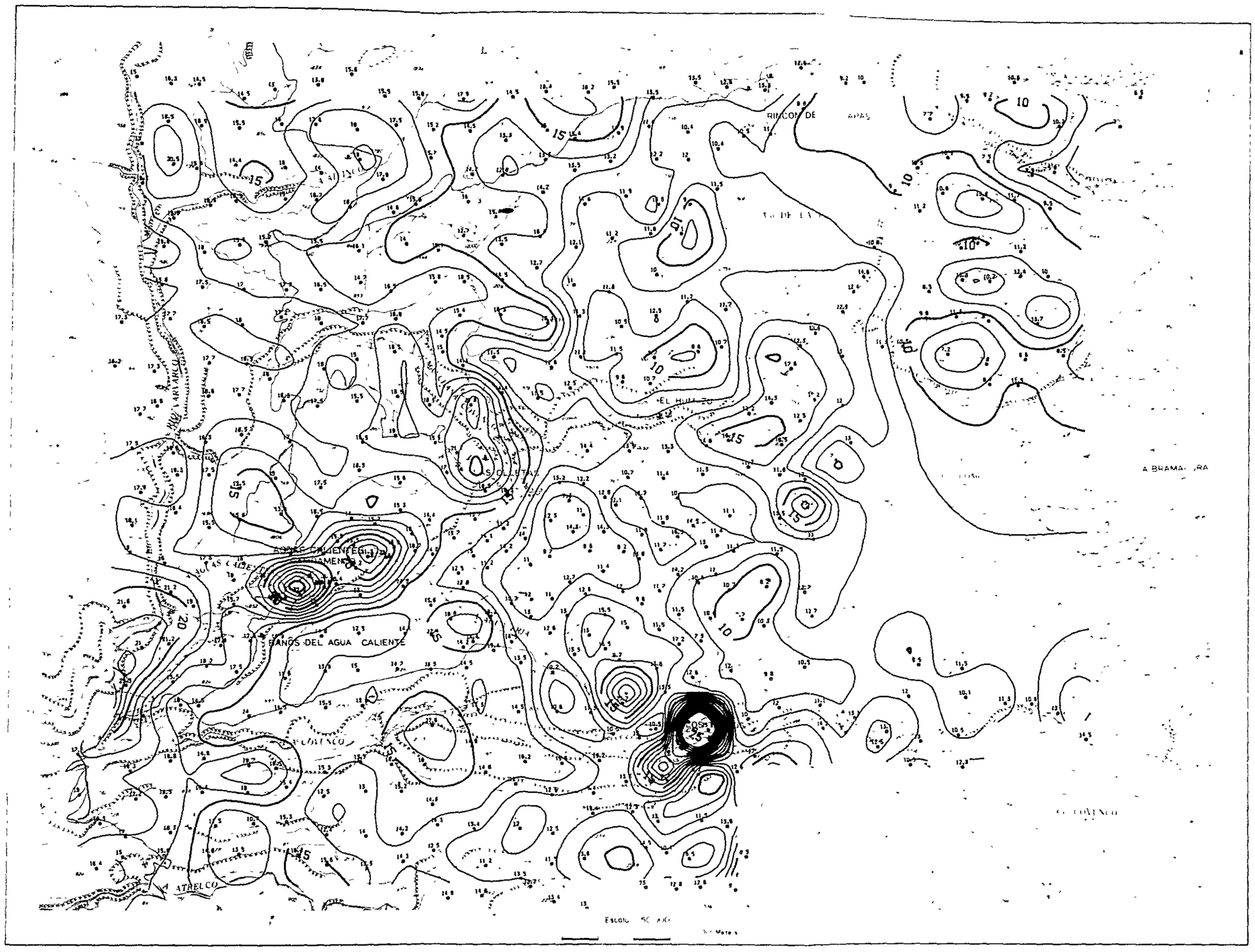

Fig.5-15 Distribution map of ground temperature at 1 meter depth

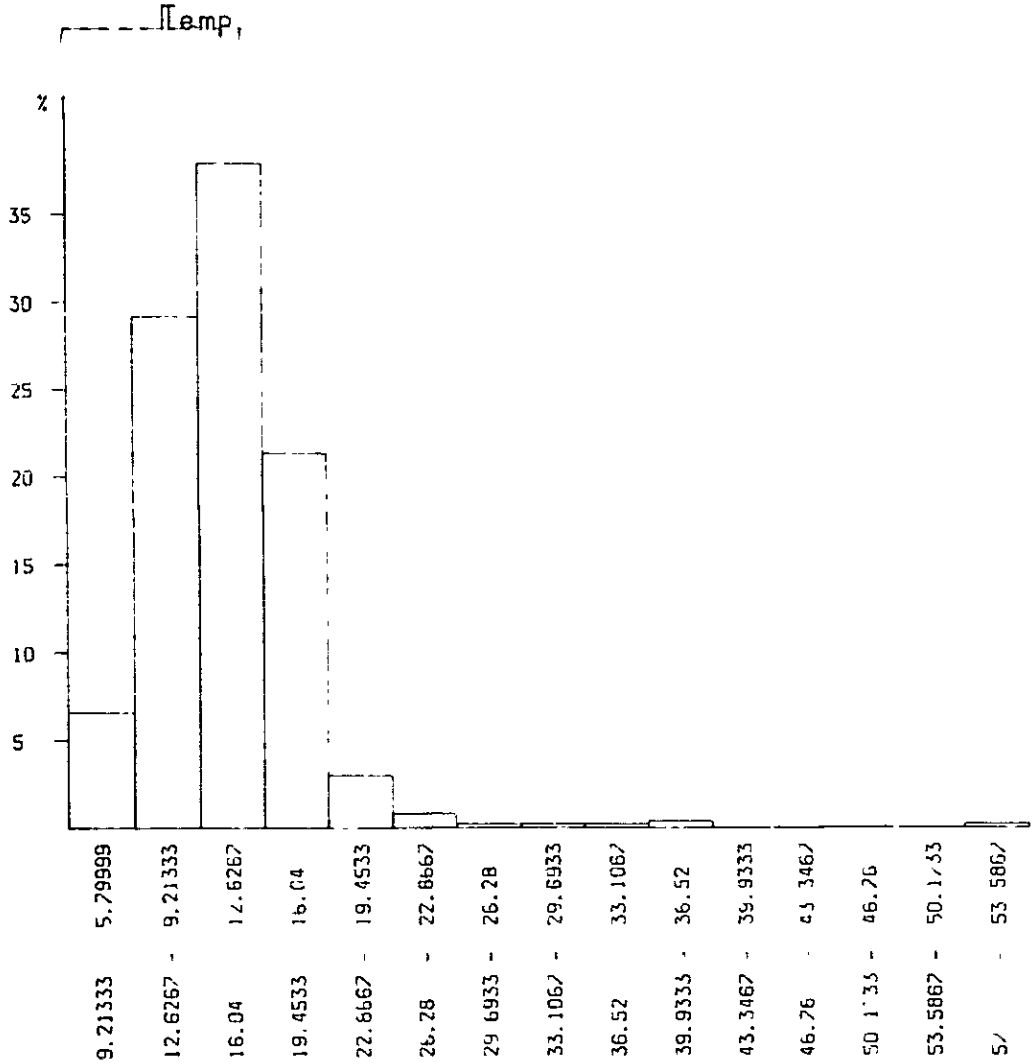

Fig.5-16 Frequency distribution of ground temperature at 1 meter depth

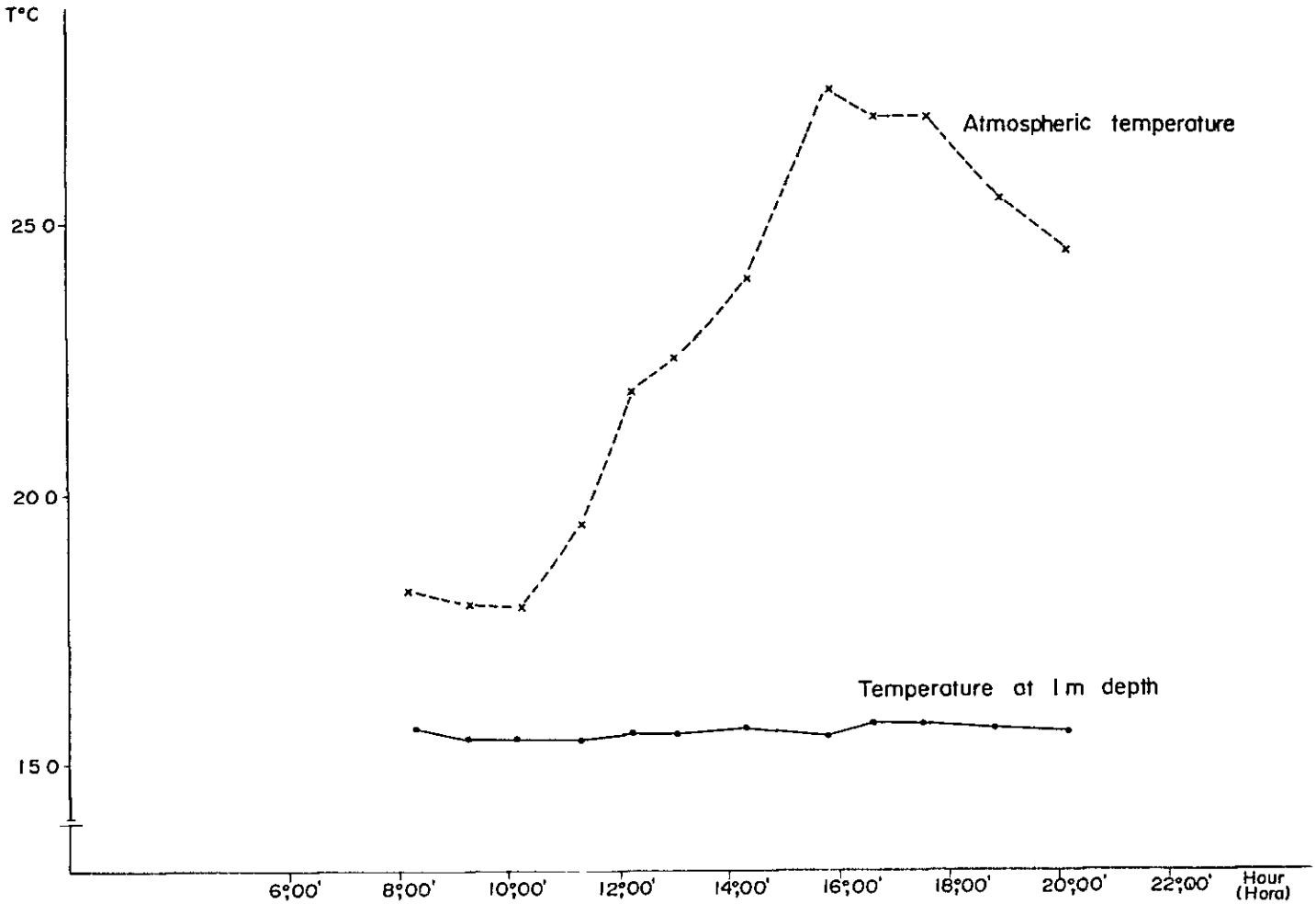

Fig.5-17 Diurnal variation of atmospheric and ground temperatures

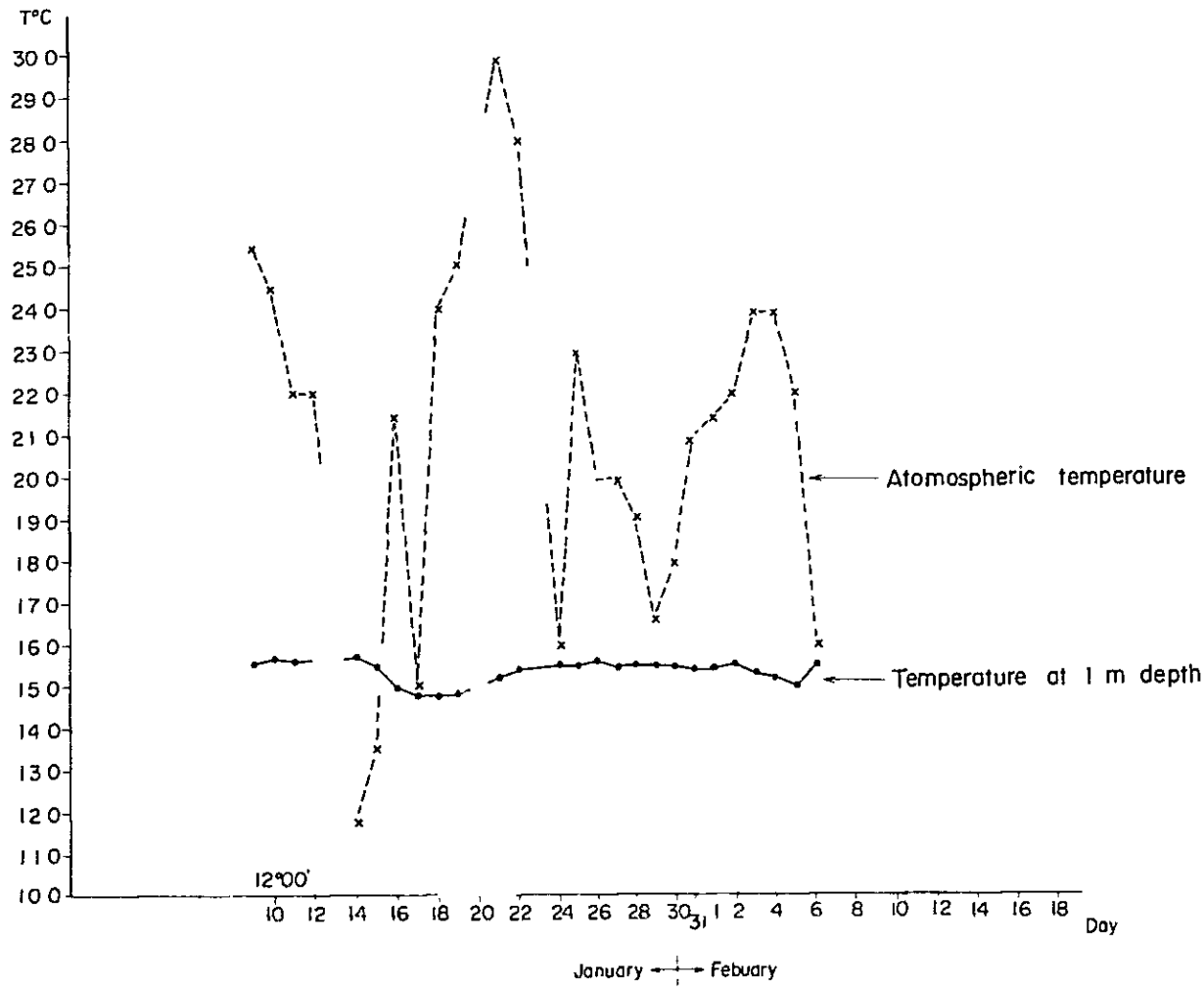

Fig.5-18 Observational results of variation of atmospheric and ground temperatures during period of 1 meter depth survey

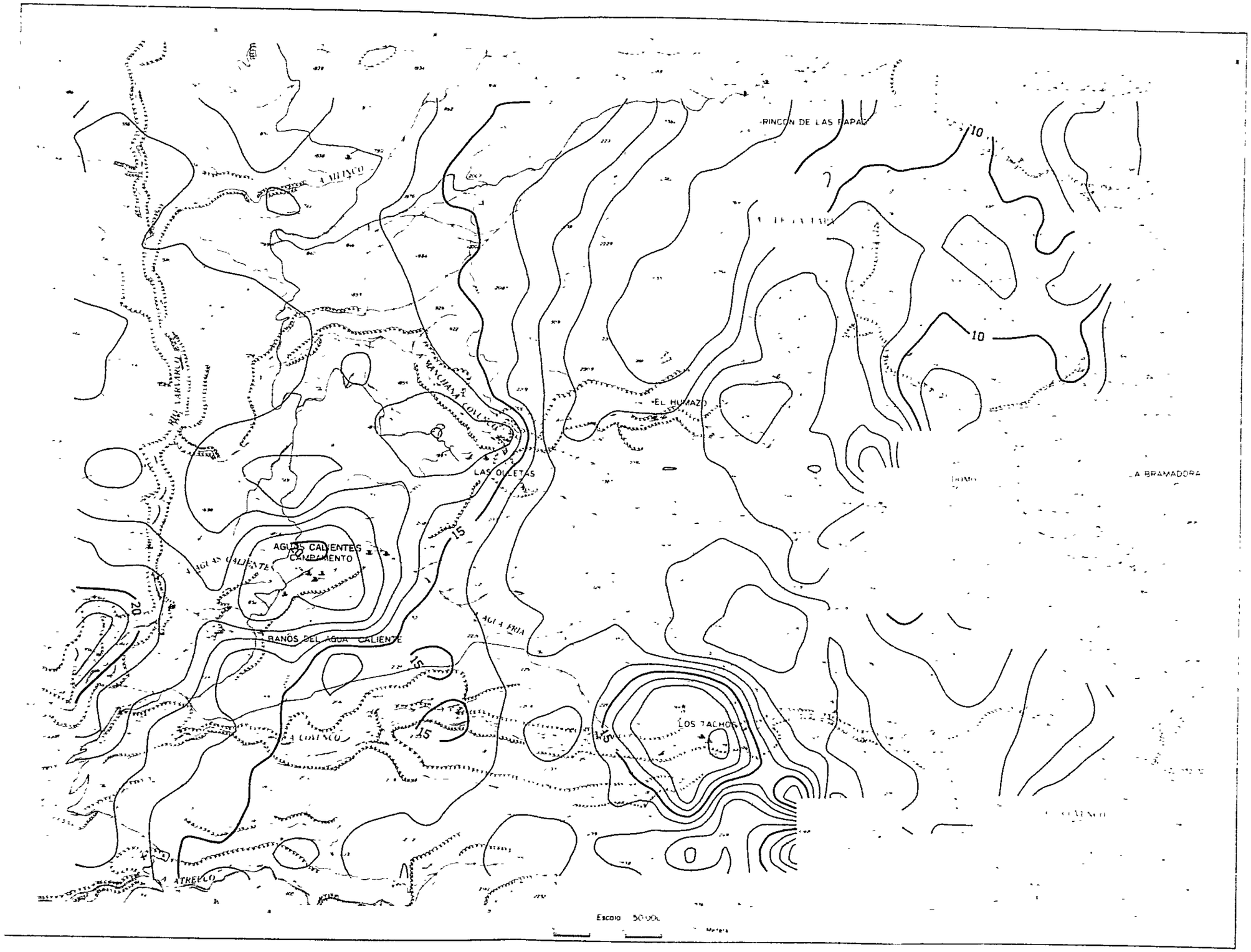

Fig.5-19 Distribution map of ground temperature at 1 meter depth by running average method

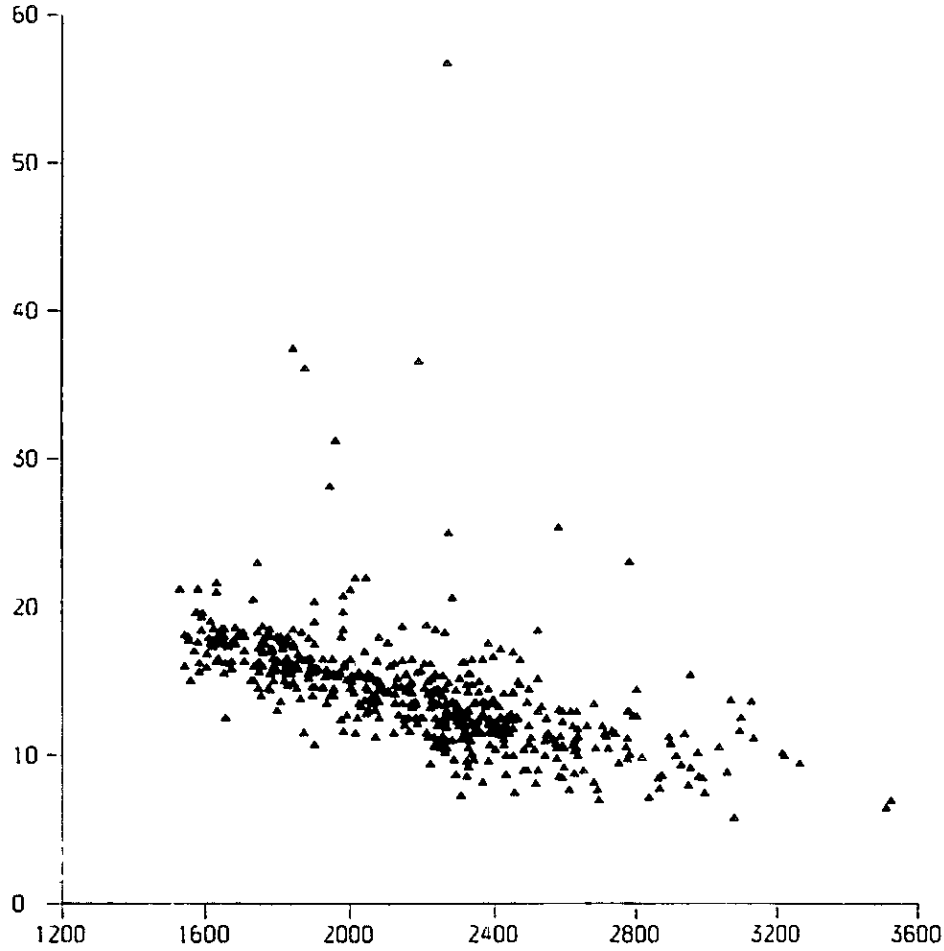

Fig.5-20 Relation between altitude and ground temperature at 1 meter depth

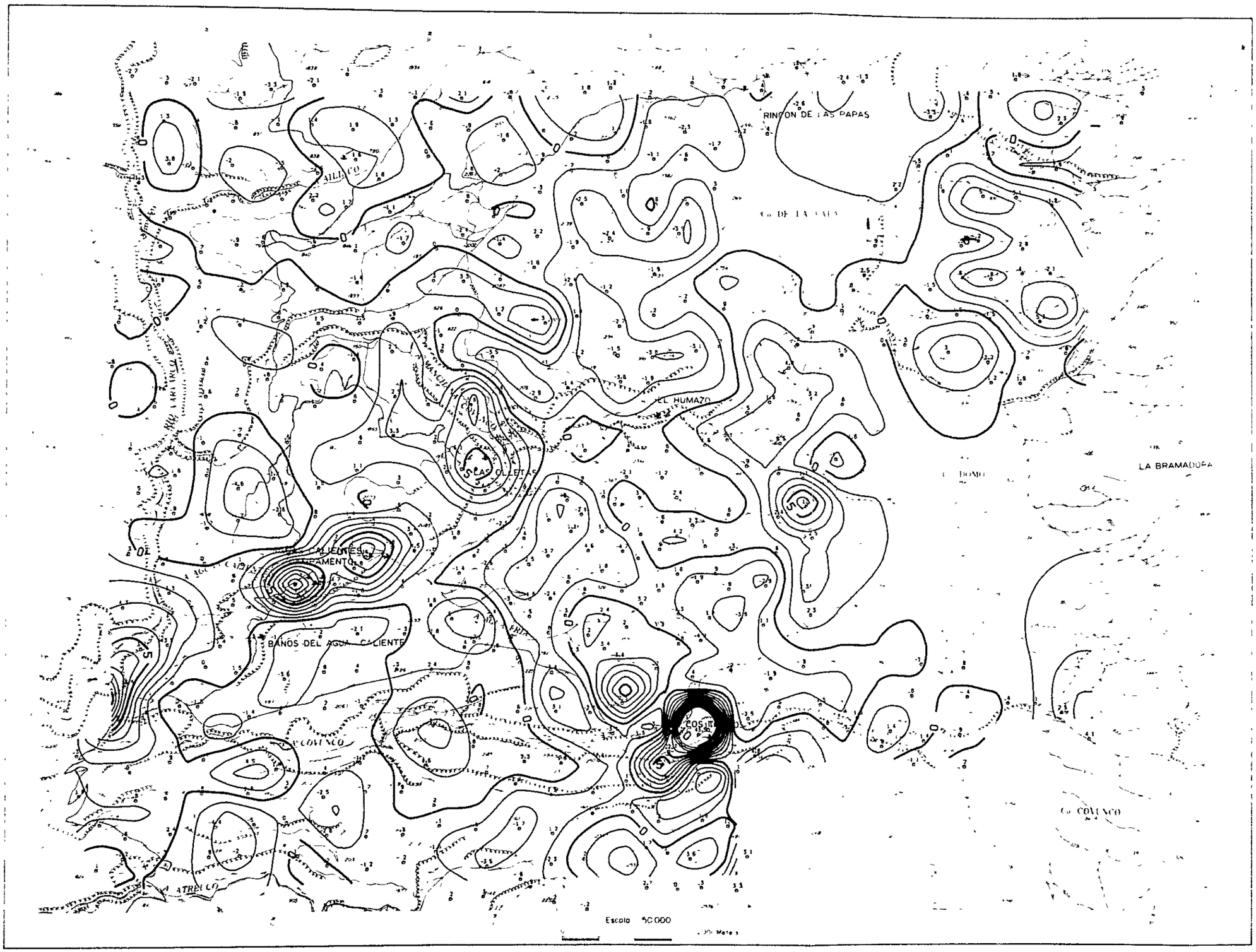

Fig.5-21 Distribution map of residual ground temperature at 1 meter depth (calculated by linear equation)

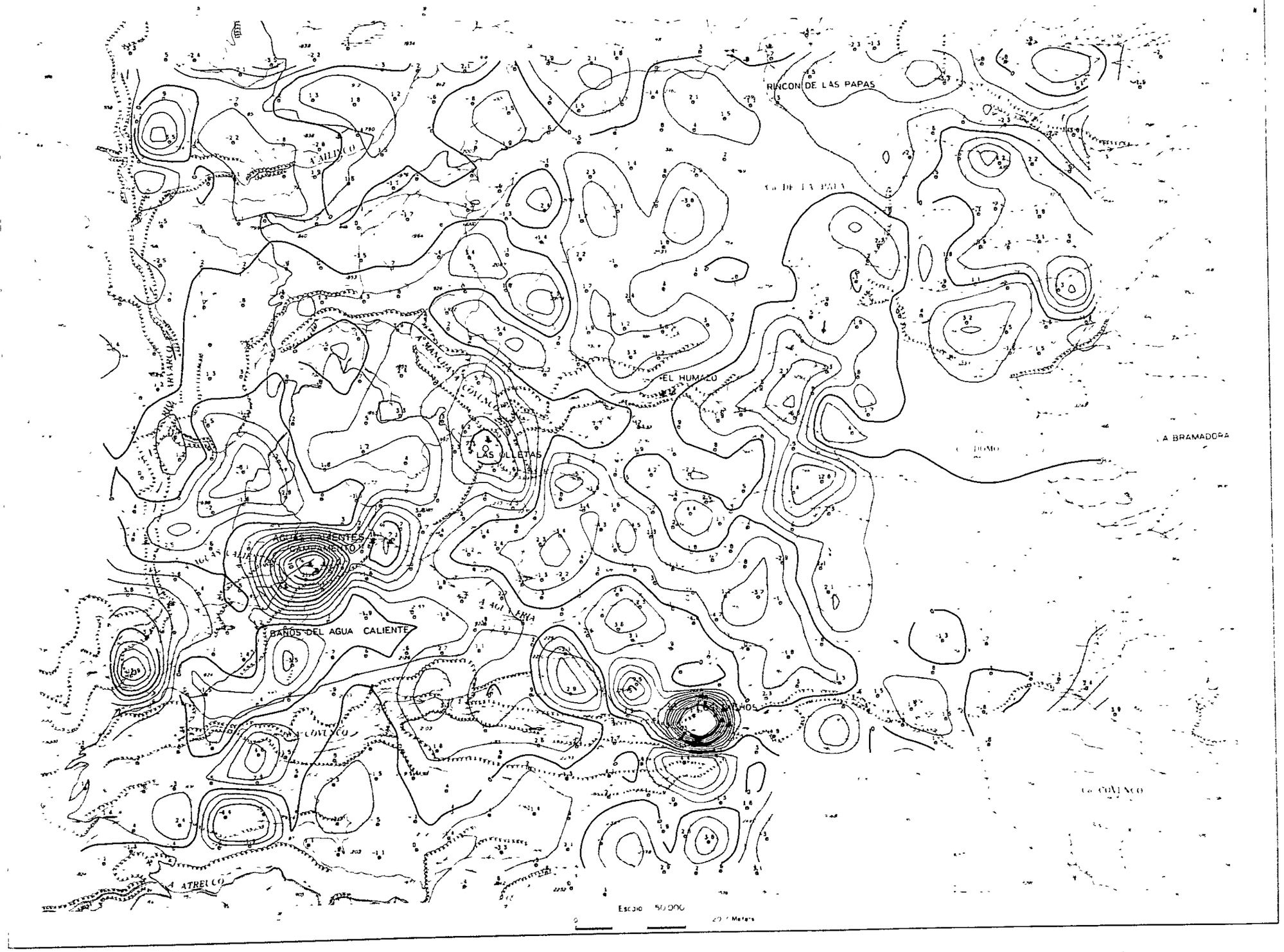

Fig.5-22 Distribution map of residual ground temperature at 1 meter depth (calculated by quadratic equation)

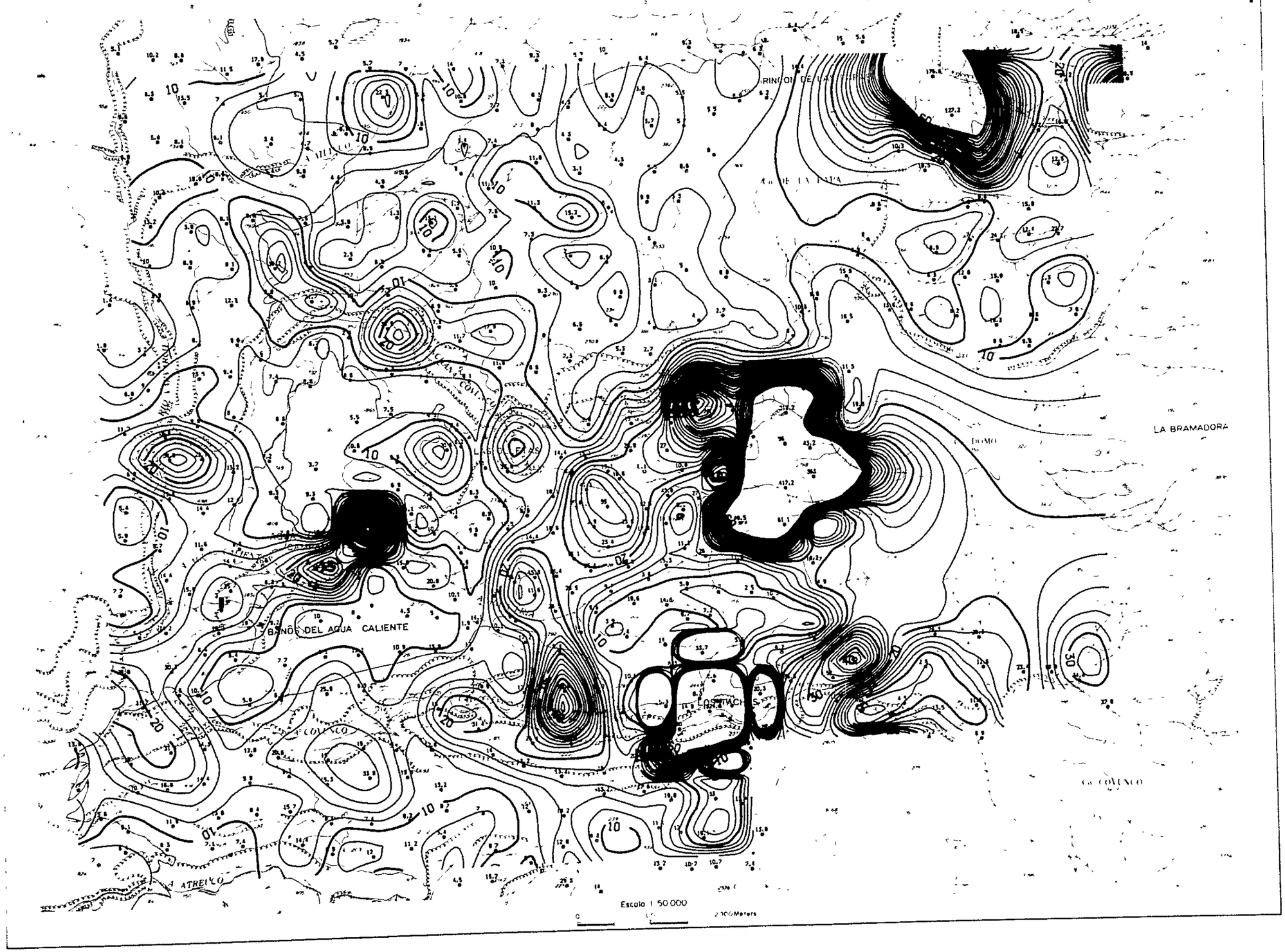

Fig.5-23 Distribution map of Hg - concentration in soil

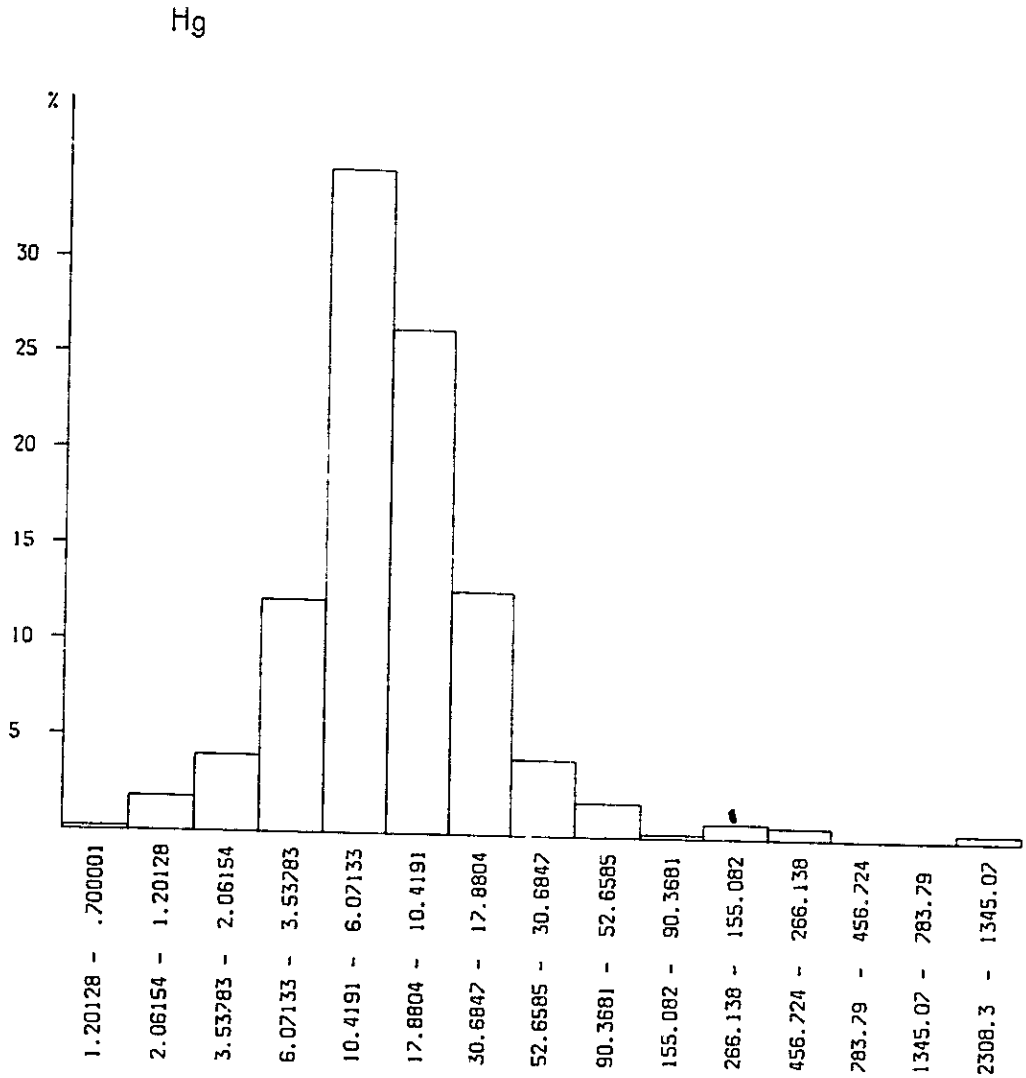

Fig.5-24 Frequency distribution of Hg - concentration in soil

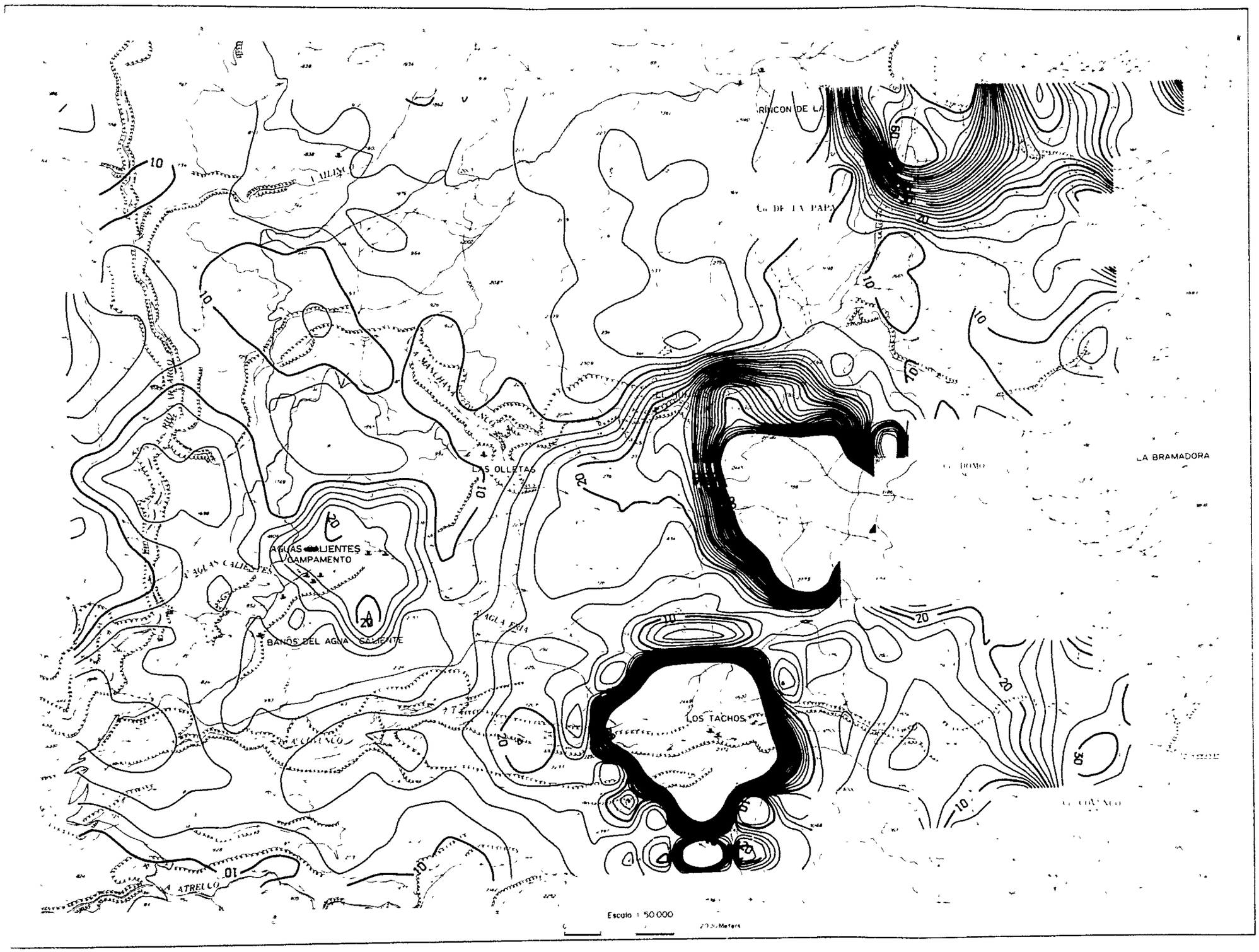

Fig.5-25 Distribution map of Hg - concentration in soil by running average method

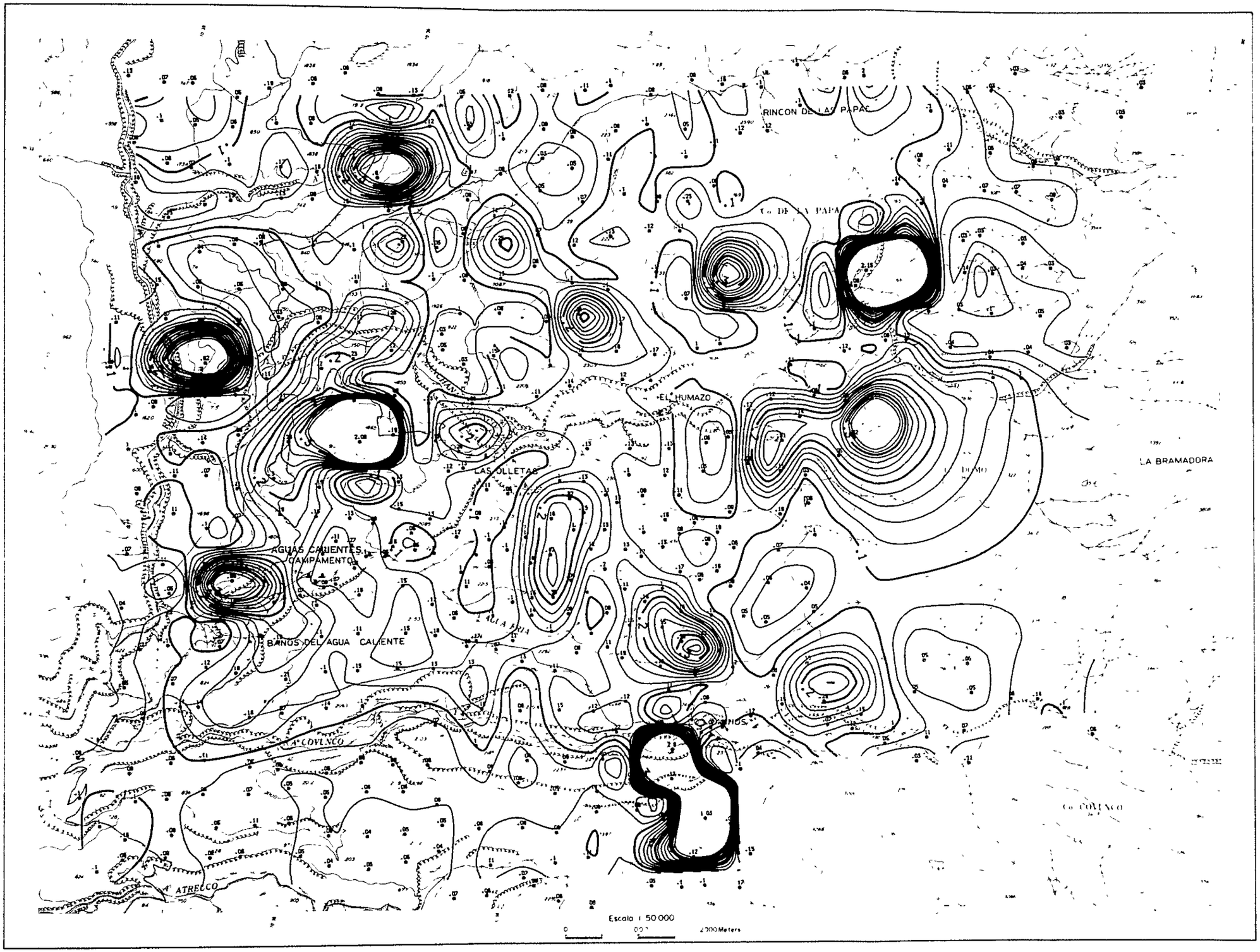

Fig.5-26 Distribution map of CO_2 - concentration in soil-air

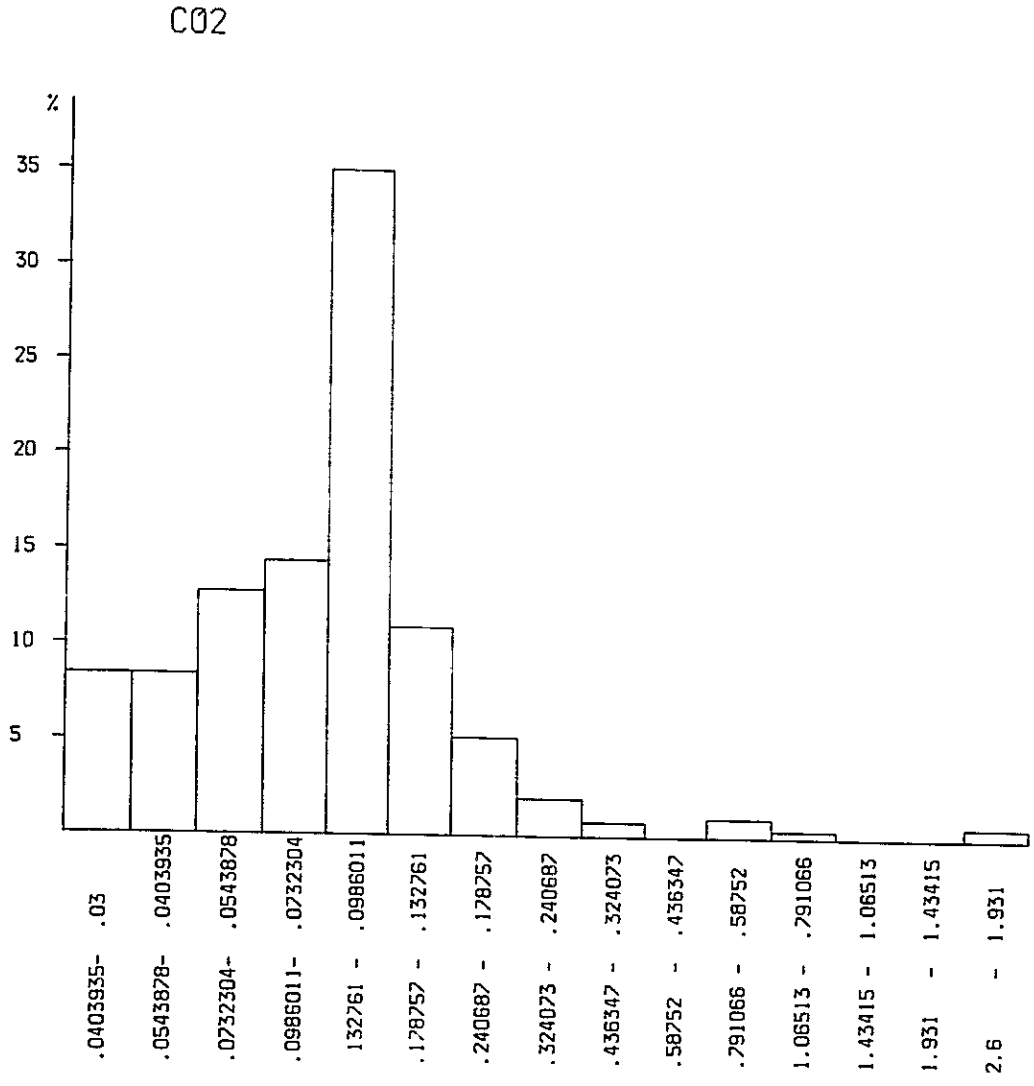

Fig.5-27 Frequency distribution of CO_2 - concentration in soil-air

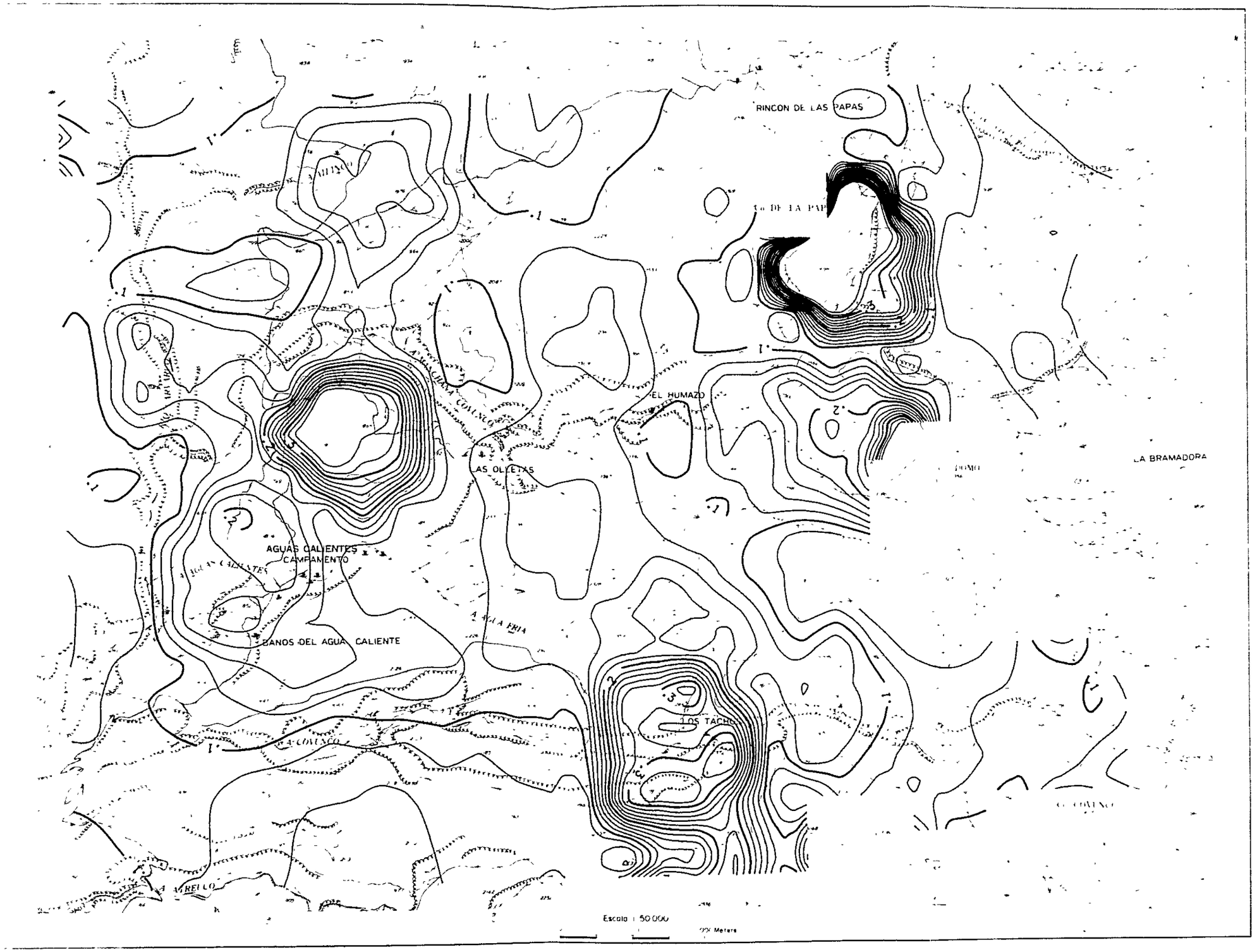

Fig.5-28 Distribution map of CO_2 - concentration in soil-air by running average method

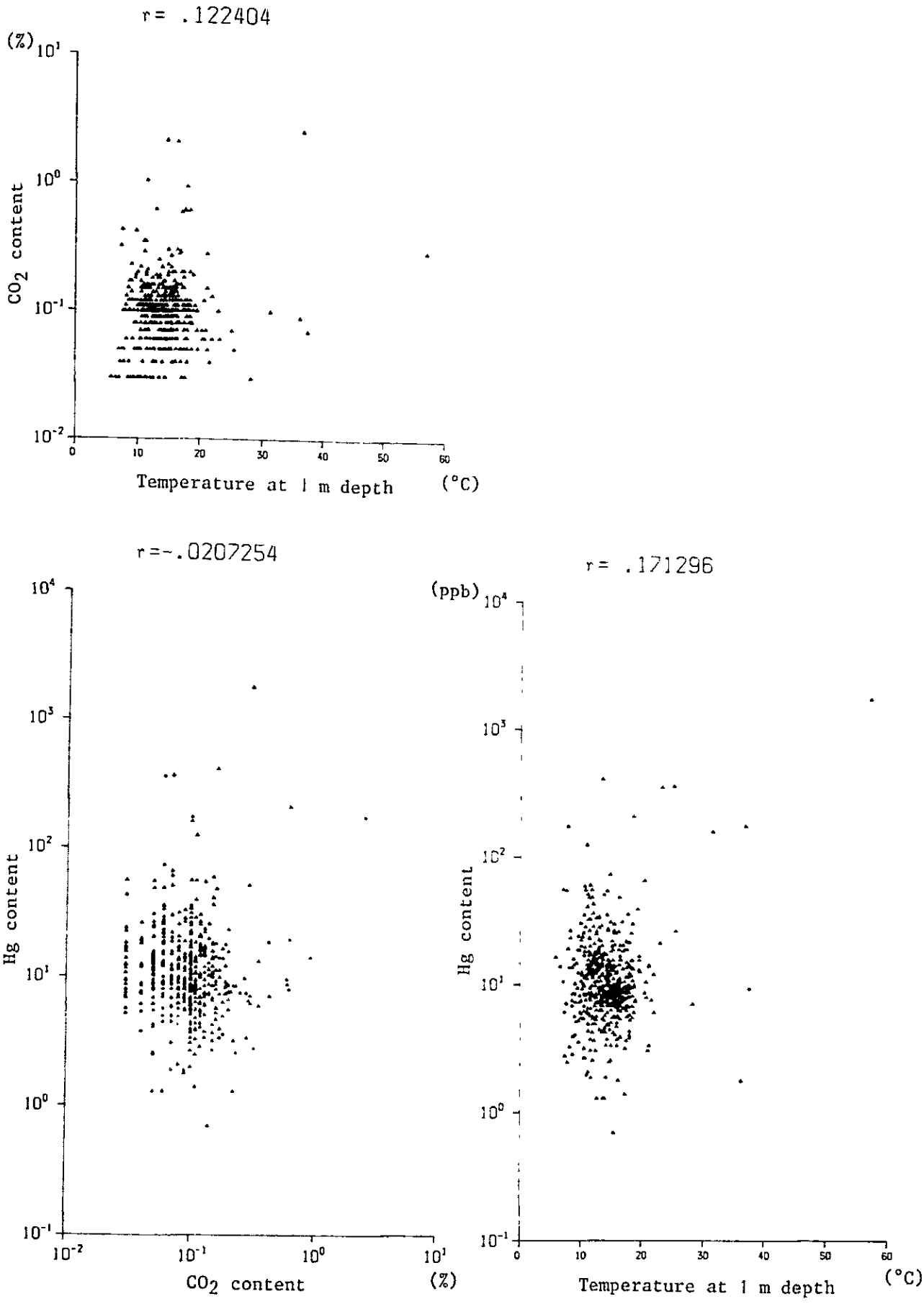

Fig.5-29 Correlations between ground temperature, and Hg and CO_2 - concentrations

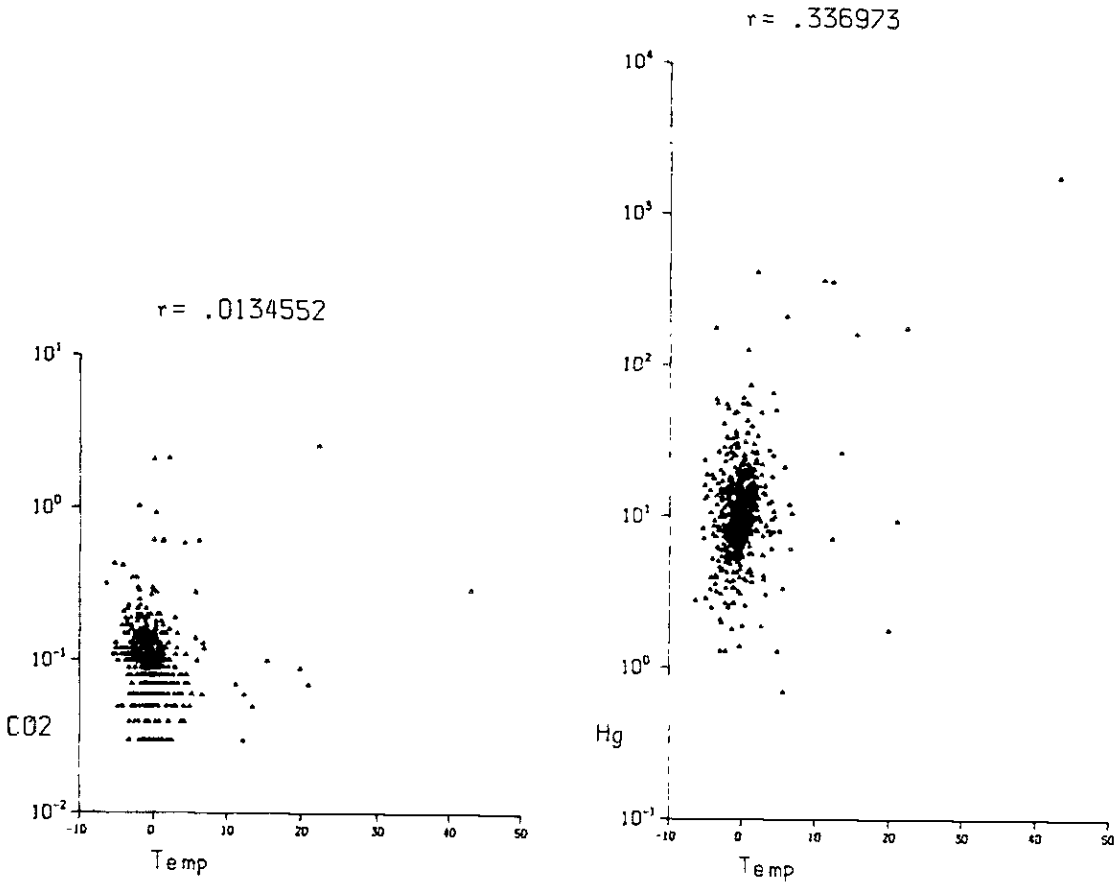

Fig.5-30 Correlations between residual ground temperature, and CO_2 - concentration(1) and Hg - concentration(2)

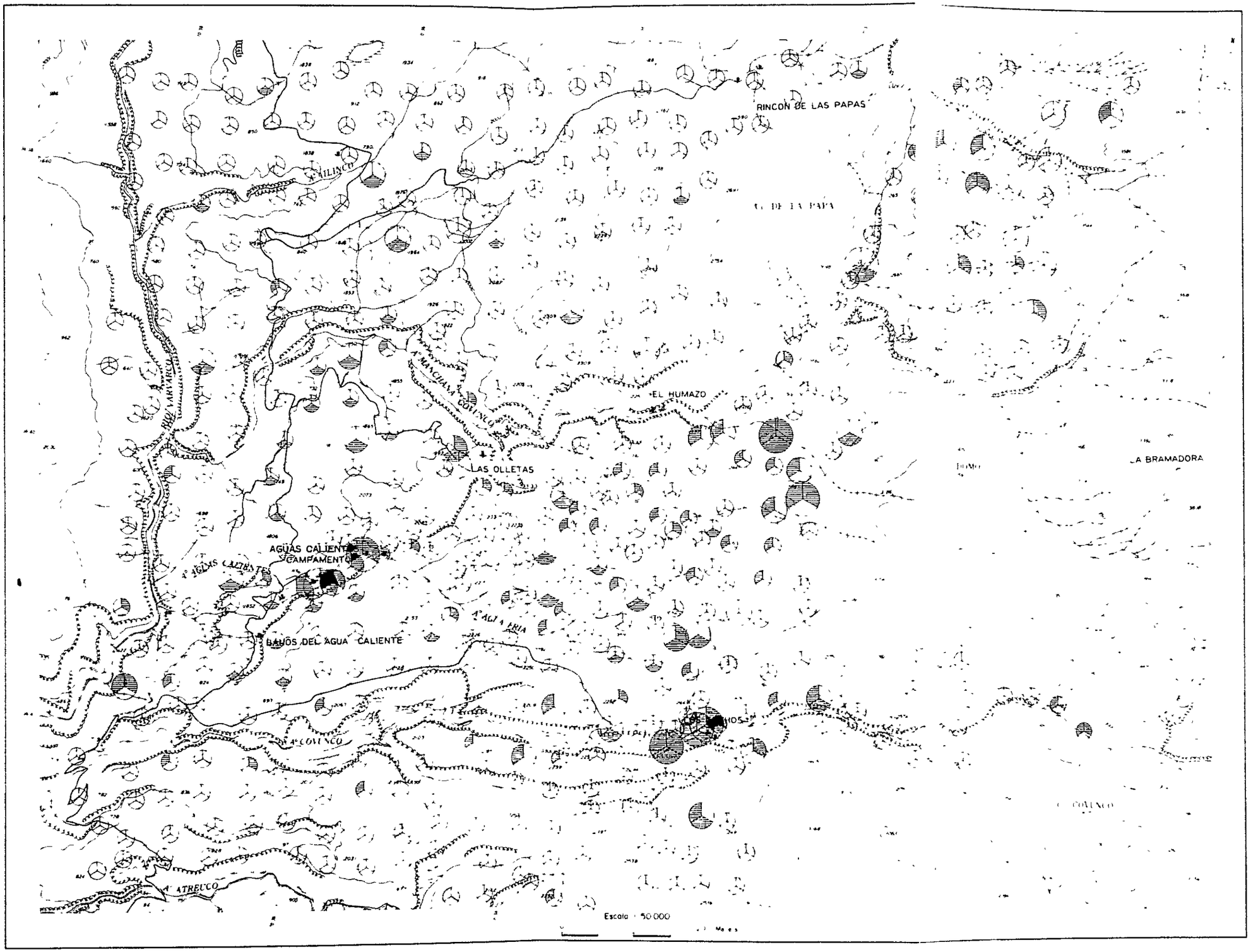

Fig.5-31 Relation map of anomalous values at 1 meter depth survey